2-1-2016

Fabrication of buckypaper with tailored porosity for application in water filtration

Ruaa Elnur

The American University in Cairo
School of Sciences and Engineering

FABRICATION OF BUCKYPAPER WITH TAILORED POROSITY FOR APPLICATIONS IN WATER FILTRATION

A Thesis submitted to the Nanotechnology Program

In partial fulfillment of the requirements for the degree of
Master of Science in Nanotechnology

By Ruaa Ibrahim Elnur
Bachelor of Science in Chemistry

Under the supervision of
Dr. Adham Ramadan, Professor of Chemistry
And
Dr. Amal Esawi, Professor of Mechanical Engineering

Fall 2016

ACKNOWLEDGMENTS

I would like to deeply thank my advisors Dr. Adham Ramadan and Dr. Amal Esawi for their constant support, guidance, and advice throughout this research project. Without their consistent feedback, never ending help and follow-up, I would never have been able to produce this work. Thank you, Dr. Adham, for accepting me in your team, and for teaching me how to be scientific and thorough in my work. I am deeply grateful for teaching me to be detailed-oriented and a problem-solver even when that meant sometimes for you to step out of your way to solve the hurdles I faced in my lab research. Thank you, Dr. Amal, for providing me with new research ideas and for following up constantly and tirelessly on my results. Thank you both for your patience and encouragement on all levels of my life, both academic and personal.

I would also like to thank the technical team that have been supporting me throughout my research. Special thanks to Youssef Jameel Science and Technology Research Centre (YJSTR) team for their constant and immediate help whenever requested. Thank you, Dr. Nahed Yacoub, Rami Wasfi, Ahmed Ghazali, Ahmed Noor, Ihab Salama for facilitating all the characterization work needed to be done. Also, I am equally appreciative for the Chemistry Department for their technical support. Special thanks to Ahmed Omaia for his unfailing help beyond limits, and to Emad, Amr, Ramadan and Abdel Aziz for always being helpful.

Having completed my master's degree is one accomplishment that I will be proud about, but gaining friends would be another thing I am equally happy about. Thank you Israa, Walaa, Asmaa, Sarah, Raghda for unfailing support you have given me a lifetime friendship. Thank you to my lab colleagues Marwa, Madina and Nouran, Norhan, Amr for making the lab time easier and enjoyable.

Moreover, there are no words to describe how much I appreciate knowing Alshaimaa, Yomna, Worood and Nada. Your support, friendship and sisterhood during the most difficult times in my life is unforgettable and nothing I do or say would show you how grateful I am to have you in my life.

My work colleagues and friends have also being big part of my support system. Thank you Sheri for being there every single moment I needed you and for teaching me when to laugh when I mostly needed it. Thank you Shaymaa for being part of my family and for especially

taking care of me without me asking. Thank you Yara and Noha for all the motivational speeches you gave me. Thank you Nermin for always pushing me to reach my maximum potential and for all your extra help. I can't thank enough Niveen, Mahmoud, and Rachael for all the support you gave me. Thank you Aya, Sandy, Nada, Somaia, Safaa, Omar, Taharqa, and Sanaa for the long support you have given me for all the years you have known me. Thank you my extended family for all the support you gave me and my family during the difficult time we went through. Special thanks to my aunt Amal.

I would like to thank my family. My mother, I only wish you were here to receive my deepest gratitude for your past presence in my life. I thank you for being a lifetime mentor and for the endless support you gave me even when that meant accepting my absence when you needed me the most, may your soul rest in peace. Thank you my dad for always being an inspiration in consistency and hardworking. Thank you my brothers Loay, Nazim and Rawie for believing in me and for accepting my absent presence. Last but not least, I would like to thank God for solving all hurdles I have faced during my work towards this degree.

Table of Abbreviations

BET	Brunauer–Emmett–Teller
BP	Buckypaper
BSE	Backscattered electrons
CNT	Carbon Nanotube
CVD	Chemical Vapor Deposition
DCMD	Direct Contact Membrane Distillation
DI	Deionized
DMF	Dimethylforamide
DWNT	Double Wall Carbon Nanotube
HA	Humic Acid
IPA	Isopropanol
MD	Membrane distillation
MWCNT	Multi-Walled Carbon Nanotube
NOM	Natural Organic Matter
PS	Polystyrene
PTFE	Polytetrafluorethylene
PVP	Polyvinylpyrrolidone
RLC	Resistor-Inductor-Capacitor
SE	Secondary Electron
SEM	Scanning Electron Microscopy
SWCNT	Single-Walled Carbon Nanotube

TEM	Tunneling Electron Microscopy
THF	Tetrahydrofuran
Trix	Triton X-100
TrOCs	Trace Organic Contaminants
UV	Ultraviolet

Abstract

The rapid development in membrane technologies and their use as a filtration medium have been based on the use and development of new materials to improve system performance. Carbon nanotubes (CNTs) represent a class of promising nanomaterial, exhibiting outstanding mechanical, electrical, thermal conductivity and adsorption properties. The idea of using carbon nanotubes in the separation and filtration industry has been put forward, but constructing macroscopic structures with controlled density, porosity, and morphology has been a challenge.

Buckypaper (BP) is a form of CNT film that is being investigated for application in water treatment. In BPs, the CNTs are oriented randomly into non-woven or paper like structure. This arrangement helps provide a large specific area with highly porous three dimensional network structures. However, the preparation of BP membranes with controlled porosity and pore size distribution entails taking into account many processing parameters.

Porosity is a key property for the use of BPs in separation applications in general. The work conducted here aims at preparing BPs with controlled porosity through the investigation of three different parameters, which impact porosity. These entail the porosity of the supporting filter membrane during the preparation of the BPs, as well as the exposure of prepared BPs to different solvents vapors and for different exposure times. The retention performance of the obtained BPs in water filtration is tested using micro-sized polymer beads.

CNT-BPs were prepared using vacuum filtration. Morphology and pore size distribution were investigated using scanning electron microscopy (SEM), nitrogen gas adsorption and mercury porosimetry. Different parameters were evaluated for their effect on tailoring the porosity of BPs. Statistical analysis was used to determine the effect of the three parameters

investigated, namely (1) the pore size of the membrane filter used in the preparation of BPs from CNT dispersions, (2) type of solvent vapors to which the prepared BPs are exposed, and (3) the exposure time to the solvent vapors, on the final membrane porosity. Results indicated that the type of solvent affects the pore size distribution with DMF giving more pores in the smaller pore size ranges. In addition, variation of pore size distribution of the BP membranes was observed upon varying the pore size of the membrane filter. On the other hand, no significant change was detected on changing the time exposure to the boiling solvent. One variable and one combination of variables were found to be successful in producing BPs with a lower average pore size. The findings confirm the potential of the solvent evaporation technique in tailoring the porosity of BP and membranes for filtration applications.

Finally, obtained BPs were tested for water filtration applications. Polystyrene beads of size ranges 0.3 µm and 0.6 µm, were chosen as model for bacteria and colloids removal, respectively. A comparison between blank BPs and modified BPs (subjected to solvent vapor for 40 minutes and prepared on specific membrane filter) was conducted. For the 0.3 µm of polystyrene beads, the blank BP showed a retention percentage of about 71% in comparison to the modified one which had a retention percentage of about 73%. For the 0.6 µm of polystyrene beads, the blank BP showed a retention percentage of about 67%, while the modified one had a percentage of about 75%. This indicates that the modified BPs possess smaller pore sizes on average than unmodified BP.

Contents

List of Figures

List of Tables

Chapter 1

Introduction

CHAPTER ONE: INTRODUCTION

1.0 The use of membranes in water filtration

Water use rates have been increasing by twice the rate of population growth in the past century. It is expected that by 2025, 1.800 billion people will be living in countries with absolute water scarcity [1][2]. Water as a resource is no longer easily accessible and obtainable in its purest form. Due to environmental challenges, urbanization impact, economic considerations and large scale industrialization, water has become an expensive commodity. Both water quality and water quantity have been one of the world major issues that need to have immediate consideration and action[3][4]. The need for cost effective water purification technology is more pressing now than ever [5].

In order to solve the issues of water quality, different technologies of water treatments have been investigated both at the lab scale and the field scale. They are generally categorized under primary, secondary and tertiary water treatment technologies. The primary technologies include techniques such as separation, centrifugation and filtration, the secondary technologies include aerobic and anaerobic treatments while the tertiary technologies include techniques like ion exchange, distillation, reverse osmosis, electrodialysis, microfiltration and nanofiltration[5][6]. Nevertheless, these technologies are not effective in removing water pollutants, as some might be too expensive to be used in commercial setups and some might not be efficient to be used in desalination applications (Figure 1). Recent improvements in membrane technologies, however, have

made them good alternative with cost effectiveness in the long run. Thus this makes them on top of other water technologies[7].

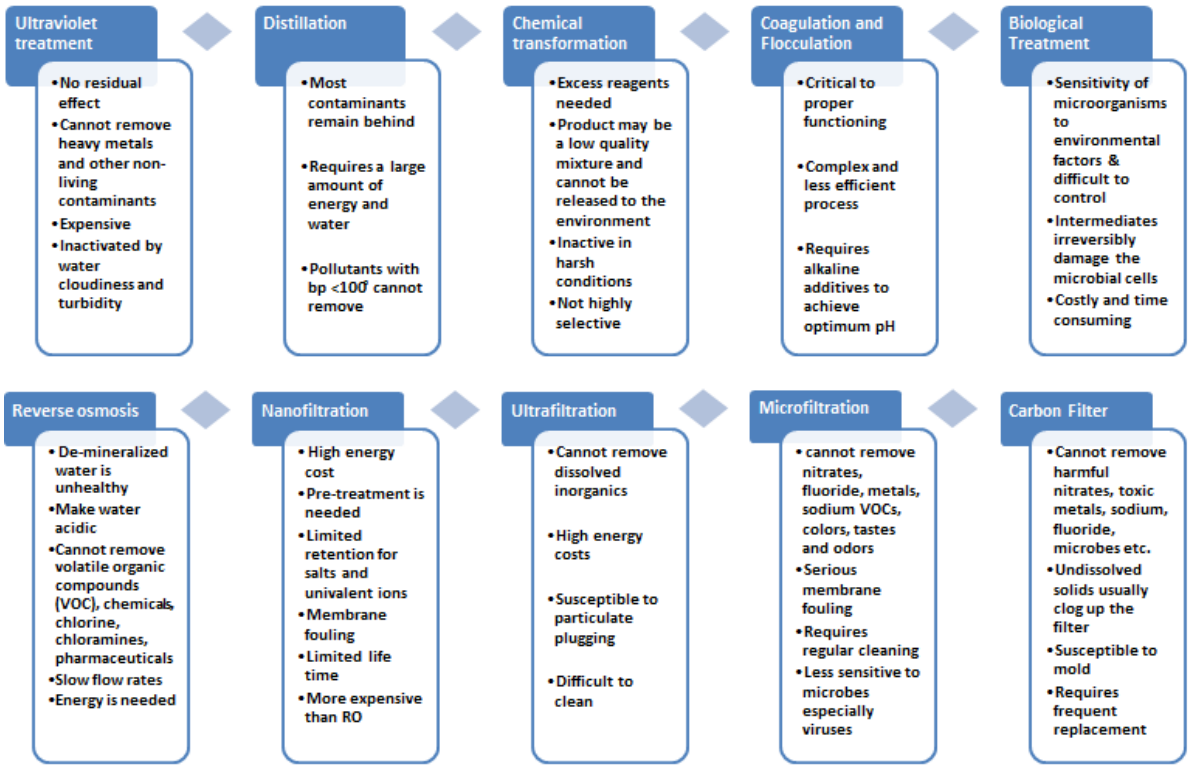

Figure 1 Major threats to existing water treatment methods

The continuous development of membranes as a filtration medium has helped provide low cost membranes with enhanced properties for water filtration applications. This is achieved with a continuing search and production for new materials to synthesize membranes with better system performance [8]. Most of the membranes that are commercially used now are made of polymeric material, and although they are cost effective compared to their counter parts, they still suffer from problems in their practical application like poor chemical and heat resistance and also fouling [9][10]. Yet, membranes based on nano-scale materials have attracted increasing interest due to their

unique properties that are most of the time superior to their bulk counterparts, and which could overcome some of these challenges[11].

1.1 CNT membranes and their properties

At present, carbon nanotubes (CNTs) are considered to be one of the most promising nanomaterials, as they exhibit outstanding mechanical, electrical, thermal conductivity and adsorption properties[12] (Figure 2). Nanotubes can be viewed as graphene sheets that are shaped into cylindrical shape, and which can be present both as single walled carbon nanotubes (SWCNT) with diameters ranging from 1-3 nm, and as a multi-walled carbon nanotubes (MWCNT) with outer diameters between 2-100 nm, and tens of walls[13]. Both SWCNTs and MWCNTs have been used in filtration application where they are useful in providing low energy water treatment solutions. However, constructing macroscopic CNT structures with controlled density, porosity, and morphology is still a challenge[4][11] [14].

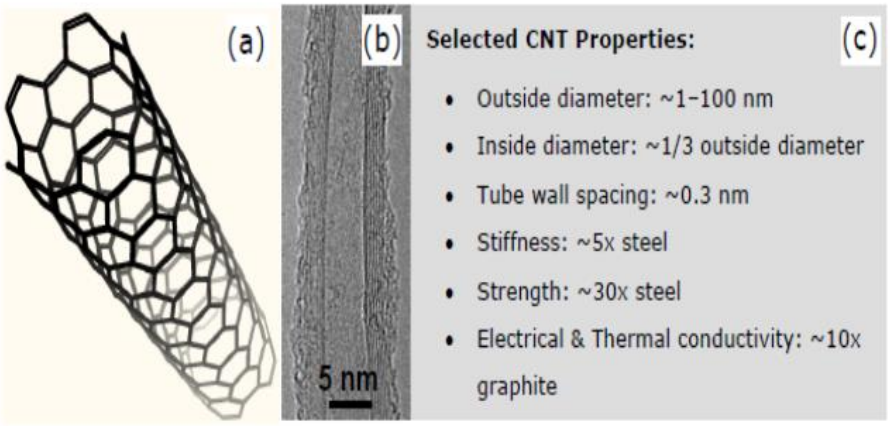

Figure 2 (a) Schematic of CNT (b) TEM image of a CNT showing a number of concentric graphitic walls (c) List of selected CNT properties[15]

Membranes made up of SWCNTs and MWCNTs possess good transport properties. The hydrophobicity of the CNTs enables frictionless movement of water molecules thus requiring minimum energy input. This, in turn, facilitates higher transport rates through these membranes[15], [16].

Some studies have established that CNTs can be exceptional antimicrobial structures. This has been found for both gram negative and gram positive bacteria. The mechanism of how this antimicrobial effect works is still not confirmed, but there are different proposed scenarios of the mechanisms of CNTs working on the bacteria, either by direct physical interaction which can disturb the intracellular metabolic pathways or through causing oxidative stress in these small organisms. CNTs are therefore considered potential candidate in terminating microbial attachment [1][17][18].

1.2 Challenges of CNT membranes

CNTs tend to agglomerate when present in a solution because of the van der Waals forces between them and their high surface area. This makes it hard for the CNTs to be dispersed in a solution or distributed uniformly in a polymer matrix. Two approaches are used to overcome this challenge.

One approach is to use surfactants such as Triton X 100, sodium dodecyl sulfate, and macrocyclic ligands, which are used to disperse CNTs in aqueous solvents. However, surfactants get adsorbed on the surface of CNTs and must be subsequently eliminated. Repeated washing and heat treatment are used methods to achieve this [19].

Another approach is to chemically functionalize the CNTs to achieve uniform CNT assemblies and produce flat CNT membranes. Previous work suggested that

functionalization helps increase the hydrophilicity of CNTs and the subsequent stabilization of CNT suspensions. CNTs can sometimes be functionalized with groups such as fluorine, amine and thiol groups by covalently grafting them onto the CNTs to help in their dispersion and crosslinking. Also, when functionalized, CNTs tend to be specific in attracting targeted pollutants. In addition, when attached with organic moieties, they make a reliable framework when present within host polymers. Methods to functionalize CNTs add to the preparation time since processes like refluxing and stirring are used[20][21].

Membranes with aligned CNTs showed promising results in filtration applications. Investigations reported in the literature showed that membranes with aligned CNTs revealed outstanding selectivity capacity for solutes based on size exclusion. MWCNTs with diameters averaging around 6.5 nm were successful in filtering gold nanoparticles that are larger than 10 nm, while letting small gold particles (around 5 nm) pass through. While membranes with aligned CNTs show promising results in water filtration, they are costly and require complex methods of fabrication that make them challenging to be produced on a large scale. Methods of fabrication such as ion milling and chemical vapor deposition with the use of hazardous materials make it difficult for these membranes to be used in large scale plants. It is for these reasons that investigations of the use of flat CNT membranes, buckypaper (BP), in water filtration are being conducted [22].

1.3 Buckypaper membranes

Buckypaper is a material composed of randomly oriented CNTs in a non-woven

or paper like structure. This arrangement provides a large specific area with highly porous 3D network structure, useful features for water filtration applications[11][23]. This however requires the control of different parameters for the preparation of BP. Longer, narrower, and purer nanotubes typically lead to stronger BPs with higher tensile strengths. With increasing MWNT diameters, the attractive van der Waals forces between CNTs become less effective, leading to BPs with lower tensile strength and poor cohesiveness[24][9].

BPs are in general described as a mat like structure of randomly entangled CNTs produced by vacuum suction. The CNTs have great tendency to self-aggregation due to the strong van der Waals attractions among them. Due to this inherent property of CNTs, BPs are easily prepared from CNTs dispersed in solution [25], [26].

BPs exhibit a number of properties rendering them good candidates for a range of applications[14]. These properties include high specific area and porosity[27], thermal[28] and mechanical stability[29], ease and relatively low cost of fabrication[14], adsorption capabilities[4], and controllable electrical properties[30]–[32].

Current applications in which BPs have been successfully used include cold field cathode emitters[30], radio frequency filters[31], substrates in biological applications [32][33], thermal interface material in electronics[28], drug delivery[34], support sorbent in extraction of milk components [35], the removal of contaminants from drinking water [4], as well as membrane distillation[27][36], gas separation[37], and filtration devices[20]. Porosity represents a significant feature of BPs, rendering them useful for separation applications in general. BPs are optimum for filtration purposes since they have large specific area, adsorption capabilities, high selectivity and low fouling[1]. Yang

et al. [20] have used functionalized carbon nanotube BPs for the removal of natural organic matter. The functional groups added to the CNTs helped in increasing the hydrophilicity of the CNTs and improved the efficiency of removing humic acid by >93%.

BPs are also used for membrane distillation (MD) processes. MD is a thermal driven process where a difference between the vapor pressures of two media separated by a hydrophobic membrane plays a central role in the process. A common process uses the hydrophobic membrane as a barrier between a feed of hot seawater/brackish water and a permeate of cold freshwater. The water vapor is the only thing that can pass through the membrane, driven by the difference in water vapor partial pressures. Dumee et al. [38] prepared self-supporting carbon nanotube (CNT) BPs and evaluated their performance in Direct Contact Membrane Distillation (DCMD). Results showed that the membranes were highly porous, majorly hydrophobic (contact angle 113^0) and exhibited good thermal conductivity of 2.7 kW/m. These attributes have proven to be useful for the membranes to be used for desalination. The only challenge was the lifetime of the membrane[36].

Pollutants like natural organic matter (NOM) are one of the major pollutants that are of interest today as they increase the toxicity level in water. They can result in producing carcinogenic byproducts formed during disinfection processes and reacting with complex metals. CNTs have good adsorptive capacity for these NOMs due to the mesoporous structure, the π-π interaction between the aromatic rings of the CNTs and NOMs that facilitate better adsorptive mechanism. [1]. Moreover, some investigations addressed the possibility of filtering trace organic contaminants (TrOCs) from aqueous

solutions using BPs. These compounds are hazardous, and can be found in water. They have the ability to disrupt the normal functionality of the endocrine system[20], [27].

1.4 Statement of purpose

This research work aims at preparing Bucky paper with controlled porosity through the variation of different parameters. The objective was to decrease the average pore size of the BPs produced and increase the number of the small pores they possess. First, varying the time of exposure of acetone vapor to the examined BPs was tested to see the change of porosity of the examined BPs. Secondly, different boiling solvents were used to see if a change of the type of boiling solvent would result in changing the porosity of BPs. Thirdly, a change of the pore size of the filter membrane (used as substrate for the BPs) was also tested as a variable to see its influence on changing the porosity. Last but not least, a statistical model was used to see what variables or combination of variables are the most influential on producing BPs with lower average pore size. The obtained membranes were tested for filtration performance using polymer beads of specific sizes comparable in size with bacteria and colloidal particles in waste water [39].

Chapter 2

Literature Review

CHAPTER TWO: LITERATURE REVIEW

BPs are prepared by vacuum suction of well dispersed CNT solution[26]. The preparation entails the purification of CNTs, their good dispersion in a suitable solvent, and their precipitation on a porous support [1]. The properties of BPs are affected by several parameters during preparation such as the type of CNTs, the vacuum pressure, concentration and dispersion of CNTs, solvents used, surface functionalization of CNTs as well as their physio-chemical properties[26]. Following is a summary of work reported in the literature investigating these different parameters.

2.1 Type of CNTs

BPs contain highly porous network with randomly oriented CNTs. Different approaches were followed to investigate the parameters that control the porosity of BP membranes. This was found to primarily depend on the type of CNTs used[40][41]. For example, Muramatsu et al.[42] investigated the pore structure and oxidation stability of BPs prepared from carbon double wall nanotubes (DWNTs) as compared to that of SWNTs. They found out that the micropore volume in BP derived from DWNTs of the former was three times greater than that of the latter. They attributed this to the fact that DWNTs have well developed inter-tube cavities as well as the fact that DWNTs possess large number of pores that range from 20 to 100 nm due to the empty spaces developed from their highly intermingled long bundles.

Rashid et al. [22], on the other hand, investigated the surface morphology of BPs prepared from SWCNTs compared to those of MWCNTs either by using functionalized CNTs or by using surfactants. By looking at the SEM images of both and carrying a

quantitative analysis of the pore openings of these materials, it was found that the surface pores of BPs prepared from MWNTs have significantly larger average diameters than those from SWCNTs. Additionally, by investigating the internal morphologies of both using nitrogen adsorption/desorption measurements, both types of membranes showed similar overall isotherms. However, when studying the isotherms further, major differences were found in pore size distribution, average internal pore diameters, and inter-bundle pore volumes. For example, the average internal pore diameter for SWNT membranes was between 2.0 ± 0.2nm and 4± 0.4nm while for that of MWNT membranes varied between 10±1 and 26± 3 nm. Not only that, specific surface areas of most of the SWNT membranes were between 360± 4 m^2/g to 790 ±4 m2/g, while those of MWNT membranes varied from 180± 0.1m2/g to 380± 2.0 m^2/g. This showed that the type of CNTs plays a role in the surface properties of BPs.

Moreover, in order to compare the thermal stability of BPs, BPs prepared from SWNTs and DWNTs to be used in electronic applications such as field emission displays was investigated. Kim et al [24] fabricated both types of BPs. Using Tunneling Electron Microscopy (TEM) and scanning electron microscopy (SEM), structural changes were observed after a thermal treatment at 2000^0C. It was observed that for BPs prepared from SWNTs, bundles of the nanotubes were structurally distorted to form larger bundles. In contrast, there was no observed change for BPs prepared from DWNTs. Therefore, it was concluded that these BPs would possess extremely stable emitting performance with a low threshold voltage when used in field emission displays.

2.2 Effect of catalyst composition

Li et al.[23] investigated the effect of catalyst composition in the synthesis of CNTs on the yield and structure of the final CNTs and also the mechanical strength of free standing BPs. They have proved that BPs made from less defected MWNTs possess higher tensile strength. The CNTs were prepared using chemical vapor deposition (CVD) of methane over Magnesium Oxide (MgO), supported Co and Mg catalysts. Different Mo/Co ratios were used from 0-3. It was found that the yield of CNTs increased from 7 wt% to 400 wt% as the ratio of Mo/Co increased from 0 to 3. Generally, the BPs obtained from CNTs prepared using different catalyst ratios showed brittle behavior as the ratio increased. The tensile strength of BP prepared from ratio of 1.5 ratio of Mo/Co (15.36MPa) for example, is five times that of BP prepared using catalyst ratio of 2 (2.77 MPa). Thus, although the yield of CNTs was increased by increasing the catalyst ratio, it led to a decrease in the mechanical quality of the BPs.

2.3 Effect of using pristine versus functionalized CNTs

With the objective of achieving a well dispersed solution of CNTs to prepare BPs, Li et al.[23] functionalized MCNTs using a mixture of nitric acid and sulfuric acid. The mixture was refluxed for four hours to produce CNTs with groups of COOH and OH on the surface of CNTs. The refluxing treatment was important for producing a continuous film after filtering the CNTs; otherwise split spots would be observed and found on the polycarbonate membrane filter which was used to filter the dispersed solution of CNTs. Zhang et al [43] also investigated the effect of oxidation by nitric acid on SWCNT BP having a mean diameter of 1 nm. It was found that by increasing the diameters of

SWNTs, a higher tensile strength was achieved. This was evident when exposing high concentrated nitric acid (10 M) to both small diameter SWNTs and large diameter SWNTs. The high acid treatment destroyed the ones with small diameters, while when exposing the high concentrated treatment to larger diameters, the tensile strength of BPs improved from 10 to 74 MPa.

Bhalchandra et al. [44] investigated changing the wetting properties of MWNTs by changing their surface properties. Chemically changing the surface of nanotubes as a way to change their wetting properties was thought to be a good approach in understanding phenomena like self-cleaning and anti-fogging. The group investigated and managed to carry chemical functionalization of CNTs leading to a change of the surface of the prepared BPs from hydrophobic to hydrophilic. Different strategies were used to functionalize the CNTs using ozonolysis, and chemical treatment of acid mixtures. The change in the wetting properties of the resulting MWNT BPs enabled a controlled heterogeneity on the surface with marginal change in the surface roughness.

Although it is useful to use functionalized CNTs to help in the critical step of dispersing them in the designated solvent, Rashid et al.[22], found this to significantly lower the mechanical strength of the resulting BPs. When comparing BPs prepared using surfactants with BPs using functionalized CNTs, it was found that those with the functionalized CNTs showed the poorest mechanical properties. For instance, MWNT-NH_2 and MWNT-COOH showed the lowest tensile strengths and poorer ductility values than those BPs prepared from surfactants. The poor mechanical properties, therefore, resulted in conducting the water permeability tests over a narrow range of applied pressure.

Sometimes, the functionalization of CNTs could be accomplished for different purposes. Dumee et al.[38], were interested in increasing the hydrophobicity of BPs to be used in direct contact membrane distillation. In this kind of application where the membrane is in contact with water of different temperature on both sides, extremely hydrophobic membrane material is needed to inhibit the processed liquid from absorbing into and wetting the membrane pores and thus forming a direct bridge-like contact between the two sides of water. The increase of membrane hydrophobicity would enhance the performance of the membrane and lower surface pore wetting and wicking which potentially limit water permeability. This was accomplished by treating first the CNTs with UV/ozone to create active hydroxyl and carboxylic active sites on the surface of nanotubes and then functionalizing CNTs with 3-glycidoxypropyltrimethoxysilane (GPTMS) for the hydroxyl group to react with alkoxysilane moieties. This was successful in changing the resulting BPs' contact angle from 120^0 to 140^0, rendering them good candidates to be used in direct contact membrane distillation.

In the same manner, Yang et al.[20] functionalized CNTs to prepare BPs to be used to filter natural organic matter (NOM) found in water. This is considered a major water pollutant, as it forms carcinogenic byproducts. According to their findings, the adsorbing capabilities seem to improve by functionalizing the CNTs using 5M sulfuric acid. The water contact angle of the resulting BP decreased from 54 ± 6^0 to 29 ± 4^0 making the BP more hydrophilic. A good removal of humic acid (HA) (>93%) was accomplished then. This was explained by the incorporation of hydrophilic functional groups to the used CNTs, enhancing their hydrophilicity and thus enabling better contact of HA solution with the BPs.

2.4 Effect of using surfactants to disperse CNTs

Another way to enhance the dispersion of CNTs used in the preparation of BPs is the use of appropriate surfactants[11]. To avoid losing intrinsic chemical and mechanical properties of the CNTs of the BP, surface functionalization is not preferred, and as surfactants interact with CNTs non-covalently, their use is preferred. However, the removal of surfactants can be challenging, possibly leading to purity challenges in the obtained BPs.

Rashid et al. [22] investigated the effect of using different surfactants when preparing BPs on BP permeability towards trace organic contaminants. Surfactants such as Triton X-100 and macrocyclic ligands were added to the CNT solution when preparing MWNT buckypaper. Permeability tests were carried out using a dead end filtration system. It was found that changing the type of CNTs (functionalized and non-functionalized) or the change of dispersants have no real effect on permeability. Permeability tests also revealed that most of the BPs prepared from the different dispersants have a good rejection of trace organic contaminants, with the lowest rejection observed being for the BP prepared using the surfactant phthalocyaninetetrasulfonic acid. This was explained by the low surface area of this type of membrane, limiting its ability to adsorb dissolved solutes. Morphology characterization was carried out using scanning electron microscopy and showed that all the membranes had similar morphologies.

2.5 Effect of using polymers to disperse CNTs

Park et al.[45] synthesized a new polyelectrolyte called polyphosphazene as a dispersing agent for SWCNTs in water. Polymers are known for their ability to exfoliate

SWNTs bundles, due to non-covalent interaction between the polymer and the surface of the SWNTs. By characterizing the obtained BPs, it was shown that SWNTs existed either as individual nanotubes surrounded by the polymer or as smaller bundles than they originally exhibited before the addition of the polymeric dispersing agent. This proved that polyphosaphazene could be a potential candidate to be used to disperse CNTS.

Liu et al.[46] prepared BPs using a novel water soluble dispersant, polyvinylpyrrolidone (PVP), to enhance the mechanical properties of the BPs. Polymer intercalation is one of the methods used to enhance dispersion by improving load transfer between the nanotubes. By fabricating the BPs this way, the tensile strength and modulus of PVP-BPs were 227% and 295% higher than those prepared using the surfactant Triton X-100. The group also found out that the improvement of the mechanical properties is not infinite: increasing the amount of PVP above a certain limit, had no additional impact on mechanical properties.

2.6 Effect of using alternative techniques

Whitby et al.[47]fabricated BPs using a novel technique they called frit compression, where neither surfactants are used nor functionalized CNTs were needed to be used. The technique was based on putting a sonicated solution of CNTs in a syringe where the solution passes through a frit with a porosity of 50 µm placed inside. A second frit was placed at the top of the solution, where both frits were pressed against each other under hand pressure, and the membrane of buckydiscs (thickness over 500 µm) was taken from between the two discs. The produced buckydiscs possessed higher porosities than ones produced using Triton- X100. They were also more flexible, robust to handle and

had a memory effect.

Another group increased the hydrophobicity more by coating the BP membrane by a thin layer of poly (tetrafluro-ethylene) to make them more hydrophobic by 23%-28% and more mechanically stable in time. These membranes were then tested in DCMD setup, which made them potential candidates for the use in DCMD, where they are highly hydrophobic because of the coating of PTFE and the high porosity due to the surface property of BPs[48].

2.7 Effect of using different solvents

Whitby et al. [47] synthesized different BPs using the frit compression mentioned earlier. They attempted synthesizing different samples using different solvents. Porosity characterization was conducted using mercury porosimetry, and it was found out that by changing the casting solvent the porosity (intertube pores, mesopores and small macropores) of the samples changed. The differences were analyzed to be due to the different packing order effect on the CNTs by the casting solvents due to differences in surface tension. For example, when hexane was used as a solvent, the resulting BPs had 9.1% intertube pores. On the other hand, when water was used, it resulted in BPs with 13.4% intertube channels. This was attributed to the fact that hexane caused rapid swelling of the CNTs while water causes agglomeration of hydrophobic nanotubes, producing more interube channels.

2.8 Effect of varying the quantity of CNTs

On a different note, the group Yang et al.[20], also attempted to investigate how different amounts of CNTs resulted in BPs having different porosities for water filtration purposes. They varied the amount of CNTs between 50 and 100 mg. It was found that BPs prepared from 50 mg and exposed to sonication for 10 minutes, had the highest porosity. In addition, BPs thickness was found to increase almost linearly with increasing CNT amount. However, Whitby et al. [47] found that there was no variation in pore distribution of samples of BPs prepared from different CNT weights, using the same casting solvent. There was generally a concentration of mesopores at 16 nm, with most of the micropores existing between 50 nm and 1000 nm, while the large macropores lied between 30 and 200μm.

2.9 Effect of varying the sonication time

In investigating the effect of sonicating the CNT solution used in BP preparation and see the effect of that on the final porosity of BPs, Yang et al.[20] varied the sonication time to 5, 10, 15 minutes when preparing the solution of dispersed CNTs. It was found that the longer the sonication time, the smaller the CNT bundles produced in the obtained BPs, and the larger the pore volume. The CNT bundle size was decreased from 137± 19 to 110± 13 nm when increasing the sonication time from 5 to 10 times, having the porosity to increase from 59.4 to 72.9 % respectively. Longer sonication times, was concluded, results in larger pore size.

2.10 Effect of using a mixture of CNTs

An attempt by Sears et al.[40] to investigate the possibility of using a mixture of CNTs to control the porosity of BPs indicated that indeed, the presence of CNTs of different outer diameters could be used to control porosity

2.11 Effect of the aspect ratio of CNTs

Another parameter that was shown to have an effect on the porosity of BPs is the length of the CNTs used. Smajda et al.[49] used CNTs of different lengths varying from 2μm to 230 nm and observed a change in pore size distribution[49].

Deneuve et al.[50] investigated the use of high aspect ratio, vertically aligned CNTs for producing BPs for H_2S oxidation into sulfur as a desulfurization process. CNTs were synthesized by chemical vapor deposition to have an aspect ratio of ca 2000. This high aspect ratio was required because it is a critical parameter to produce BPs which are both flexible and have good chemical resistance. In addition, when comparing using CNTs of different aspect ratios, the group found that the higher the aspect ratio the more stable the CNTs in their solvent. For example, the CNTs of aspect ratio 2000, was stable in an ethanol suspension for 24 hours, while the others with low aspect ratios, 100-200, quickly settle at the bottom of the container an hour after the same ultra-sonication treatment. Thus, changing the aspect ratio of the CNTs affects their dispersion in the solvent designated, and thus affect the mechanical and chemical properties of the BPs produced.

Another group was investigating the effect of using CNTs with different aspect ratios on the pore size and pore distribution of the BPs [51]. They found out that when

BPs are prepared using longer CNTs with smaller diameters, this results in having BPs with smaller average pore width values and better distribution of pores. While those BPs prepared from larger diameters generally have larger pore sizes. BPs produced from shorter CNTs generally have a larger pore size distribution.

2.12 Effect of changing the filtration pressure

In their investigation, Zhang et al. [52] were more concerned about changing the applied pressure during the filtration process of the CNT solution on the porous support. The group investigated changing the conventional filtration setup technique with a syringe technique that would allow them to change the filtration pressure by applying constant load on the syrine. The effect of changing pressure is then investigated on the porosity, the mechanical, and thermal and electrical conductive properties of the BPs prepared. In doing that, it was found that an increase of the applied pressure (from 1 atm to 12 atm), the porosity of the BPs was reduced by ~1.9%. Also, the gaps between within the entangled CNT bundles decreased in size resulting in a higher intertube interaction, which in turn led to enhanced mechanical and conductivity properties of the BPs.

2.13 Effect of applying mechanical pressure

Arif et al. [53] investigated the effect of applying mechanical pressure on prepared BPs in order to change their porosity and mechanical, electrical and thermal properties. Two types of BPs were investigated, uncompressed BP which were prepared by vacuum filtration and compressed BP also subjected to compressive forces between platen presses. The compressed BP showed pore ranges between 5 to 50 nm while the

uncompressed BP showed larger range between 5 to 70 nm. In addition, the compressed one showed a much higher number of pores between 0 and 30 nm than the uncompressed one. In general, the compressed BP showed enhanced thermal and conductivity properties, while no difference was observed for the mechanical properties.

Chapter 3

Theoretical Background

CHAPTER THREE: THEORATICAL BACKGROUND

3.1 Scanning Electron Microscopy (SEM)

SEM is a popular tool to examine the morphology of solid specimens. The different properties that it possesses range from high lateral resolution, different imaging modes, to a relatively easy handling and preparing of the samples imaged [54]. The magnification of imaging ranges between 5X-10,000,000X, which makes detection of nanomaterials possible [55].

The principle of the SEM relies on the deflection of electrons when exposed to a magnetic field. Unlike the light microscope which uses light beam as a source of energy, the SEM uses a high energy electron beam.

When the beam reaches the sample, interactions between the electrons and the specimen produce different signals such as backscattered electrons(BSE), secondary electrons, X-rays, Auger electrons and cathodoluminescence that can all be used to form an image [56][57].

BSE have high energy that could provide information about composition and topography deep beneath the surface. [56]The SE signal gives a good topography of the specimen surface where the image appears with bright edges and dark empty spaces[55], [56]. In case the vacancy left by the SE is filled by an electron from higher energy orbital, X-rays of equivalent energy are emitted. This results in having characteristic x-rays that can provide chemical information of the specimen. Auger electrons have energy that is considered to be of a characteristic energy that allows the determination of chemical

composition. Last but not least, there are some materials that result in emitting excess energy in the form of photons when holes are filled by recombining of electrons and this is called cathodoluminescence [50] [51].

3.2. Brunauer Emmett-Teller (BET)

The BET theory is based on the Langmuir theory, which is a relationship between gas molecules that form a monolayer on a solid surface and the pressure of that gas on that surface. The Langmuir theory is based on a number of assumptions: (1) Ideal behavior of gaseous molecules; (2) Only one monolayer of gas molecules onto the solid sample surface; (3) All sites on the surface of the solid specimens are identical, meaning that they are all energetically favorable for the adsorbate (like the nitrogen gas); (4) There are no interactions between the adsorbent and the adsorbate; (5) the adsorbed molecule is immobile [58].

The Langmuir theory has some flaws that are addressed by the BET theory. The BET theory basically extends the former theory to multilayer adsorption with three more assumptions:

1. There is an infinite physical adsorption of gas molecules on the surface;
2. There is no interaction between the different layers;
3. The BET theory can be applied to each layer [59].

When a sample is analyzed using the BET method, five different adsorption isotherms could be produced (see Figure 3) [60].

Type I isotherm:

This type is similar to the Langmuir isotherm because it results from a monolayer adsorption. Materials with micropores with diameters that are less than 2 nanometers, result in this type because once these micropores are filled with adsorbate gaseous molecules, there is no longer external surface area to adsorb molecules upon. On the curve, there is an initial steep slope which shows the strong adsorption between the adsorbate and the adsorbent. Then, the plateau describes the area where there is no more adsorption. Type I (a) is due to microporous materials with micropores in pores in the size < 1nm, while Type I (b) is due to materials with larger range of micropores and possibly narrow mesopores (< 2.5 nm). The steeper the B region, the quicker the monolayer completion takes place.

Type II isotherm*:*

This type is different from the Langmuir isotherm. This type is the most widely produced isotherm when using the BET technique. For materials with diameters exceeding micropores, the pores are filled with nitrogen gas at the low pressures. Monolayer formation then begins to take place where there is a rounded knee at the beginning of the curve, while the formation of multilayer appears at medium pressures The absence of hysteresis in this curve denotes that there is adsorption and desorption from non-porous surface.

Type III isotherm:

This type shows the formation of multilayer and no monolayer is formed. BET, therefore, cannot be applied. This type occurs because the interaction between the different layers is

greater than the interaction between the adsorbate and the surface of the adsorbent. The absence of point B is the indication of no monolayer formation.

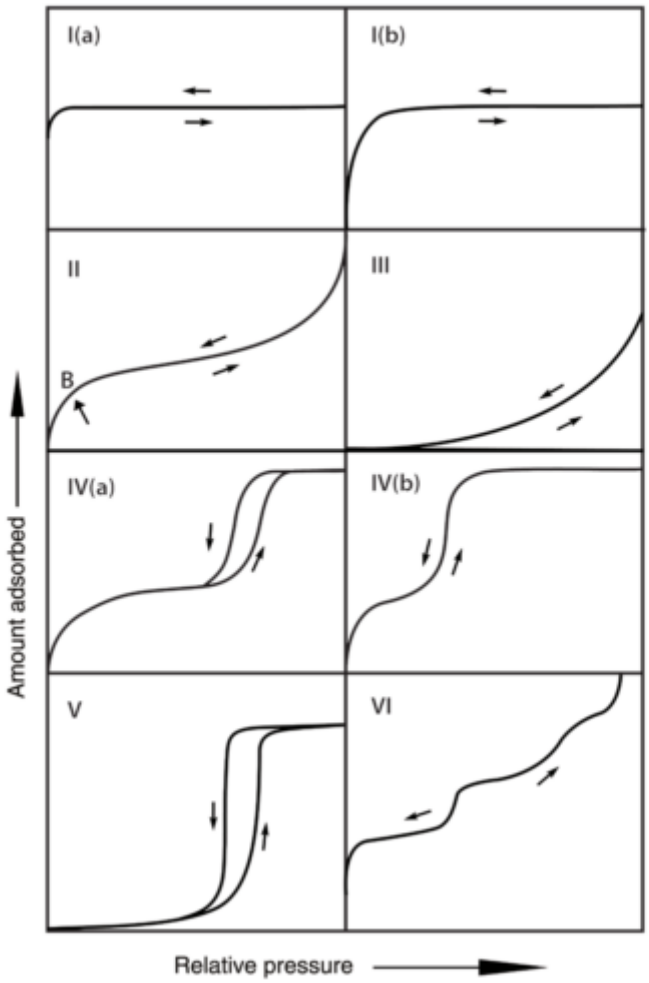

Figure 3 Isotherm types[60]

Type IV isotherm:

This type occurs mainly because of capillary condensation. Gases tend to condense in the pores of the examined solid at pressures that are lower than the saturation pressure of the adsorbate gas. Monolayer formation occurs at low pressures followed by multiple layer formation. Mesoporous materials (2-50 nm) result in this type of isotherm. A typical feature of this isotherm is a saturation final plateau. Type IV (a) is accompanied by hysteresis for materials with pore widths > 4 nm. The hysteresis is dependent on the adsorption system

and the temperature of the adsorbate gas. Type IV (b), on the other hand, are obtained with materials having conical and cylindrical pores.

Type V isotherm:

This isotherm results from the greater interaction between the layers than those of the adsorbate and the adsorbent, like in type III isotherm. This occurs usually in materials with pore diameter between 1.5 to 100 nm. On the curve the lack of knee represents extremely weak interaction between the adsorbate and the adsorbent. This type is commonly observed for water adsorption, and hydrophobic mesoporous and macroporous adsorbents.

Type VI isotherm:

This type represents layer by layer adsorption on the surface of a uniform nonporous material. The height of each step in the curve is a representative of the capacity of each adsorbed layer, while how steepness of the step is dependent on the temperature and the adsorption system.

*The produced hysteresis loops, on the other hand, are classified into four types (*Figure 4) *[*[60]*]:*

H1 loop: This one has a vertical and parallel adsorption and desorption isotherms. This one is famous with adsorbents that tend to have uniform and small range of distribution of pores.

H2 loop: This loop seems to have a broad loop since it has slow adsorption mechanism and quick desorption. It is found with porous materials that possess networks of interconnected pores with variety of pore sizes and shapes. H2 (a) is observed with

materials like porous glasses, silica gel and ordered mesoporous materials. While H2 (b) is observed with materials like mesocellular silica foams.

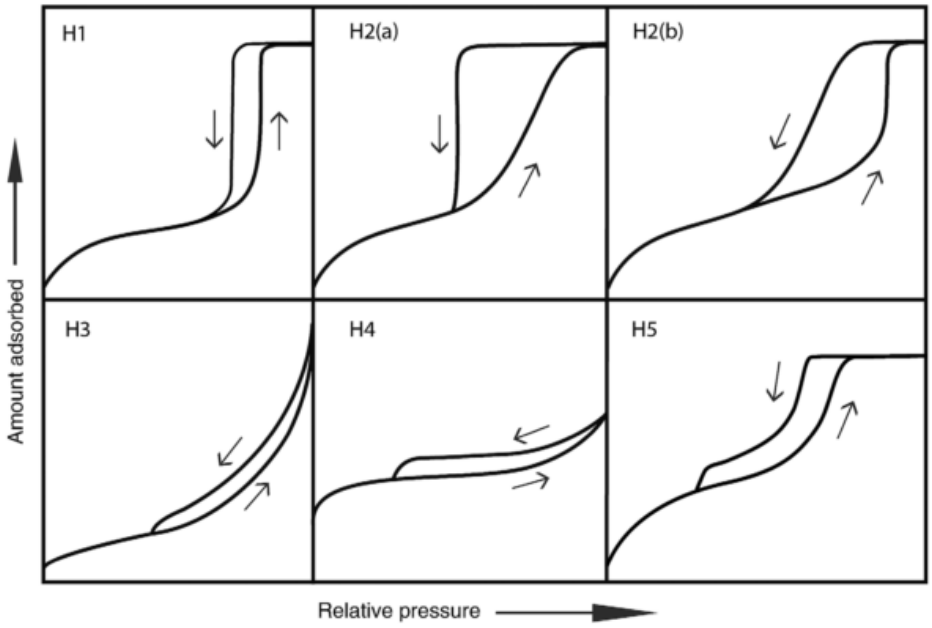

Figure 4 Types of hysteresis loops [60]

H3 loop: The curve does not terminate in a plateau at large pressure values which results in having a limited desorption boundary curve that is not easy to determine. This loop is mostly defined with structures solid materials that have aggregates with particles or solids having slit shaped pores.

H4 loop: This is the same as the H3 loop; it doesn't terminate in a plateau. It is associated with solids like meso-microporous carbons, and mesoporous zeolites.

H5 loop: This type is unusual. It is often associated with certain structures of pores that are both open and partly blocked. An example of this type is plugged hexagonal template silicas.

The phenomena of physical adsorption of a gas on the surface area of a solid can be used to determine the surface area of that solid. This is achieved by calculating the volume of the adsorbate gas forming a monolayer on the surface. Physical adsorption occurs as a result of the relatively weak van der Waals forces between the adsorbate gas molecules and the adsorbent surface area of the examined solid [61].

The Brunauer-Emmett-Teller method is derived to measure the surface area from physisoroption isotherm data. The BET equation gives the volume of the gas needed to form a monolayer on the sample surface:

$$\frac{p}{n_a(p_0 - p)} = \frac{1}{n_m C} + \frac{(C-1)}{n_m C} \cdot \frac{p}{p_0} \qquad (1)$$

where:

$\mathbf{n_a}$: the amount of the gas adsorbed at relative pressure p/p_0

$\mathbf{n_m}$: the monolayer capacity

C: a constant that depends on the isotherm shape

p: partial vapour pressure of adsorbate gas at equilibrium with the surface at 77K.

$\mathbf{p_0}$: saturation pressure of the adsorptive at a given temperature

From the equation, a linear relation is obtained if $p/n_a(p_o-p)$ is plotted against $\mathbf{p/p_o}$, where $\mathbf{n_m}$ is obtained. However, the linearity of the plot is only limited to the part of the isotherm that is not beyond $p/p_o \approx 0.3$[59].

The slope (**(C − 1)/n_mC)** and y intercept (**1/n_mC**) are obtained. Once n_m is obtained, the specific surface area (**S_t**) is calculated using the following equation:

$$S_t = n_m .L. a_m \qquad (2)$$

where:

L is Avogadro's number

a_m is the adsorbate cross sectional area which is equal to 0.162 nm^2 for adsorbed nitrogen molecule.[59]

3.3 Hg Porosimetry

Mercury porosimetry is one of the widely used techniques for the characterization of porous materials. Materials with pores between 500 μm and 3.5 nm are more suitable to be investigated by mercury porosimetry [62], [63]. Usually the analysis time of mercury porosimetry is shorter (around half an hour) than that by gas adsorption (which could take more than 12 hours). It can provide information like the pore size distribution, porosity (the total pore volume), density and specific surface area of the sample.

The concept behind mercury porosimetry measurement lies in the measurement of the volume intruded by mercury, a non-wetting liquid, into a porous material as a function of the applied pressure [63], [64]. Mercury will therefore not penetrate the pores of the sample by capillary action [62]. The liquid has a high surface tension. To resist the surface tension, an external pressure is applied to overcome this resistance of mercury penetration into the pores.

Washburn equation governs the relationship between the external pressure and pore size, by assuming the cylindrical shape of the pores.

$$p = -\frac{2\gamma cos\theta}{r} \quad (3)$$

where p is the absolute applied pressure, γ is the surface tension of mercury (which is approximately 0.48N/m) **r** is the radius of the capillary and θ contact angle of mercury[62], [65]

In order to determine the pore volume or the the pore size distribution of a sample, the sample must first be evacuated to remove air and contaminants from the pores. Mercury is then injected gradually increasing pressure. At each pressure value, a corresponding volume of the injected mercury is recorded[62]. Two types of measurements are carried out:

1. *Low pressure measurment*

Mercury is entered first onto the sample at low pressure. The pressure is then increased using air or nitrogen. This allows the mercury first to penetrate the empty spaces between the sample particles as well as the largest pores of the sample. The first readings are usally taken around 0.5 psi. The pressue is then increased until it reaches the maximum required presssure and an intrusion curve is produced. Extrusion curves can also be obtained when decreasing the pressure gradually and the mercury is withdrawn from the sample.

2. *High pressure measurment*

This follows low pressure measurements, and entails presurizing the mercury to higher pressure values using a hydraulic fluid. This allows the mercury to intrude into the smaller

pores of the sample. Extrusion curves can also be obtained when decreasing the pressure gradually and the mercury is withdrawn from the sample [64]

3.4 Contact Angle Measurement

Contact angle measurement is crucial to determine the wettability of surfaces resulting from the interaction between a solid and a liquid. Wettability is usually measured by the contact angle established between a solid surface and a liquid drop [66]. Contact angles which are less than 90^{o} indicate high wettability, while those larger than 90^{o} indicate low wettability [67].

As a liquid resides on a surface of a solid (Figure 5), a contact angle is formed. By definition, the contact angle is the intersection of liquid-solid interface and the liquid vapor interface. This constitutes the tangent line that originates from the point of contact along the liquid vapor interface in the profile of the droplet. Figure 5 indicates that a liquid spreads out on the solid surface when the contact angle is small, while it appears that when the liquid is barely touching the surface of the solid, the contact angle is large. [67], [68].

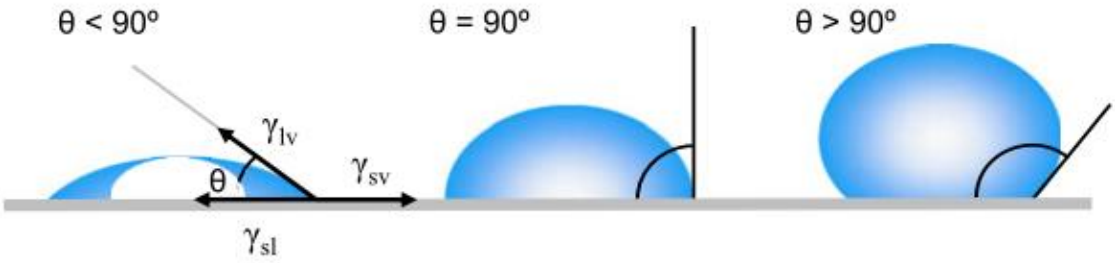

Figure 5 Illustration of the contact angle formed between a liquid and a homogenous solid surface[67]

Moreover, the liquid droplet's shape is determined by the surface tension of the liquid. In the case of a pure liquid, each molecule in the bulk of a liquid is pulled out by equal forces from all the adjacent molecules in every direction having a net force of zero (Figure 6). However, those at the surface of the liquid are pulled inward by the adjacent molecules, resulting in an internal pressure. This in turn makes the liquid contracts to allow for the least surface energy. The intramolecular force that makes the surface contract is called the surface tension, and it is the reason behind the shape of the droplet formed. Gravity forces also play a role in the shape of the liquid droplet, thus the contact angle is measurement of both the surface tension and external forces like gravity. Consequently, a contact angle is theoretically considered to be a characteristic for a given liquid-solid system in a certain environment [67], [69].

Figure 6 An illustration of the unbalanced forces at the surface of the liquid that causes surface tension[67]

According to Thomas Young, a contact angel (θ) of a liquid droplet on a homogenous solid surface is defined as the mechanical equilibrium between the three interfacial tensions: the liquid-vapor (γlv), the solid vapor (γsv) and the solid liquid (γsl) [67].

$$\gamma lv \cos \theta = \gamma sv - \gamma s \quad (4)$$

3.5 Ultra-Violet Spectroscopy

Spectroscopy techniques in general entails the interaction of light with matter which gives an indication of its structure or concentration [70]. The technique is widely used to quantitatively determine amounts of inorganic, organic and biological molecules[71].

UV radiation is involved with electronic transitions, because it has enough energy to excite valence electrons in many atoms or molecules. Technically, visible light acts in a similar way to the UV light so it is considered part of the electronic transition region.

Consequently, commercial UV/Vis spectrophotometer operates with wavelengths between 200 nm- 800 nm. [72]

When a molecule absorbs ultraviolet radiation of a certain frequency, a transition occurs to an electron from a lower energy level to a higher energy level. This energy difference is given by the equation:

$$\boldsymbol{E = hv} \qquad (5)$$

where E is the energy of the photon, and it is equal to the difference between the ground state E_0 and the excited state E_1, h is Planck's constant (h=6.64× 10^{-34}Joules.seconds) and v is the frequency of the radiation. Vibrational, transitional and rotational energies make up for the total energy f or a molecule.

Exposing a compound to electromagnetic radiation does not necessarily result in electronic transitions. There are two types of transitions: allowed and forbidden. Electronic transitions are limited by some restrictions. Transitions that involve a change of a spin quantum number, an excitation of a number of electrons at the same time, a change of a symmetry in the molecule or the electron state itself can result in the transitions not occurring, i.e. forbidden transitions. These transitions are usually not observed, and might have weak intensities. However, transitions that are allowed have higher intensities of absorption [70].

In general, the greater the number of molecules absorbing light at a certain wavelength, the greater the absorption that occurs. The concentration of a species,

therefore, can be determined by the amount of light it absorbs at the specific wavelength, according to Beer-Lambert Law:

$$\boldsymbol{A} = (\mathbf{log}\, \boldsymbol{I}_{\circ}/\boldsymbol{I}) = \varepsilon \mathrm{c}\boldsymbol{l} \quad \text{for a given wavelength} \qquad (6)$$

where **A** is the absorbance that is equal to $\log I_{\circ}/I$, I being the intensity of the incident light, I is the intensity of the transmitted light, Ɛ is the molar absorptivity, **c** is the concentration of the solute and **l** is the sample cell length. The molar absorptivity is a function of the molecule going through electronic excitation and its maximum value determine whether the transition type is allowed or forbidden. Values that are more than 104 have absorption of high intensity and they are allowed transitions, while values that are below 103 have absorption of low intensities and they are forbidden ones [73] .

3.6 Densification of Carbon Nanotubes

In order to test for the change of variables of preparing the BPs to see the effect of that on the porosity, a mechanism based on solvent evaporation is adopted. Recent studies have shown that solvent infiltration of carbon nanotubes can lead to the densification of the bundles. The concept is based on a capillary condensation phenomenon.

Volder M. et al.[74] investigated the condensation of CNTs using vapours. This is achieved by the evaporation of a boiling solvent, such as acetone. The vapor of the solvent rises up and condenses on the substrate with the CNTs. Due to capillary rise, the solvent is drawn into each CNT microstructure individually. It was reported that solvent withdrawal can result in densifying adjacent CNTs individually by capillary forces where van der Waals forces become stronger. After the exposure to the vapor of the boiling solvent, the substrate is removed to let the solvent evaporate from the substrate in room temperature.

Carbon Nanotube forests were densified through solvent infiltration and evaporation process.

Additionally, recent studies had suggested solvent infiltration within CNT macro-bundles can lead to high density and aligned CNT. According to Dumee et al. solvent withdrawal leads to adjacent CNTs to densify under the influence of capillary forces, thus enhancing the van der Waals potential and leading to localized high density regions within structured materials. Figure 7 below shows the mechanism behind the CNTs densification. In this figure, CNT forests were immersed in either pure solvent or mixed solvents, in order to avoid the solvent front advancing through the forest fast which would have resulted in densifying the aligned arrays as shown [23].

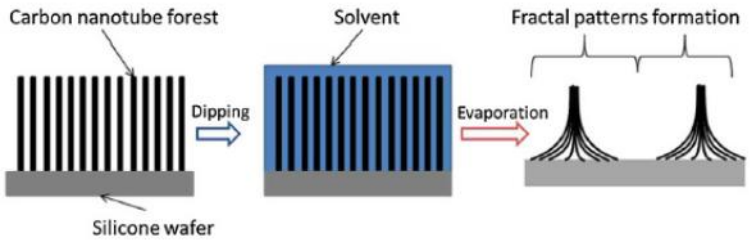

Figure 7 Densification procedure of CNTs by Dumee et al. [23]

It is thus important to note that the densification concept tackled by these two groups was used in this work differently, since the randomly oriented CNTs arrangement is different from the arrangement of the CNTs forest. In this work, the concept was introduced to see if exposure to boiling solvents would in general lead to a change of porosity of the BPs examined, and if this change of porosity would result in the creation of smaller pores.

Chapter 4

Material and Methods

CHAPTER FOUR: MATERIALS AND METHODS

4.1 Materials

All MWCNTs in this work are Elicarb produced by Thomas Swan (England) with a diameter of 10-12 nm, tens of microns in length and a density of 1.7-1.9 g/cm^3. Triton X-100 (Trix;*Sigma Aldrich*) was used as a dispersant. Deionized (DI) water was used from Millipore- Q as a solvent. Acetone (*Sigma Aldrich*), Isopropanol (IPA; *Aldrich*), Dimethylforamide (DMF; *Sigma Adlrich*) and Tetrahydrofuran (THF; *Carlo Erba*) were used as boiling solvents for densifying the CNT buckypaper. Also, filter membrane with different pore sizes were purchased from *Whattman* (0.2, 0.45, 1, 10 µm).

4.2 Preparation of Buckypaper (BP)

4.2.1 Preparation of CNT solution

Weighing Step: The CNT powder was weighed in an Aluminium weighing dish. 25mg of Carbon Nanotubes (CNTs) were placed into 800 ml of DI water in different beakers with 28ml of surfactant Triton X 100 (Trix). The quantity was divided into four equal beakers. Each beaker took 6.25 mg (DI) [17] [22][51].

Sonication Step: The powder is then mixed with DI as a solvent, and Triton X-100 (Trix) as a surfactant. The mixing, however, happened in multiple steps. First, 200 ml of water is put into 500 ml beaker and sonicated for five minutes to allow for the water molecules to be dispersed and ready to receive the surfactant that would be added. Then, a surfactant of 7 ml is added dropwise to the water while it was being sonicated, and then left for 15

minutes. This allowed the surfactant to disperse within the water molecules and to be ready to receive the CNT powder. Since the CNTs are mixed with IPA and DI water, this mixture was added dropwise to the solution being sonicated. After that, the whole mixture (DI+Trix+CNTs) was to be sonicated for 15 minutes to allow for the CNTs to disperse and not aggregate[24]. The sonicator water bath temperature was set at 30^0C.

4.2.2 Preparation of BPs

Filtration Step: After sonication is complete, the solution was filtered. A typical vaccum filtration system was used as illustrated in Figure 8. The reservoir is where the CNT solution is poured and then filtered. The reservoir is connected to the support base using a clamp. The support base is used to accommodate a filter membrane through which the solution was filtered and on which the BP is formed. The support base is connected to a suction pump. The filtration of the solution which is approximately 800 mL (4 times of the 200 ml), took around 24 hours.

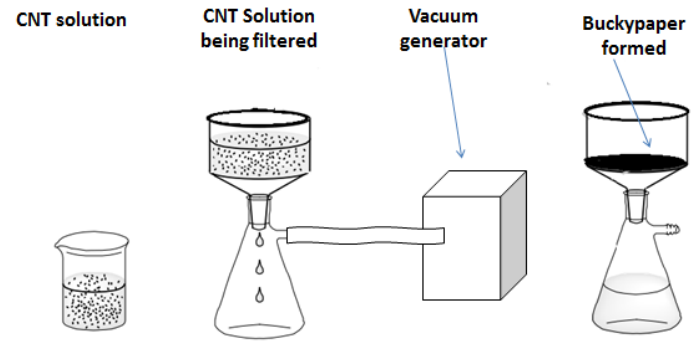

Figure 8 vacuum filtration system used

Drying: After the filtration was complete, a BP is formed on top of the filter membrane. In order to facilitate the peeling of the BP from the membrane, it is allowed to dry overnight at room temperature[75].

Peeling: The BP is carefully peeled off the filter membrane using tweezers.

Washing: Since surfactant TRIX 100 is used, the washing step of the BP was critical and is done in multiple of steps. The BP was first washed in 50 ml of DI water for two hours, then in 50 ml of IPA solution for five hours, then in 50 ml of DI water again for two hours. The BP was then left to dry overnight[47][46].

4.2.3 Notes on Preparation

After filtration the BP obtained was attached to the membrane filter it was filtered on (in this case, Nylon membrane with a pore size of 0.45 µm). In order to separate the BP from the filter membrane, different drying conditions were investigated. Changing drying conditions by heating at certain temperatures 80˚C or 300˚C or drying at room temperature for different durations of time, did not facilitate the peeling process. The use of new membrane filters (Teflon membranes with also 0.45 µm pore size) was suggested. This resulted in having the BP peeled off completely from the filter membrane (Figure 9).

Figure 9 First BP to be peeled off completely

4.3 Changing the parameters of preparation

In order to see what variables affect the porosity of the BP, certain parameters were chosen to be changed. Pore size of the membrane filter, the type of the solvent used for evaporation, the time duration during which the membrane will be exposed to this boiling solvent.

I. Type of boiling Solvent

It was decided for the work presented here to investigate the use of the same concept of densification of CNTs forest introduced in chapter 3 to evaluate whether or not it will be effective in drawing together randomly aligned CNT bundles (BPs) by strengthening the van der Waal forces, and thus creating closer arrangements of the CNTs, leading to potentially smaller pores in the BP. According to this, BPs were exposed to the vapors of different boiling solvents. Basically, after the BP was exposed to the vapor flow for the specified duration, the BP was removed and left in ambient conditions for the solvent to evaporate. Later, other solvents than acetone were used to test for the effect of different boiling solvents on the arrangement of CNTs.

Four different boiling solvents were used.

a. Acetone

b. IPA

c. THF

d. DMF

II. Exposure of BPs to boiling solvents

150 ml of the solvent was poured into a beaker and boiled using a hot plate. The beaker with the solvent was covered with a wire mesh on which the BP was placed. A beaker with a similar size was placed on top of the bottom one, right above the wire mesh to ensure the passage of the vapor to the membrane (Figure 10).

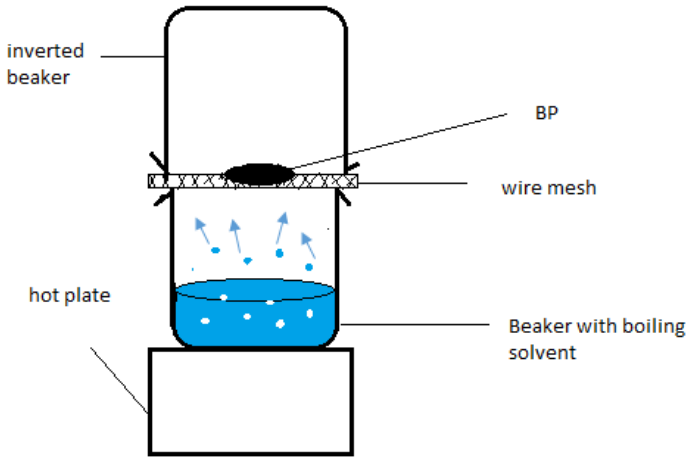

Figure 10 Schematic of the setup used to expose the BP to boiling solvent

III. Exposure time of boiling solvent

The time of exposure varied between 5 and 40 minutes when acetone was used, by an increment of 5 minutes every time. Thus, an exposure time of the BPs to the acetone vapor was 5, 10, 15, 20, 25, 30, 35, and 40 minutes. Nitrogen adsorption at 77 K using the BET method and Hg porosimetry analysis were carried out starting with prepared samples exposed to 20 minutes.

IV. Filter membrane

The BP was filtered at the beginning on a Nylon membrane of 0.45 µm. When the peeling problem persisted, PTFE filter membranes of different pore sizes were tested.

Four different pore size filter membranes were tested.

a. PTFE membrane filter of pore size 0.20 µm.
b. PTFE membrane filter of pore size 0.45 µm
c. PTFE membrane filter of pore size 1 µm
d. PTFE membrane filter of pore size 10 µm

V. Statistical Analysis

The studied variables were analyzed through experimental design and statistical analysis. The objective of this analysis is to learn the variables that have the most influence on the response of interest, and in this case they are the average pore width and

the BET surface area. This is done by changing the three variables discussed earlier (exposure time of acetone, type of boiling solvent, and pore size of filter membrane) at the same time. In other words, each trial will have a combination of a change of the three variables.

Table 1 below shows how the design of experiment was conducted. Three factors were chosen to be tested and only the highest and the lowest values of the variables were tested.

a. Factor one (Pore size of the filter membrane): The highest value is 10 µm and the lowest is 0.2 µm
b. Factor two (Type of boiling solvent): The highest value is acetone because it has the highest vapor pressure and the lowest is DMF because it has the lowest vapor pressure.
c. Factor three (Exposure time to the boiling solvent: The highest value is 40 minutes and the lowest is 5 minutes.

Table 1 Design of Experiment table showing the three tested variables.

		Factor Three Exposure to Acetone			
		L		**H**	
		Factor Two (Type of boiling solvent)			
		L	**H**	**L**	**H**
Factor One (Pore size of filter membrane)	**L**	Trial #1	Trial #3	Trial #5	Trial #7
	H	Trial #2	Trial #4	Trial #6	Trial #8

Each run, then, would have different combinations of low and high values of the three factors. The experimental design, including 3 factors and two levels, was adopted to study the process. The resulting design was 2^3 factorial design, representing 3 two level factors. Thus, a total of -8 (2^3) experimental runs were conducted. Each trial has a result of an average of three samples done in the lab.

The statistical analysis is then carried out using the software package Design expert 10.0 developed by stat-ease. Also, analyses of variance (ANOVA) was used. The software basically generates the order of the runs (experiments) to be carried out in the lab. After obtaining the results of the average pore width and the BET surface area from examining the BPs using the BET instrument, their values are entered for each respective run. The analysis is then carried out to measure if the model is adequate or not by examining the p-value. In addition to that, the software also checks if the model satisfies normality assumption, non-constant variance, and independence assumption (refer to appendix). The software then tells you if the model is significant; meaning that the variables tested have any significance on the responses or not.

4.4 Filtration of Polystyrene beads:

A solution of polystyrene beads of 10 ml was filtered on the BPs to measure for the retention percentage of the BPs for these beads. Two BPs were tested in this application: one is a blank BP (a BP with no modification at all) and a modified BP which is modified based on the results of the statistical model. Two types of the polystyrene solutions were tested, one with 0.3 µm PS and the other one with 0.6µm. For each BP, a number of three

trials were measured for each type of the solution. The concentration of the feed solution was prepared with a concentration of 0.15 mg/ml for both the 0.3 µm and the 0.6µm solution. After the solution is filtered through the respective BPs, the concentration of the permeate solution is measured. The retention percentage is then measured by the following equation

$$Retention\ Percentage = \frac{\text{Conc. of feed solution} - \text{Conc. of permeate solution}}{\text{Conc. of feed solution}} \times 100\% \quad (7)$$

An average of the retention percentage for the three trials is then considered to compare results between the blank BP and the modified for the two solutions of PS. A standard deviation is then calculated to account for the error bars.

4.5 Characterization of BP

4.5.1 Scanning Electron Microscopy

Scanning Electron Microscopy was used to investigate the morphology of the BPs. The SEM used was a Leo Zeiss supra 55 field emission scanning electron microscope (FESEM). Both the surface of the BP as well as its cross section were imaged. Cross sections of the BP were prepared by snapping with tweezers after freezing in liquid nitrogen. The magnifications used to image the samples were 700X, 15,000X, 20,000X, 50,000X, and 100,000X. The working distance (WD) used was 4.00mm, and Extra High tension (EHT) of 8.00 kV using the in lens detector.

4.5.2 Brunauer–Emmett–Teller (BET) Instrument

The instrument used is a Micrometrics ASAP 2020. BPs were cut into small pieces (~ 3×3 mm) and inserted in the instrument's sample container. A single test used three BP samples, to ensure enough sample weight in order to reduce the percentage error in measurements. The degassing of the sample took around 7 hours at a temperature of 30℃.

4.5.3 Mercury Porosimetry

The instrument used is a Quantachrome PoreMaster Mercury Porosimeter. The cut BPs used in the BET method was used again and inserted in the instrument sample container. Low pressure mode was chosen to be the only mode to work with, since several samples were tried to be tested at the beginning with high pressure mode that resulted in no significant peaks to analyze.

4.5.4 Contact Angle

The contact angle equipment used is Kruss Drop Shape Analyzer (DSA25). For each BP sample, the contact angle was measured three times and the average value used.

4.5.5 Filtration Setup of the PS solution

A filtration setup was designed to use as shown in Figure 11 below. The setup consisted of a burette that holds the permeate solution (10 ml) of the polystyrene beads that was adjusted for the rate of a drop every 16 seconds, while it passed through the BP which was centered on the sintered glass. The BP's diameter (3.4 cm) is larger than the diameter of the sintered glass of 2 cm, and this ensured that no leakage of the permeate solution occurred around the BP. The filtration was facilitated through the vacuum created by the pump attached to the conical flask holding the sintered glass.

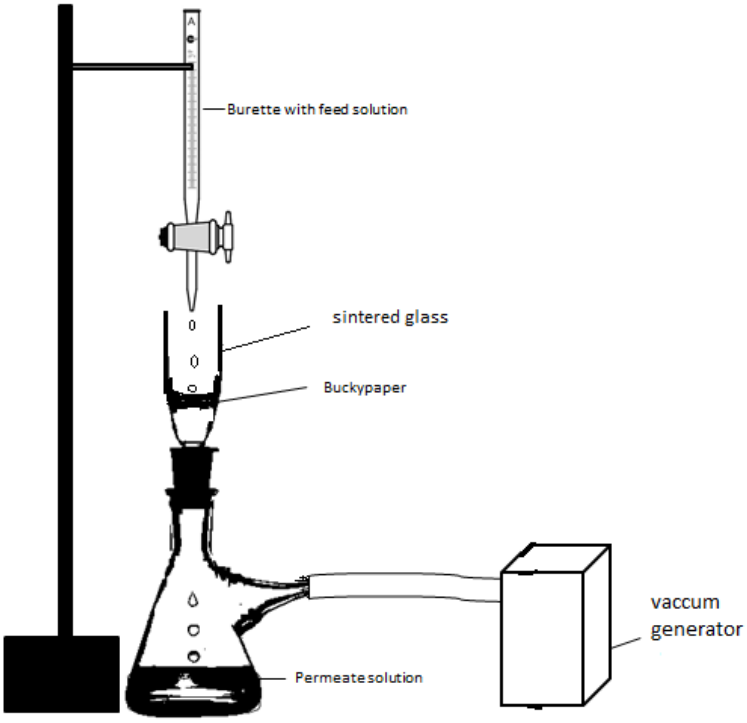

Figure 11 Filtration Setup used for the filtration of polystyrene beads

4.5.6 UV –Vis Spectrophotometer

Concentrations of the polystyrene beads were measured using a Jenway UV-Vis 6800 double-beam spectrophotometer. The absorbance of the polystyrene beads in the filtrate and permeate solutions was measured at respective λ_{max} values and using previously-plotted calibration curves (appendix), the concentrations were determined.

Chapter 5

Results and Discussion

CHAPTER FIVE: RESULTS AND DISCUSSION

All BPs prepared for the analysis were prepared using the same procedure explained in the previous chapter. In comparison to the literature where it was reported that a proper time to sonicate MWNCTs using the surfactant Triton X-100 is 30 minutes [17], the CNTs in this work were sonicated for 15 minutes only since longer sonication times were recently found to produce membranes with greater pore volumes [20].

5.1 Filtration on Membrane Filter

5.1.1 Nylon Membrane Filter

The filtration of the CNT suspension was first carried out onto a nylon filter membrane of a pore size of 0.45 µm. The filtration procedure was done smoothly except for the part when the BP needed to be peeled off from the Nylon membrane filter. The BP adhered to the nylon membrane, so it was hard to separate the two from each other and some parts of the BP were stuck to the Nylon filter membrane. Figure 12 represents an SEM image of the Nylon filter membrane (upper part) adhering to the BP (bottom part).

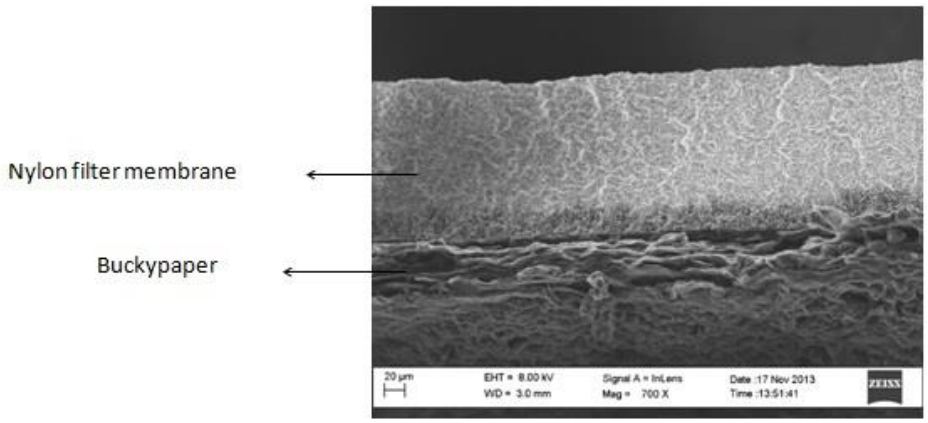

Figure 12 SEM image of the BP adhering to Nylon Membrane Filter. Top part (Nylon Filter) Bottom part (buckypaper) of magnification of 700 X.

Different drying conditions were used to facilitate the peeling process. The nylon membrane along with the BP adhering to it, were exposed to different oven temperatures to see if this would facilitate the peeling process. They were, first, exposed to 80^0 for two hours, then for 12 hours, and then they were left for 24 hours. None of these trials helped in the peeling. On a different trial, the membrane was exposed to 300 ^{0} C for up to 24 hours. All trials failed to facilitate the peeling.

An SEM image (Figure 13) was taken at a higher magnification than (Figure 12) after the 300 ^{0}C treatment in attempt to understand the interaction that is present between the Nylon membrane and BP more. It is clear that the CNT network is somewhat entangled with the lamellar crystals of the nylon filter".

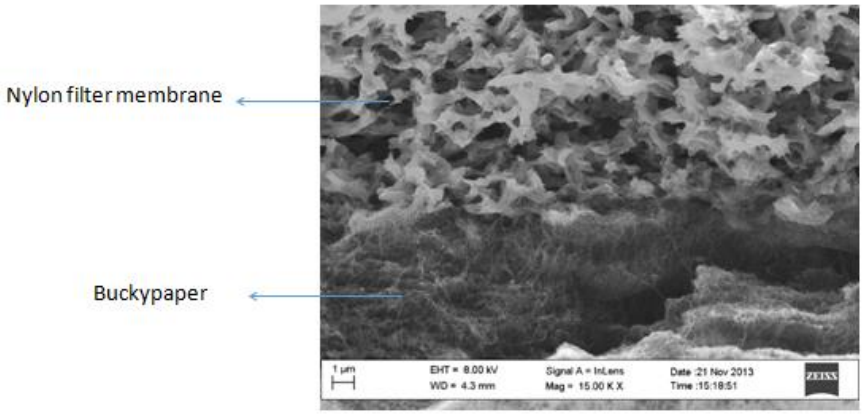

Figure 13 Nylon Filter still adhering to BP after heat treatment of 300^{0}C. Top part (Nylon Filter), Bottom Part (Buckypaper) of magnification of 15,000X

5.1.2 Polytetrafluorethylene (PTFE) membrane filter

By going back to the literature, an overview of the use of different membrane filters used in the preparation of BPs was investigated. The most commonly used one was found to be polytetrafluoroethylene (PTFE) membrane filter [20], [22][27]. Upon trying a PTFE membrane with the same pore size as Nylon (0.45 µm), the peeling process was carried out smoothly (Figure 14).

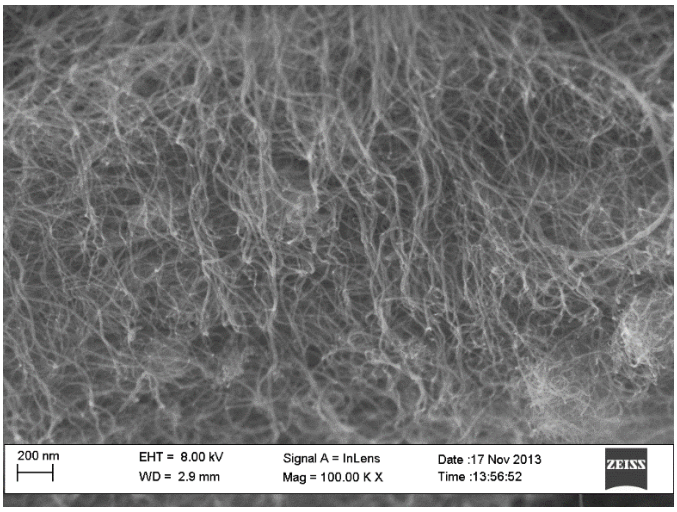

Figure 14 SEM image of buckypaper successfully peeled off from the PTFE membrane filter of magnification of 100,000 X

In order to investigate the differences between the Nylon and the PTFE membrane filters, , an analysis on the contact surface on both membranes was carried out using the drop contact analyzer. By measuring the contact angle of the surface on the Nylon membrane and on the PTFE membrane, the angles turned out to be 48°(Figure 15) and ~

88° (Figure 16), respectively. This means that the PTFE has more hydrophobicity than Nylon, which made it easier to detach from the BP.

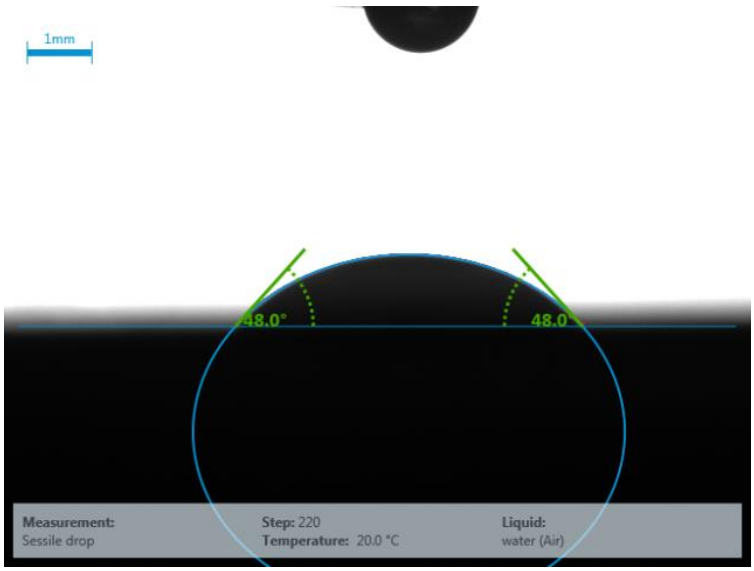

Figure 15 Contact angle of the Nylon filter membrane

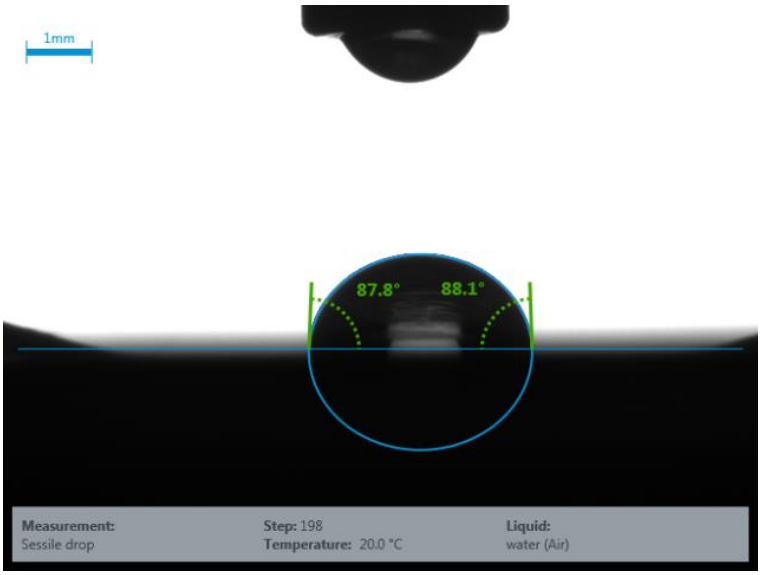

Figure 16 Contact Angle of the PTFE filter membrane

5.2 Exposing Buckypaper to Acetone Vapor

5.2.1SEM imaging

At the beginning, only SEM imaging was used to see if the arrangement of the CNTs would change if the acetone vapor exposure time increases from 5 minutes to 25 minutes with an increment of 5 minutes (Figure 17 (a-f)). The SEM images were found to show number of similarities to each other and to that of the blank BP sample that was not exposed to any acetone vapor. In general, they all show a highly entangled mat of CNTs and some CNT aggregates, with relatively comparable dimensions.

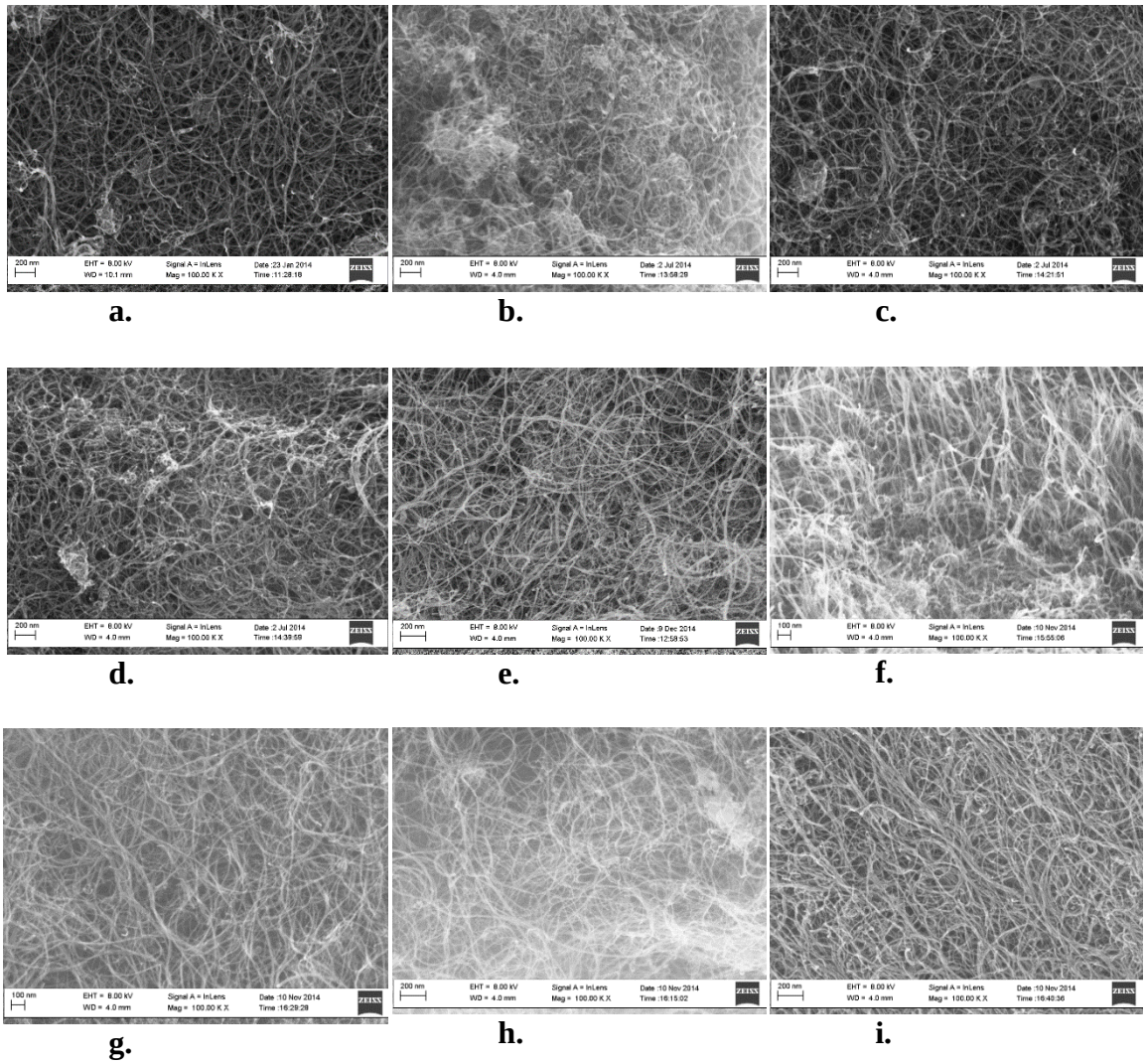

Figure 17 SEM imaging of different buckypapers exposed to acetone vapour. a. 0 mins (blank sample}, b. 5 minutes, c. 10 minutes, d. 15 minutes, e. 20 minutes, f. 25 minutes, g. 30 minutes, h. 35 minutes, i. 40 minutes

This shows that the surface morphologies of the BPs are somehow similar to each other, meaning that the time interval increase of the vapor exposure does not have much effect on the surface features of the membrane surface except for the sample exposed to 25 minutes of acetone (Figure 17 (f)) which shows some kind of alignment. According to Wang et al.[76], different degrees of densification could be controlled by the different

exposure times to solvent vapor. Shorter exposure times might lead to the densification of some parts and leave the other parts, while longer exposure timings can lead to the full densification of the CNTs exposed. The images obtained here indicate that within exposure times of 40 minutes, no significant change of surface features could be observed.

However, the one directional arrangement structure that appeared in the sample exposed to 25 minutes of acetone was further investigated. The arrangement was then confirmed by preparing three more samples and exposing them to 25 minutes of acetone. Two of the three samples showed a one directional arrangement structure of the CNTs (Figure 18). This confirmed the fact that acetone exposure can result in a change of the arrangement of CNTs, and it was thought that this might also be a factor in changing the porosity of the samples.

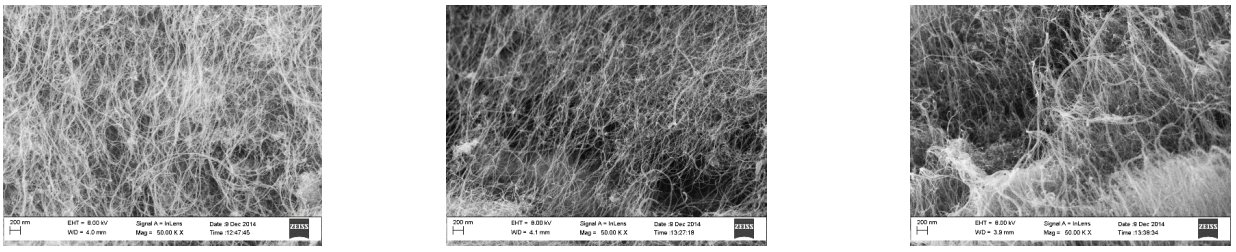

Figure 18 SEM cross section images of BP exposed to 25 minutes of Acetone Vapor

In general SEM images of BPs showed similar structure of BPs prepared by Triton-X 100 as a surfactant compared to other work in the literature [17], [22] (Figure 19).

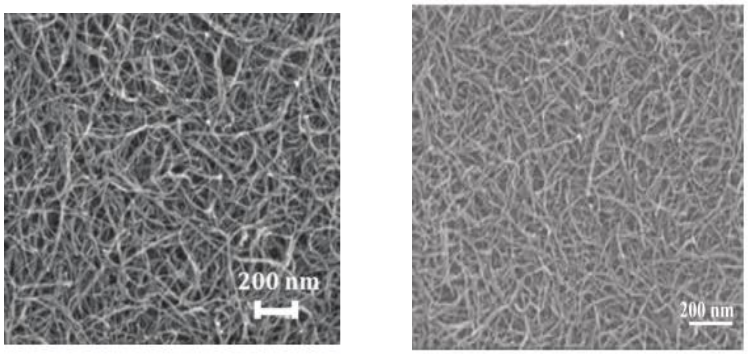

Figure 19 SEM images from previous work done, both BP prepared by Triton X 100 as a surfactant [17][22]

5.2.2 Hg Porosimetry

With mercury porosimetry, larger pores can be measured as compared to pores that are detected by the BET method. The determination range is 0.003 µm to 200 µm.

Pore Range (0-200 µm)

Exposure of sample to acetone vapor (5 minutes) vs. no exposure:

In order to investigate for the change in porosity when BPs were only exposed to 5 minutes of acetone in the beginning, a porosity investigation using Hg porosimetry was first carried out along with the SEM imaging discussed in the previous section. Figure 20 shows that there are distinct pore widths (>~4µm) at sizes between 4 µm and 15 µm and pores at distinctive sizes of 26, 53, 123 and 154 µm for both membranes. By looking at the figures below (Figure 20 and Figure 21), displaying the delta volume vs. pore width and the delta surface area vs. pore width, there are higher values for the pore widths less than 10 µm, relative to the larger pore widths >14 µm. This shows that there are

significant numbers of these smaller pores relative to the larger ones for both the acetone exposed BPs as well as the BPs with no exposure. An increase in surface area of all the pores means an increase in the number of pores, and so the average pore size decreases since the total pore volume is the same. Two features are important to note. In Figure 20, it is clear that exposure to acetone led to an overall decrease in average pore size for pores >14 µm. In addition, for pores smaller than 10 µm, the acetone exposed BPs exhibit a larger number of pores than BPs not exposed to acetone, as reflected in the value of delta surface area (Figure 21). Both observations demonstrate that the exposure to 5 minutes of acetone, even for as a short period as minutes, did in fact lead to the creation of more small pores, which could not be visually detected in the SEM images.

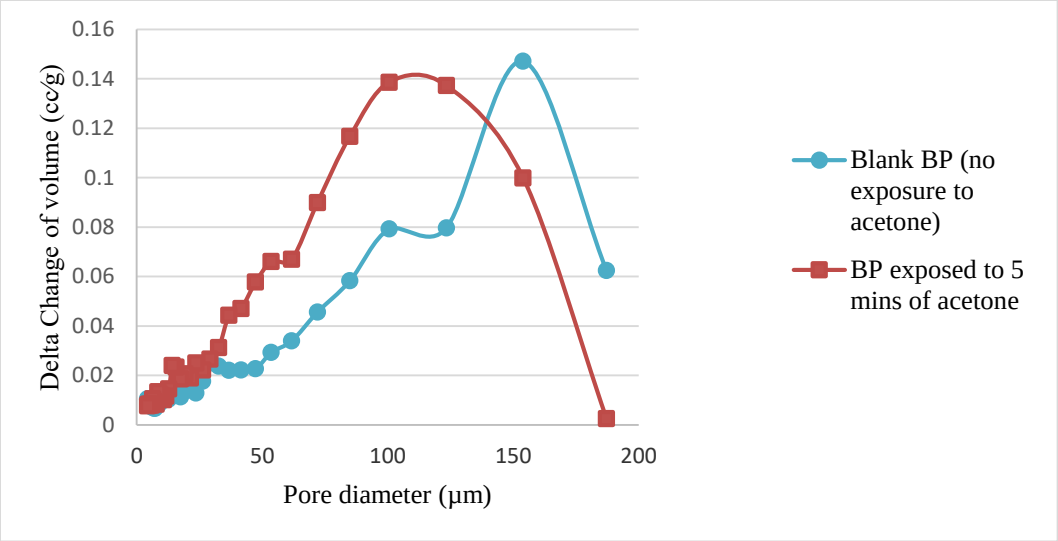

Figure 20 Delta volume intruded versus pore diameter comparison between a blank BP and a BP exposed to acetone for 5 minutes

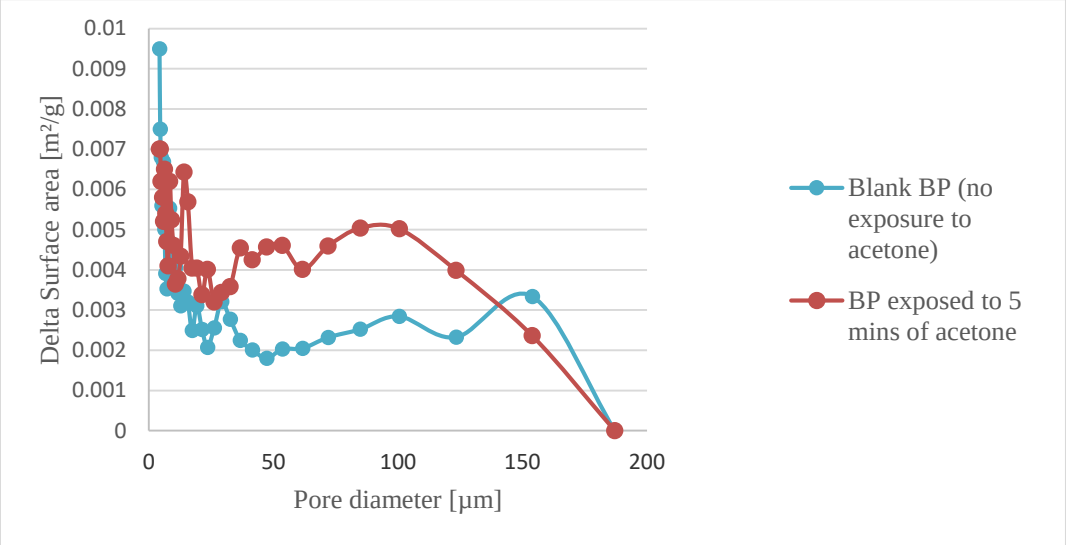

Figure 21 Delta surface area versus pore diameter comparison between a blank BP and a BP exposed to acetone for 5 minutes

Comparison of membranes exposed to 20, 25, 30, 35, 40 minutes of acetone:

Since a change was observed in the distribution of pores between the blank BP and the BP exposed to 5 minutes of acetone, a further investigation was carried out for the BP

samples exposed to acetone starting 20 minutes of acetone. Figure 22 and Figure 23 show the delta change of volume as a function of pore width and the delta surface area as a function of pore width, respectively for samples exposed to 20, 25, 30, 35, 40 minutes of acetone compared to the blank BP, which was not exposed to any acetone vapor at all. From these two figures, the blank BP showed the highest differential surface area at the distinct pore at 4.8 µm, exceeding all the other membranes. Other membranes showed less surface area than the blank for the pore diameter range < 20 µm. Since this sample did not get exposed to any acetone vapor, a possible explanation could be that an increase in porosity from the solvent vapor was evident in the other samples starting certain pore diameters larger than 30 µm. BPs that were exposed to 20 and 25 minutes of acetone, showed distinct pore diameters at 46.8 µm, 66.6 µm and 104 µm, while those exposed to 30 and 35 minutes of acetone showed distinct pore diameters at 129 µm.

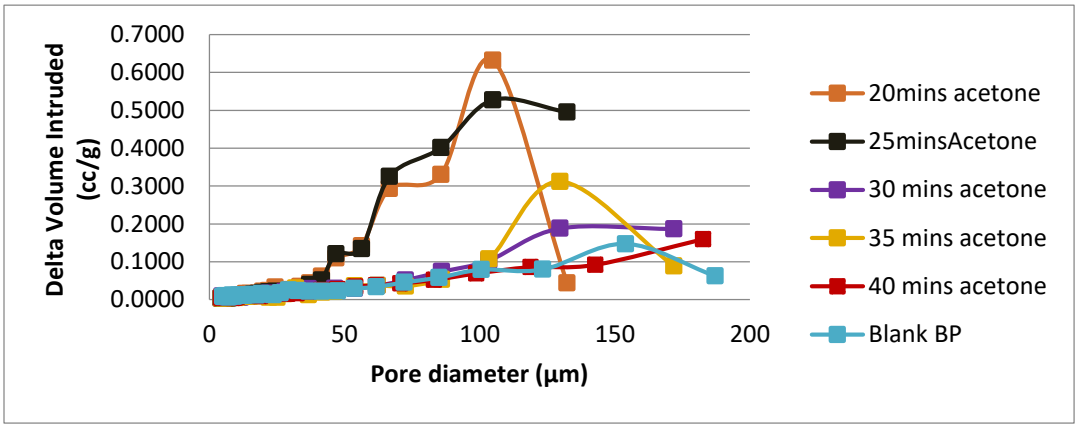

Figure 22 Change of volume versus pore width comparison between BPs exposed to different times of acetone vapor (0,20,25,30,35,40 mins of acetone)

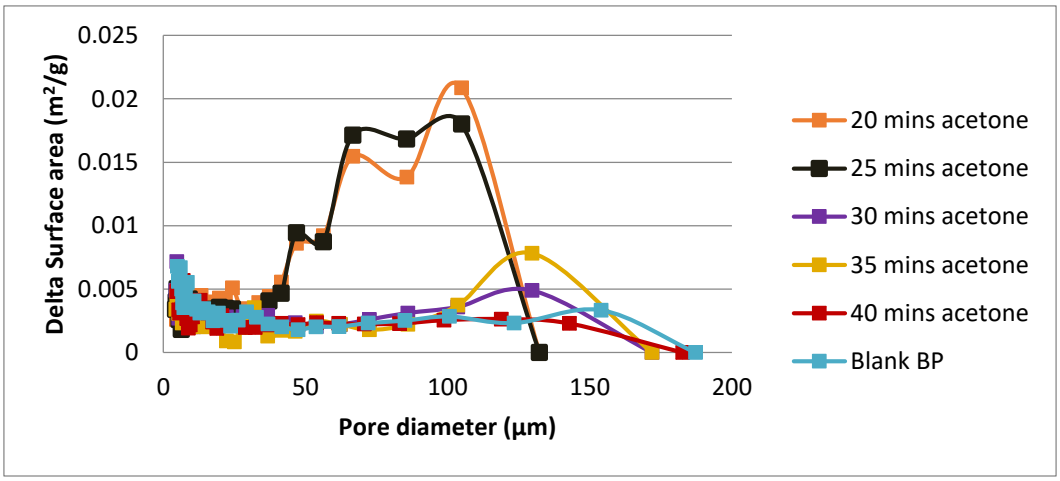

Figure 23 Differential surface area versus pore width comparison between BPs exposed to different times of Acetone vapor ((0,20,25,30,35,40 mins of acetone)

For samples that were exposed to 20 and 25 minutes of acetone vapor, a different behavior is observed from the blank and from those of the other BPs exposed to other timings of acetone vapor beyond pore width of 40 µm. A higher volume at these distinct pores (46.8 and 66.6, 104 µm) means that these pores consume the largest volume of all the other pores in the BP, while a higher surface area means that the number of these pores increased. This change of behavior with samples exposed to 20 and 25 minutes of acetone might be in line

with the change of surface features observed in samples exposed to 25 minutes of acetone which show a different pattern from the other BPs exposed to acetone. Other membranes exposed to 30, 35 and 40 minutes of acetone including the blank BP show comparable behavior and less amount of almost no distinct pores at these values. They both have comparable delta volume and delta surface area values as shown in Figure 22 and Figure 23.

Pore range (0-40 µm)

In order to have a better understanding at the pore distribution happening between 0 and 40 µm, Figure 24 and Figure 25 were constructed. Both Figures show the delta volume and delta surface area as a function of pore diameter, respectively. The different samples don't necessarily follow the same trend at the distinct pore sizes. Samples, in general, show distinct pore sizes at around these pore diameters 4.6, 5.9, 7.7, 10.7, 13.2, 19.2, 24.3, 31.8 µm. Two things are to be noticed from these two graphs. First, all samples show comparable delta volume to the blank sample, yet the blank has the highest delta surface of all for pore diameters between 0 and 20 µm. This means that the exposure to acetone resulted in wetting of the CNTs bundles pushing them towards each other, and so narrowing the pore diameters are in the small range between 0 and 20 µm. Second, the sample exposed to 25 minutes of acetone shows higher delta surface area at pore diameters of 24.3 µm. Also, sample exposed to 35 minutes of acetone show higher delta surface area at pore diameter 31.8 µm. Again, it can be inferred from these results that the longer the

exposure to acetone vapor for certain durations like the 20, 25, 35 minutes of acetone results in creation of higher pore diameters.

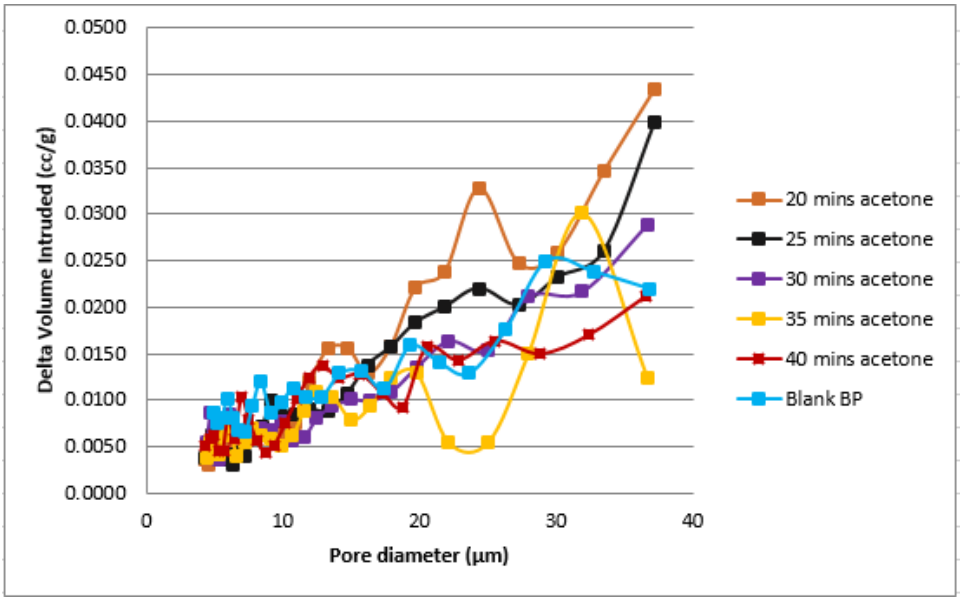

Figure 24 Change of volume versus pore width comparison between BPs exposed to different times of acetone vapor (0,20,25,30,35,40 mins of acetone) –pore range (0-40µm)

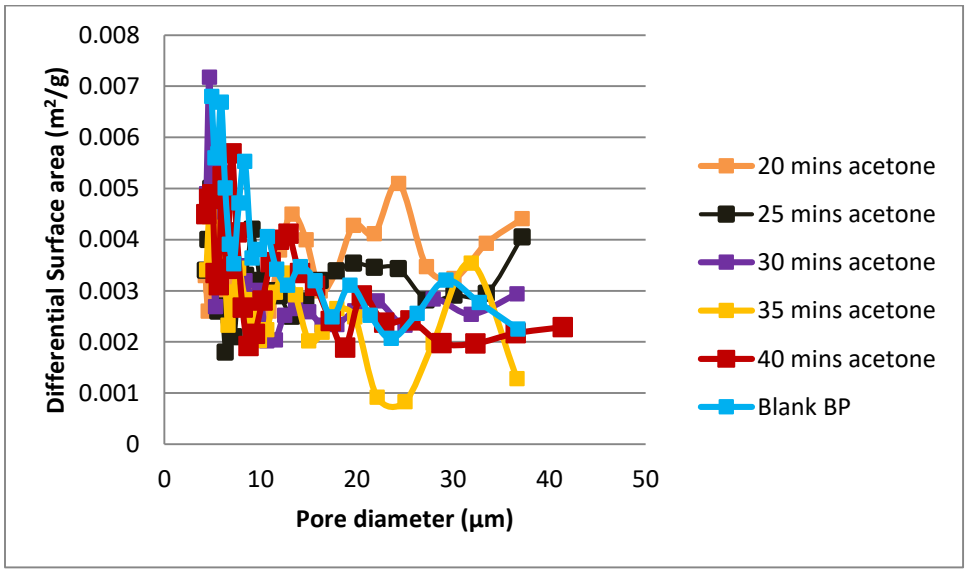

Figure 25 Differential surface area versus pore width comparison between BPs exposed to different times of Acetone vapor ((0,20,25,30,35,40 mins of acetone) –pore range (0-40µm)

5.2.3 BET Results

Pore range (0-120 nm)

In order to investigate more on the change of porosity on the small range of pore widths on the samples exposed to acetone, a BET analysis was carried out. Figure 26 presents the differential pore volume as a function of pore width for the membranes exposed to different durations of acetone starting from 20 minutes along with the blank. Figure 26 shows that for all the membranes, the larger pores (>~ 20 nm) accounted for most of the differential pore volumes, with distinct values at pore widths of 25 nm, 37 nm, 50 nm, 54 nm, 68 nm, and 86 nm. Not all the samples exhibited maximum differential pore volume at the same pore size. Membranes exposed to 20 and 35 minutes of acetone vapor showed maximum pore volume distribution around 54 nm, while the membrane exposed to 40 minutes of acetone vapor exhibited maximum differential pore volume at pore width of 68 nm, while membranes exposed to 25 minutes, and 30 minutes showed maximum differential pore volume at pore width of 86 nm. Although the graphs of the different membranes follow a similar trend, there is no linear relationship between increasing time of exposure to acetone and the differential pore volume. In general, blank BP graphs seem to fall noticeably under all the graphs of the BP samples exposed to acetone vapor after the pore size of 58 nm, which indicates that there has been an increase in the number of pores at the pores size ranges (58 nm, 63 nm, 68 nm, 73 nm, 79 nm, 86 nm, 93 nm, 100 nm, 108 nm, 117 nm) for all BP samples which have been exposed to acetone vapor.

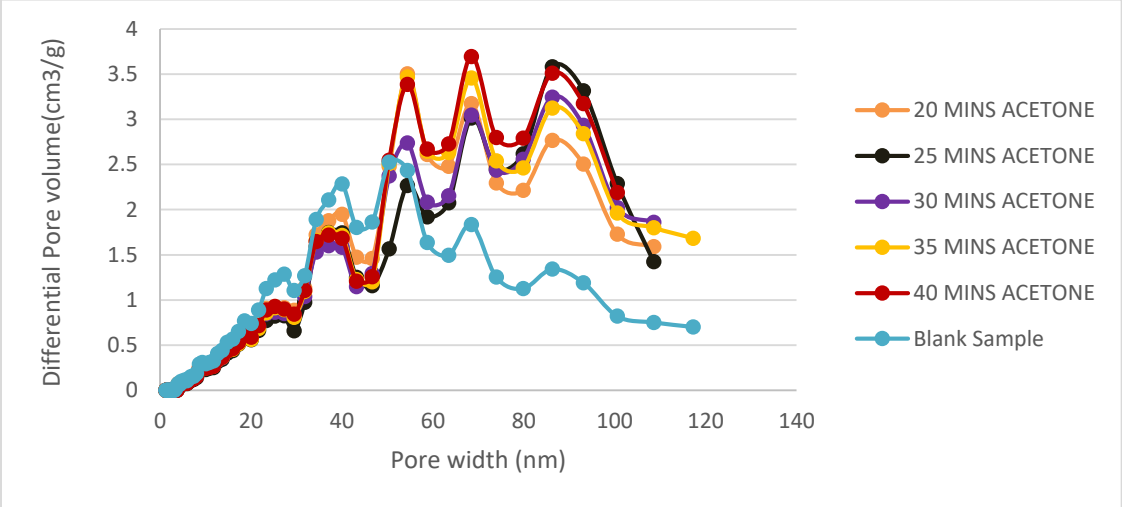

Figure 26 Differential Pore volume vs Pore width – The effect of varying exposure time of Acetone Vapor on BP (0-120 nm)

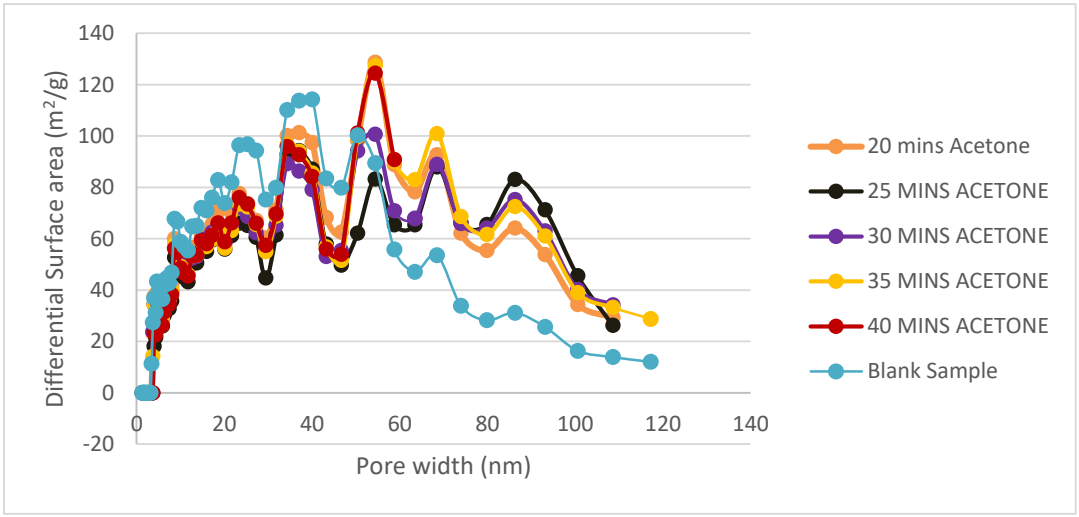

Figure 27 - Differential Surface area vs. Pore width – The effect of varying time of Acetone exposure on BP porosity (0-120 nm)

Figure 27 shows the corresponding differential pore surface area distribution versus the pore width for the samples exposed to acetone vapor for various durations of time. On comparing Figure 26 and Figure 27, the small pores (<20nm) exhibit the lowest differential pore volume but also one of the higher differential surface area denoting that

their numbers must be significant in their membranes. All membranes showed pores at the same distinct values stated earlier.

In general, the blank sample showed the lowest differential surface area for pore sizes that are larger than 58 nm meaning that it has lesser number of pores of these sizes than the samples exposed to acetone. In the blank sample, there is a shift in trend relative to the other samples smaller and larger about 50 nm: (<~50 nm) the blank sample showed the highest differential surface areas and (>~50 nm) it showed the lowest. This means that there is higher number of the small pores (size less than 50 nm) than the other samples (exposed to acetone), and vice versa after the 50 nm. Thus, the exposure to acetone resulted in an increase of the pores larger than 50 nm in pores and in blocking some of the small pores. This might be an indication that those samples that were exposed to acetone resulted in the wetting and pushing of the individual CNTs and CNTs bundles towards each other resulting in blocking some of the small pore sizes that are smaller than the 50 nm in comparison to the blank sample which exhibited the highest differential surface area in this same range. However, after the 50 nm the blank sample showed the lowest differential surface area for pore sizes that are larger than 58 nm meaning lesser number of pores of these sizes than the samples exposed to acetone. This could be an indication that the exposure to acetone that resulted in the wetting of CNT bundles by acetone did not have the same effect percentage on the larger pore sizes, as it has on the small pores. Since the CNTs and CNTs bundles are wetted and pushed towards each

other to the same degree, they have a more pronounced effect on the decrease of porosity in the small pores than on the larger pores.

Pore range (0-16 nm)

In order to investigate the behavior of each graph at the small distinct pore widths, the graph in Figure 26 was further investigated in Figure 28 because Figure 26 does not show clearly the breakdown of the differential volume of the small pores.

Figure 28 shows the differential pore volume as a function of pore width for pore widths between 0 and 16 nm. Small pores accounted for limited differential pore volumes with distinct pore widths of 4 nm, 4.6 nm and 5.4 nm, 7.9 nm, 8.6 nm, 12.6 nm (Figure 28). These pores account for pores lying between aggregates of nanotubes as explained by Rashid et al. The small pores found between 5 and 6 nm in the MWCNT BP prepared by their work were found to be those pores present between the aggregates of the nanotubes [22]. The general trend of the graphs is that the graph of the membrane of the blank BP is always exceeding the other graphs in the differential pore volume. In general, the plot indicates that the blank BP has more pores of the pore width range (0-16 nm) than samples exposed to acetone. This means that samples exposed to acetone vapor lost porosity within this pore width range. Starting only from around 58 nm a significant increase in differential pore volume is exhibited by samples exposed to acetone as explained earlier (Figure 26).

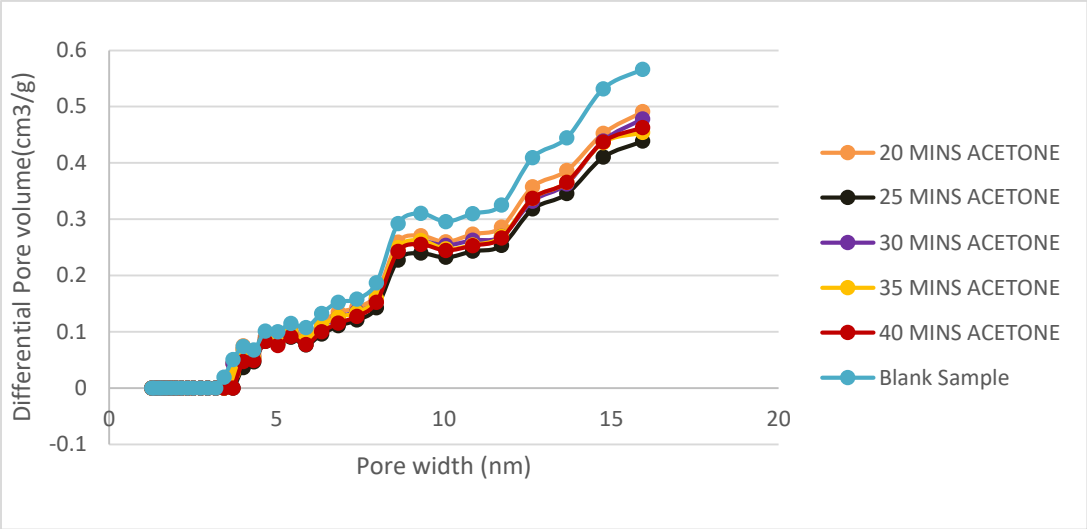

Figure 28 Differential Pore Volume vs. Pore Width –The effect of varying time exposure of Acetone vapor on BP for pores (0-16 nm)

Figure 29 shows the differential surface area of the different membranes at the same distinctive pore widths discussed above for the differential pore volume in the same range (0-16nm). The graphs of the different membranes range from the blank BP featuring the highest differential surface area in all the distinctive pores. Following the blank sample's graph, is the graph of the BP exposed to 20 minutes of acetone which exceeds in differential surface area the other BPs being exposed to other timings of acetone. This indicates that the BP being exposed to 20 minutes of acetone exhibits the largest number (after the blank BP) of pores in this size range.

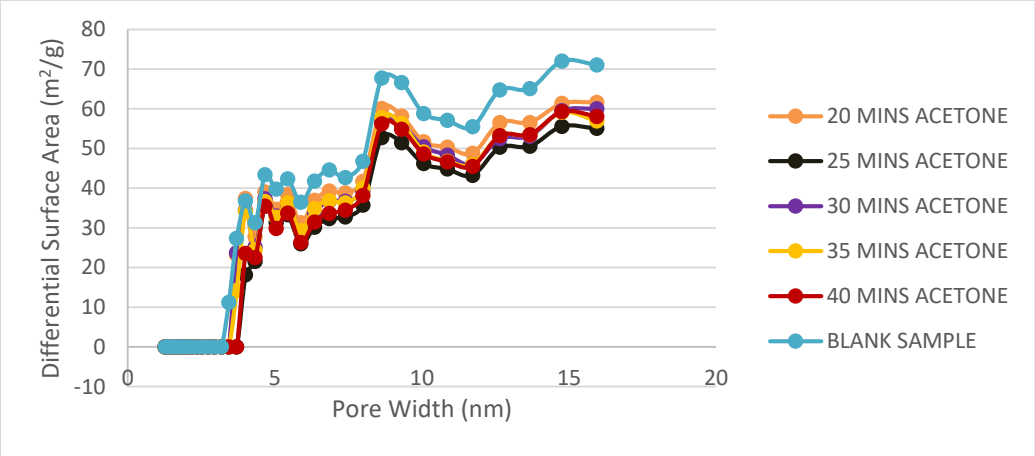

Figure 29 Differential Surface area vs. Pore width – The effect of varying time of Acetone exposure on BP porosity (0-16nm)

The membranes show distinctive pore widths at of 7.9 nm, 8.6 nm, 12.6 nm The order of the graphs (in this range) from the highest value of differential surface area to the lowest are the blank, 20, 30, 35, and 40 minutes of acetone with all BPs displaying almost the same pattern. This indicates in general that the longer time of acetone exposure, the lower the differential surface area, thus the more pronounced effect of the wetting of CNTs bundles on the small pore range, the lesser the number of the pores on this small range of pore widths. On the other hand, the BP being exposed to 25 minutes of acetone is not included in the previous pattern, as it shows the least differential surface area along with the BP exposed to 40 minutes of acetone in this pore width range.

Average Pore size and BET surface Area

Table 2 shows the BET surface area and the average pore width of the different membranes. The values of the BET surface area are consistent with previous values reported in the literature for MWNCT BP [22][27]. Again, the average pore size of the BP (16.5-22.6 nm) corresponds well with the literature[22]. The membrane exposed to 40 minutes of acetone shows the highest surface area with a value of 186.03 m^2/g. There is a

general increase of surface area and general decrease of average pore size as the time of acetone exposure increases.

Table 2 Comparison between the surface area and average pore widths of BPs exposed to different duration of Acetone.

Time of exposure of acetone vapor (in minutes)	**0**	**20**	**25**	**30**	**35**	**40**
BET surface area (m^2/g)	167. 3	172.9	170.4	180.6	180.6	186.0
Average pore width (nm)	22.6	18.7	18	16.1	16.04	16.5

In general, the BP sample which was not exposed to any acetone had the lowest surface area and the highest average pore width. This means the more the exposure to acetone, the higher the number of pores regardless of their pore size, the higher the surface area. On the other hand, the decrease in the average pore size could be explained by that all samples including the blank BP show comparable quantities of the small pores widths less than the 50 nm. Beyond, the 50 nm, samples exposed to acetone show higher numbers of pores in the large pore width range greater than 50 nm. Since, the average pore width is a measure of the sum of pore sizes over the total number, and since the number of pores of the exposed samples before the 50 nm of comparable quantity while beyond the 50 nm in the blank BP is less than the other samples, then the average pore width should be of a larger value for the blank than for the other samples. In contrast with previous studies[78] related to CNTs forest, a group have investigated the effect of porosity by densifying the CNTs forest. They found out that the porosity of the forest has decreased from 97% to 72%. This was explained by the fact that when liquids are

exposed to high porous CNT forests, the pores collapse as an effect of the capillary forces and so a densely packed solid is created.

In order to have a better picture of the change of porosity that occurred as a result of the exposure to acetone, a comparison between the micron and nano ranges of the pore sizes according to the Hg porosimetry and the BET results is shown in Figure 30. Samples exposed to acetone vapor have showed an increase number of pores for pore sizes between 50 nm and 120 nm, according to the BET analysis. Samples exposed to 20 and 25 minutes of acetone, showed higher number of pores for the range size between 20 µm and 105 µm. Also, higher number of pores were shown for samples exposed to 30 and 35 minutes of acetone for the pore size range between 105 µm and 200 µm. Thus, these ranges of pore sizes show where the change of porosity was observed for the samples exposed to acetone throughout the nano- and the micron- range of the pore sizes.

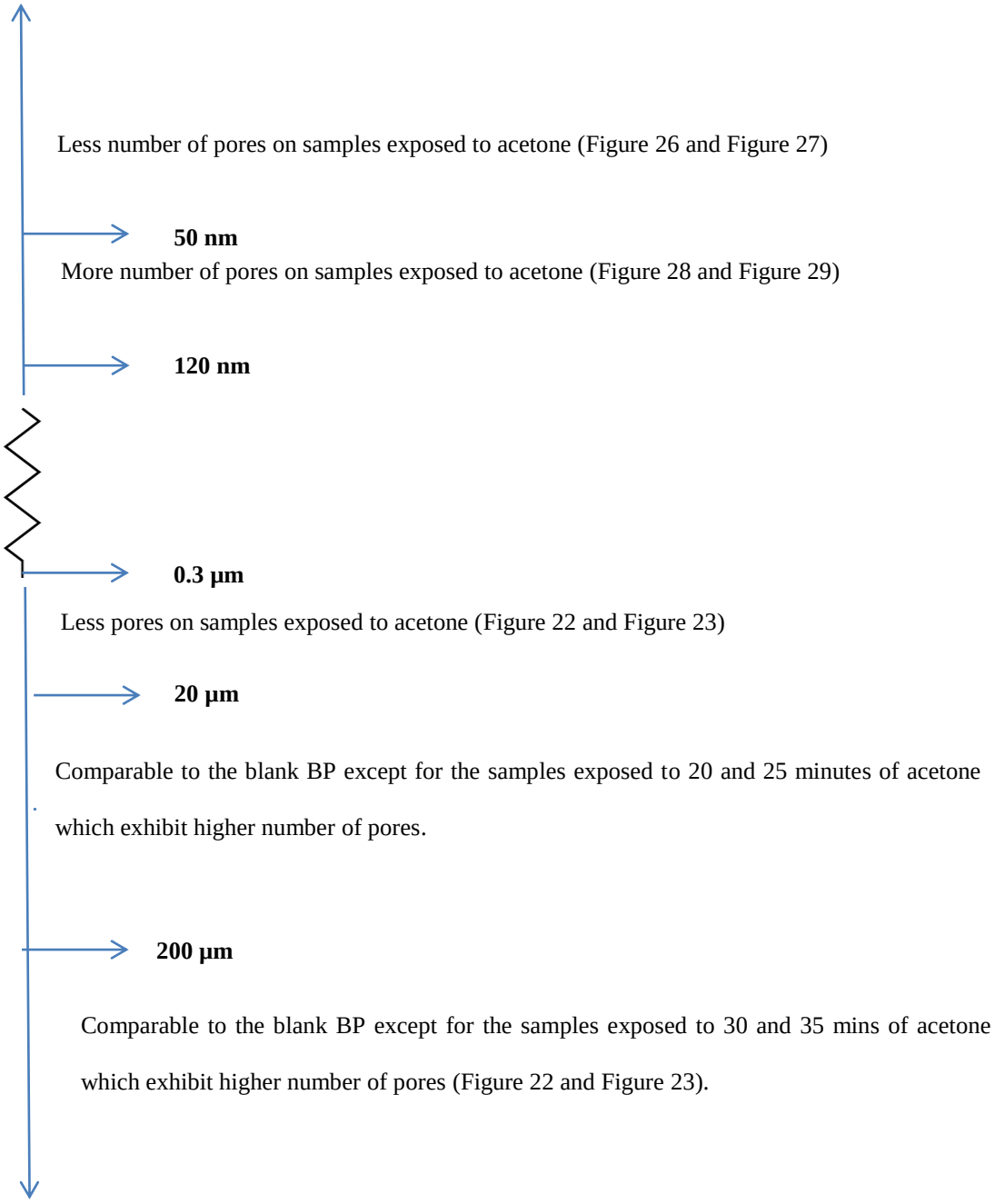

Figure 30 Comparison between the micron and nano ranges of the pores sizes according to Hg porosimetry and BET analysis

5.3 Comparing BPs exposed to different types of solvents

Hg Porosimetry, BET analysis and SEM imaging were carried out to see the effect of changing the boiling solvent on the porosity of the examined BPs. All the BPs here were exposed to 40 minutes of boiling solvent since this was the time that gave the highest BET surface area and the one of the smallest average pore size (Table 2), when BPs were exposed to acetone.

5.3.1 Hg Porosimetry

Pore Range (0-200 µm)

By looking at the figures below (Figure 31 and Figure 32), displaying the delta volume vs. pore width and the delta surface area vs. pore width for the BPs exposed to different boiling solvents for 40 minutes, including the blank BP, pore widths <~10 µm constitute most of the differential surface area for all the samples exposed to the different solvent. The blank BP shows the highest differential surface area of all at the pore width of 4.8 µm, while this value tends to decrease much for the exposed BPs to the solvents. This seems to mean that the exposure to the solvents have resulted in the drawing of the CNTs bundles towards each other, blocking some of these small range of pores. Another notable feature present in these two figures, is the plot of the BP exposed to the solvent THF. This plot shows higher differential pore volume than the other plots at the pore widths of 68 µm and 97 µm, while it also shows higher delta of the surface area at the pore diameter of 68 µm. This shows that there are significant numbers of pores at this pore diameter relative to the other BPs exposed to the other boiling solvents. Thus, the BPs exposed to the different solvents show comparable behavior to the blank BP for the micron range of the pores, except for the THF which shows an increased number of pores

at the pore width of 68 µm. Further investigation for the change of porosity is then performed using the BET analysis for the nano- range of pores and the SEM imaging.

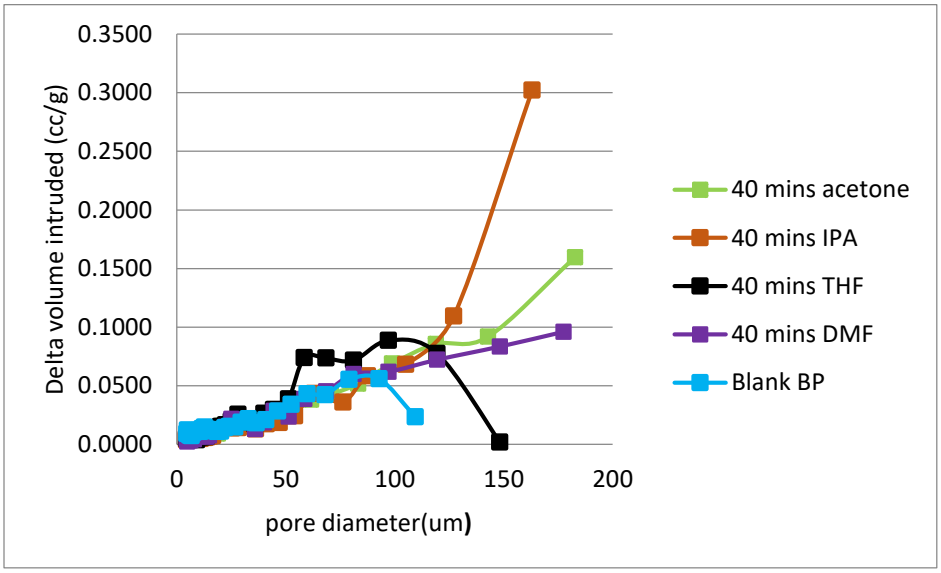

Figure 31 Delta volume intruded vs. pore diameter for BPs exposed to different boiling solvents

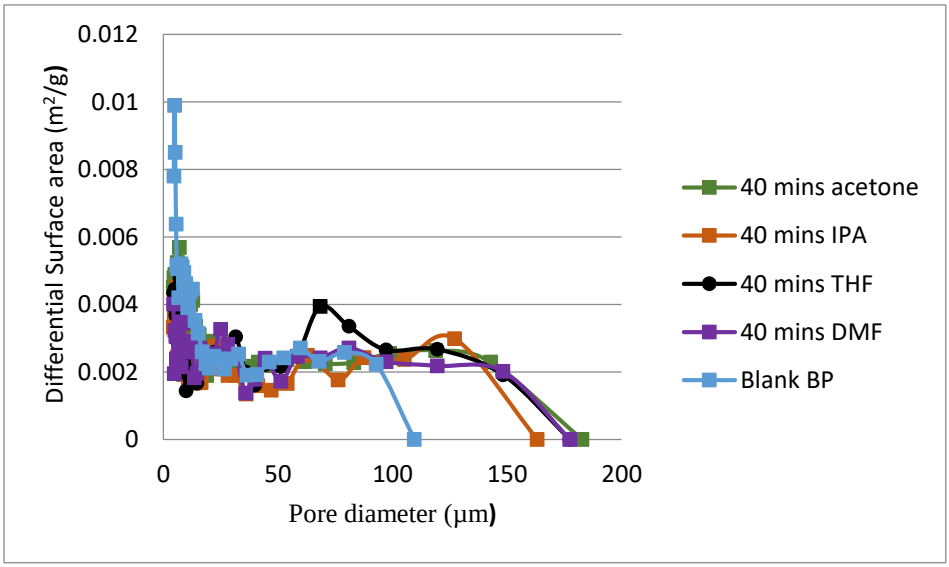

Figure 32 Delta Surface area vs. pore diameter fo BPs exposed to different types of boiling solvents

5.3.2 BET Results

Pore Range (0-120 nm)

Figure 33 and Figure 34 present the differential pore volume and differential surface area as a function of pore width, respectively, for BPs exposed to different solvents: acetone, IPA, THF,and DMF. All figures include Blank BP which has no exposure to any solvent vapor. Figure 33 shows that for all the membranes, the larger pores (>~ 20 nm) accounted for most of the differential pore volumes, with distinct values at pore widths of 25 nm, 37 nm, 50 nm, 54 nm, 68 nm, and 86 nm which are of similar values to those of BPs exposed to different times of acetone.

Also, the graph of differential surface area (Figure 34) showed a noticeable decrease in BP surface area upon exposure to DMF compared to other solvents. It is also clear that the graph of the BP exposed to DMF lies lower than the other graphs for pore widths >~10 nm denoting that it has relatively lower values of differential pore volume compared to the others in that pore width range (Figure 33). Also, the blank BP graph generally constitutes the highest differential pore volume of all the graphs for the ranges of pore width < 50 nm, and then it becmoes comparable to the THF, IPA and acetone graphs for the pore width ≥ 50 nm. On the other hand, the blank BP graph alternates between the THF, IPA, and acetone graphs fore pore widths >~10 nm. The BP exposed to 40 minutes of acetone, on the other hand, showed the maximum differential volume and differential surface area starting the pore width of 54 µm.This means that the change due to the exposure of 40 minutes of boiling solvent resulted in larger number of pores for the samples exposed to acetone at pore widths 54 nm and 68 nm. Acetone, was thus, the most effective boiling solvent for producing greater number of pores at the large pores.

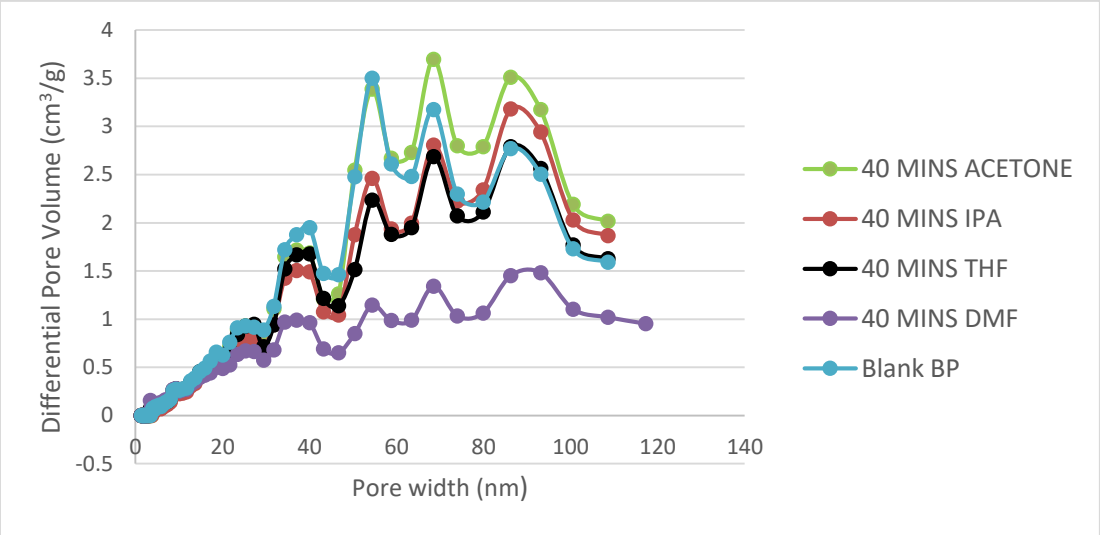

Figure 33 Differential Pore Volume vs. Pore width- The effect of different boiling solvent on BP (Pore size (0-120 nm)

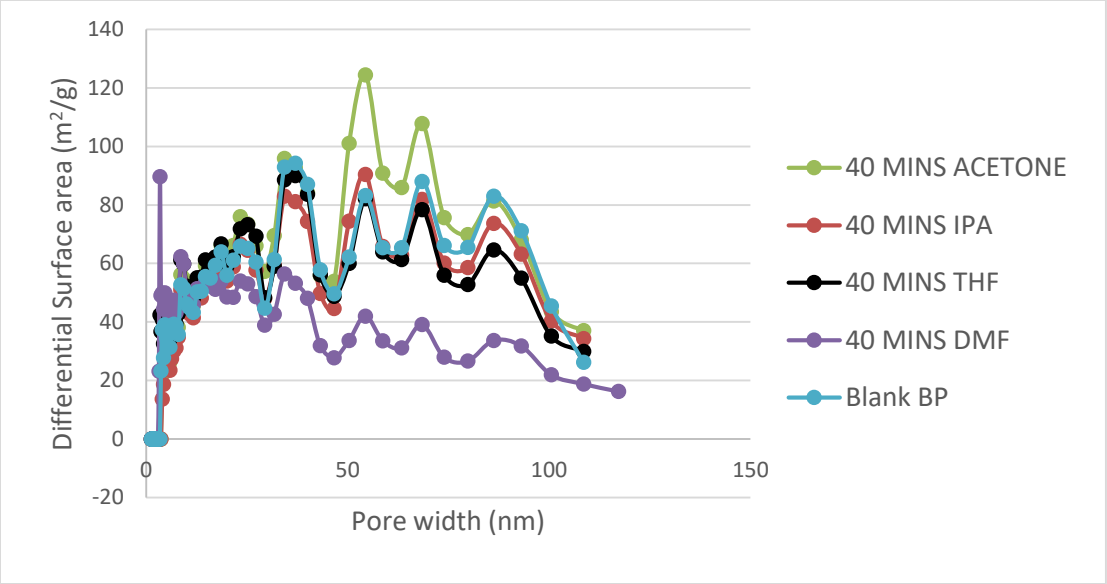

Figure 34 Differential Surface Area vs. pore width -The effect of different boiling solvent on BP (pore size 0-120 nm)

Pore range (0-16 nm)

Figure 35 and Figure 36 show the differential pore volume and differential surface area versus pore width, respectively, for pore range between 0-16 nm. DMF exposure resulted in relatively higher differential pore volumes compared to other solvents in the pore range (<10 nm). Moreover, DMF shows a peak at 3.4 nm equivalent to a differential pore volume of 0.15 m3/g which is much higher than that THF (the second lowest after DMF) (0.07 m3/g). This could be a result of the fact that DMF has the lowest vapor pressure and the highest surface tension of all the solvents used. This agrees with the work presented by Lu et al.[78] where electrospun fibres made of polystyrene were synthesized using DMF and THF as different solvents to investigate for their effect on the internal porosity of nanofibres. It was found that DMF was important in producing pores in the interiors because of the low vapor pressure it exhibits. On the other hand, THF did not result in producing interior pores but more of a rough surface as it has relatively higher vapor pressure than DMF. In the contrary, in a related work done on buckypaper cast from various solvents by Whitby et al. [47] to see the effect of the different solvents on porosity, it was explained that high vapor pressure solvents result in distribution of small macro-pores because the high vapor pressure prevents the collapse of the larger pores as the solvent evaporates.

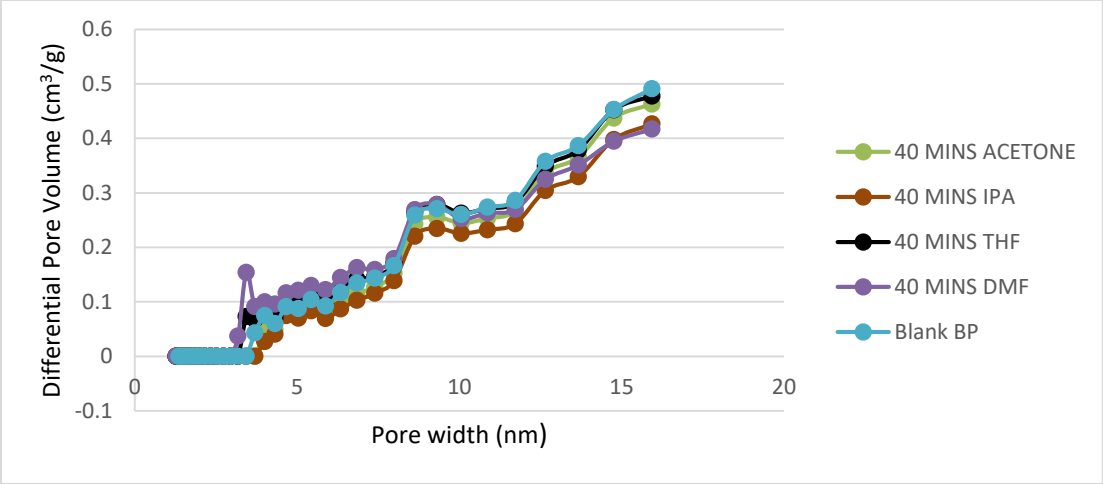

Figure 35 Differential Pore Volume vs Pore width- The effect of different boiling solvent on BP (Pore size (0-16 nm)

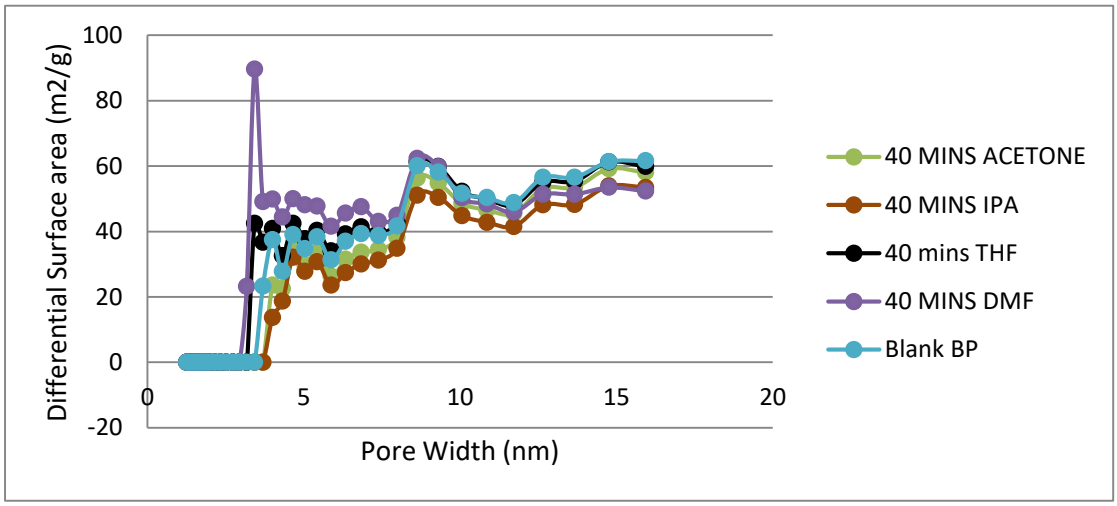

Figure 36 Differential Surface Area vs. pore width -The effect of different boiling solvents on BP (0-16nm)

In Figure 35 of (pores between 0-16 nm), it can be observed that small pores accounted for limited differential pore volumes with distinct values at pore widths of 3.4, 4.0, 4.6 nm 5.4 and 9.3 nm. However, these pores are of the same size as that of the BP exposed to acetone vapour for differernt times, except for the 3.4 nm where only BP exposed to THF and DMF exhibit. The blank BP graph lies under the graphs of the THF and DMF, while above those of acetone and IPA for this small range of pore width. This could be due to

the fact that THF and DMF have lower vapor pressure in comparison to their counterparts IPA and Acetone (Table 3), and as explained by Whitby et al. too [47].

Consequently, by looking at the general order of the differential volume and differential surface area for the different solvents involved for pore widths less than 20 nm, DMF exhibits the highest differential pore volume and differntial surface area, followed by THF, then IPA and, acetone. This is the same order for the surface tension, DMF being the highest and acetone the lowest. In light of the explanation offered by Whitby et al. above, the order is right. As the surface tension decreases, more wetabillity is experienced by the CNTs, as the solvent manges to enrobe the CNTs better. Therefore, it seperates them better and so the number of pores increases as reflected by the differential surface area and differential volume figures above for the large pores. Since Acetone and IPA have the lowest surface tension (Table 3) then they both contribue to the highest number of pores in the large range of pores relatively to the others. However, the highest the surface tension (as in the case of DMF), the lower the wettability, and so the solvent works more on the bundles of CNTs rather than enrobing the CNTs seperately. As it does that, the bundle of CNTs are pushed towards each other, resulting in the creation of the small pores generated by the DMF at 3.4 nm.

Table 3 The BET surface area and average pore width of BPs produced by the different boiling solvents

Boiling solvent	Surface tension (mN/m) at 25°C	Vapour pressure (KPa)
acetone	23.3	30.80
THF	26.7	21.60
IPA	23.0	6.02
DMF	34.4	0.44

By comparing the results produced by the different solvents in comparison to the results produced by acetone at different times, it could be observed that all membranes exhibit the same distinct pore width in all cases. However, the exposure of the BP membrane to DMF did result in a higher differential surface area values than the BPs exposed to different timings of acetone. For example, the BP exposed to 20 minutes of acetone at the pore width of 4 nm (the highest among all the BPs exposed to acetone at this pore width) exhibited a differential surface area of 37 m^2/g while the BP exposed to DMF exhibited a differential surface area of 49 m^2/g. In addition to that, BP exposed to DMF exhibited the highest differential surface area in both pore widths of range 4.6 nm and 68 nm, of all the BPs exposed to different timings of acteone, and to BPs exposed to other solvents.

It is then safe to conlclude that DMF has the highest influence of all the solvents in producing the smallest number of pores with the highest number of all as seen in Table 4 below. In regard to the table, which shows the average pore sizes exhibited by the BPs exposed to different types of solvents. The BPs that were exposed to 40 minutes of DMF showed the smallest average pore size of all the other BPs exposed to all the other

solvents and the blank BP, and to those exposed to differenent timings of acetone. This is in alignment with the results shown by the BET analysis, where the BPs exposed to DMF had the highest differential surface area in the small range in comparison to the other BPs.

Table 4 Average pore size of the BPs produced by the BPs exposed to the different solvents.

Exposure to boiling solvent exposure	Average Pore size (nm)
Blank BP	22.6
40 minutes acetone	16.5
40 minutes THF	17.0
40 minutes IPA	16.8
40 minutes DMF	14.0

5.3.3 SEM images:

The morphologies of the prepared BP membranes exposed to different boiling solvents are shown in Figure 37. The BP exposed to acetone shows aligned and compacted morphology, whereas that exposed to THF is not as smooth as the other ones, and this could be an indication of the different features of porosity it showed using the Hg porosimetry where it showed the highest number of pores at the distinct pore of 68 µm. IPA and DMF exposed BPs have similar morphologies except that the DMF one appears to have a more compacted structure, with smaller pores which is in alignment with the BET results where DMF showed the smallest average pore size.

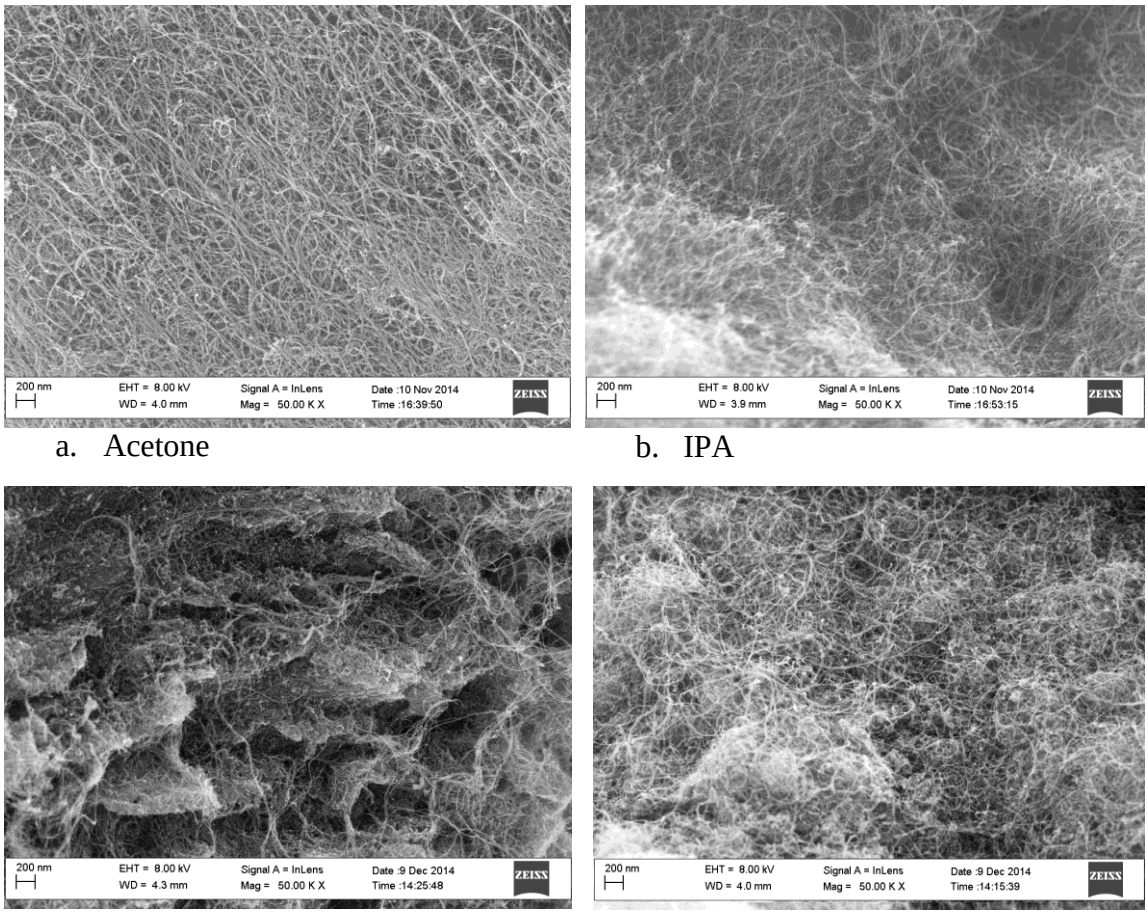

a. Acetone b. IPA

c. THF d. DMF

Figure 37 SEM images on the effect of the different boiling solvents on the porosity of the BP

Thus, the differences between the BPs exposed to the different solvents which are evident in the BET graphs and in the SEM images could be attributed to the different surface tensions and vapor presssure (Table 3) which affected the capillary condensation effect which occurs in two steps: first the CNTs are drawn together through capillary forces, and secondly when the solvent evaporates upon drying of the BP, the van der Waals between the CNTs adhere the tubes closer[75][79][80]. DMF has highest surface tension, which could be the reason for the more effective closure of the CNT network observed as discussed above. A possible explanation was offered by Whitby et al, that explains by referring to the BPs having the strongest MWCNT-MWNCT interactions and MWCNTs-

solvent repulsion forces in the highest surface tension solvent (DMF, in this case) and the weakest in the least surface tension solvent (in this case acetone and IPA). In agreement with this expalantion, another group who was involved in fabricating BPs using different solvents, concluded that the use of DMF as a solvent resulted in having lower ranges of pore sizes because of the strong MWCNT-MWCNT in liquids with higher surface tension[81].

5.4 Comparing BPs produced by different membrane filters

By comparing the effect of different solvent vapor exposure on BPs, DMF was found to be the most effective solvent to produce a high number of small pores on BPs exposed to 40 minutes. Consequently, BPs exposed to 40 minutes of DMF were prepared on PTFE membrane filters of different pore sizes (0.2 µm, 0.45 µm, 1.0 µm and 10 µm). This was done to test the effect of changing the pore size of the membrane filter on BPs porosity.

5.4.1 BET Results

Pore range (0-120 nm)

Figure 38 shows the differential pore volume as a function of pore width for the BPs exposed to filter membranes of the different sizes. It shows that for all the membrane filters, the larger pores (>~ 20 nm) accounted for most of the differential pore volumes, with distinct values at pore widths of 25.3 nm, 40.0 nm, 54 nm, 68 nm and 86 nm for all. This is in accordance with the same pore sizes in the same range of the other BET graphs shown above when testing the other parameters on the porosity.

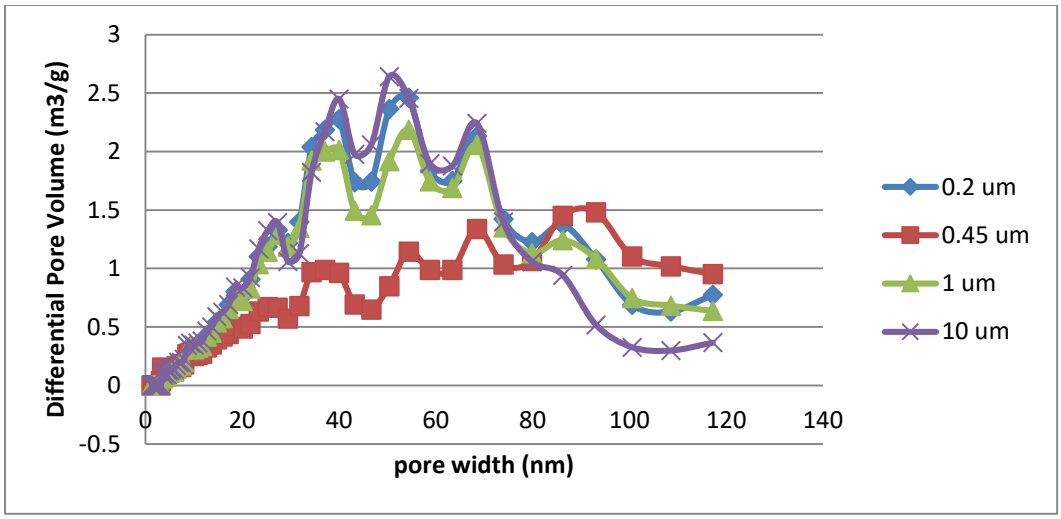

Figure 38 Differential pore volume versus pore width-The effect of changing the membrane filter size on BP (Pore size of membrane filter between (pore width0-120 nm

It is noticeable that not all the samples exhibited maximum differential pore volume at the same pore size. It is clear that the graph of BP produced by the 0.45 µm substrate lies the lowest of all graphs for most of the pores (<80 nm) denoting that it has relatively lower values of differential pore volume compared to the others. This means that the distinct pores (< 80 nm) that were produced in the BP on the 0.45 membrane filter have relatively smaller volume than the same distinct pores in the other BPs produced by the other pore sizes of the membrane filters. Also, by looking at the range of small pores, it can be observed that small pores accounted for limited differential pore volumes with distinct values at pore widths of 3.4 nm and 9.3 nm. This is similar to the same pore distribution discussed above in the other BET graphs.

Figure 39 shows the differential surface area versus pore width for the BPs produced by membranes of the different pore sizes. Figure 39 showed a noticeable decrease in BP surface area produced by the membane filter 0.45 µm after pore width

(>10 nm). On the other hand, it showed the highest differential surface area (89.6 m^2/g) at small pore widths (3.4 nm) confirming a considerable increase in the number of small pores due to the pore size of the substrate (0.45 µm).

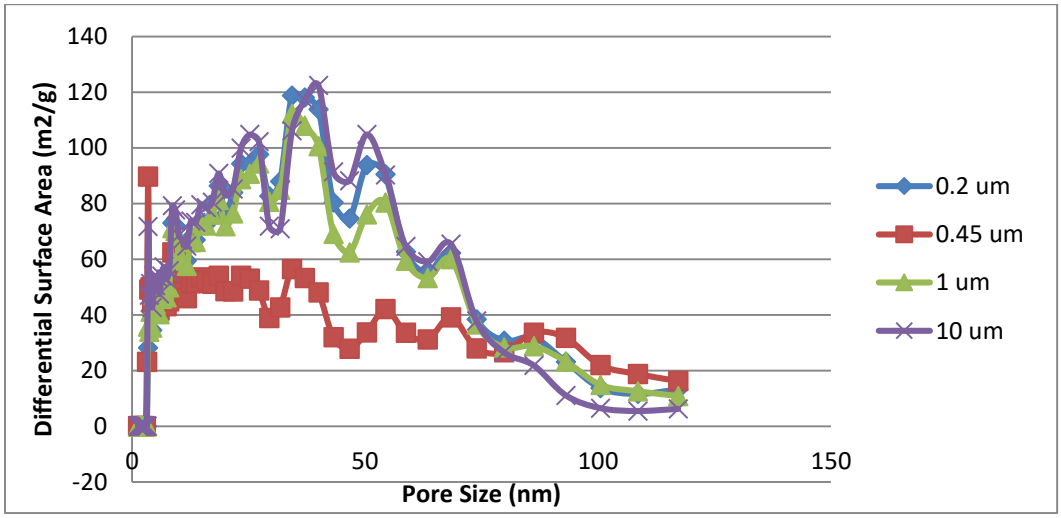

Figure 39- Differential Surface area vs. pore size of the BPs produced by different membrane filters (pore size range 0-120 nm)

Generally, this shows that there is a general trend observed between all the BPs produced by the different BPs having the same distinct pore widths, except for the 0.45 um where it had the highest differential surface area before the 10 nm and the lowest after the 10 nm. The rest BPs produced by the other membrane filters exhibit more or less the same behaviour with 0.45 µm and 10 µm having higher values of the differential surface area than the other two. This is again confirmed with the values of the BET surface area and the average pore size of the different BPs produced by the different substrates Table 5. The BP produced by 0.45 µm has the least average pore size of all, while the avearage pore size for the rest of membranes are comparable to each other.

Table 5 The BET surface area and the avearge pore size of BP produced by the differenet membrane fitlers

	0.2 µm	0.45 µm	1 µm	10 µm
BET Surface area (m^2/g)	180.7	173.8	179.7	184.3
Average Pore Size (nm)	21.1	14.0	20.2	20.1

Again, by looking at the table, there is no direct relationship between the increase in the pore size of the substrate and the average pore size of the BP or the BET surface area. It was expected that a decrease in the pore size of the substrate would lead to the decrase of the average pore size of the BP as was predicted from the work of Muhlbauer et al. [82]. In this work, Muhlbauer et al. tested the effect of the pore size of the substrate on the electrical response of CNT films. The pore size of the substrate was reported to affect how the network of CNTs was formed onto the substrate and accordingly the electric resistance was influenced. Since the vaccum filteration process happens using a constant vaccum source, then the pore size should have an effect on the formation of films on the surface of the substrate and through the thicknesss of the substrate itself. It is anticipated that the MWCNTs will not form on the surface of the substrate if the pore sizes of the substrate are much larger than the MWCNTs. On the other hand, if the pores of the filter membrane are of the same size of the CNTs, then the CNTs will rather bridge the pores and thus a much less deposition of CNTs will be pulled down through the thickness of the filter. If the substrate pore size is smaller, then the MWCNTs are able to cover the surface of the substrate and a more complete network of MWCNTs would be shown. Thus, with this explanation the use of substrates with different pore sizes was expected to have an effect on the porosity of the BPs. The CNTs used by Muhlbauer et al. were of

0.2-5 µm, and so when CNTs of this size were deposited on filter membranes of 5 µm and 25 µm, a higly dense network of CNTs formed for the 5 µm filter membrane, while the network formed on the 25 µm showed high density regions of CNTs seperated by empty regions where CNTs were missing. In this work, however, all the membrane filters used are of a smaller size than the size of CNTs whose lengths are tens of microns, except for the 10 µm filter membrane the pores of which might be similar in size to the CNTs used. Therefore, BPs produced by all the membrane filters used should be expected to have a good network shape, because the CNTs will form bridges on the pores of the filter membranes, as explained by the Muhlbauer et al. [82]. The 10 µm filter membrane is expected to result in having the CNTs deposited both on the surface and some within the thickness of the filter membrane.

Additionaly, the fact that the BPs produced by 0.45 µm possessed the highest number of the pore size 3.4 nm, was confirmed as shown in Table 5 . It can be seen that the BP produced by the substrate with pore size 0.45 µm exhibits the smallest average pore size of all (14.01 nm) as compared to (21.1, 20.2, 20.1 nm) produced by the other substrates (0.20, 1.0, 10 µm) respectively. . This means that the change of the pore sizes of the filter membrane prepared by this work have no effect in changing the average pore width and the BET surface area of the BPs. However, in another work by Liu et al.[83], the change of pore size of fitler membrane did change the average pore width of the BPs prepared by them. In their work, when they changed the pore size of the PTFE membrane filter they are using between 0.22 µm, 0.8 µm, and 1.2 µm, the average pore widths of the respective BPs changed to 19, 31, 40 nm respectively. They concluded that a decrease of the pore size of filter membrane results in a decresae in the overall average pore width of

the BP.

In comparing the BPs produced by the different sizes of pore widths of membrane filters to those produced by other solvents between pore widths (0-120nm), it was found that the same pore widths were produced by these filters including the 3.4 nm. However for the pore width 23 nm, the BPs produced by this category (changing the pore size of filter membrane) exhibited relatively higher differential surface area values than those of other solvents or those exposed to different times of acetone. For example, the highest differential surface area exhibitied by the BP at 23 nm is 124 m^2/g, while for the ones exposed to the other solvents was 79 m^2/g , and for the one exposed to the different times of acetone is 76 m^2/g. Another observation was noticed is that, starting from pore widths 50 nm and 68 nm, the differential surface area values for this category (104 m^2/g, 65 m^2/g, 33.6 m^2/g) are lower than the other BPs exposed to different solvents category (121 m^2/g, 110 m^2/g, 80 m2/g) and to those exposed to different times of acetone (124 m^2/g, 100 m^2/g, 83 m^2/g) respectively. This means that the BPs produced by different membranes generally exhibited lower number of pores at these distinct values.

5.4.2 SEM Images

The surface morphologies of the BPs produced on membranes of different pore sizes appear to be different from each other as seen in Figure 40. For the BP produced by 0.20 µm, the CNT's network is randomly distributed similar to the BP produced by the susbtrate of pore size 10 µm, yet the SEM image of he 10 µm show much more condensed network (Figure 39). This could contribute to the difference seen in the BET differential surface area diagram where the BP produced by 10 µm exhibited the second highest number of the small pore size. For the BP produced by 0.45 µm , the surface

consists of scattered networks that have MWNTs with high density networks. Finally, the BP produced on 1 µm membrane filter in Figure 40 (c) shows wider CNTs network than all of the other BPs. The 1.0 µm showed the most widspread network of all, which is also in agreement with the BET differential surface area plot, where its graph shows mostly the lowest differential surface area of all, after the 0.45 µm filter membrane graph (Figure 39).

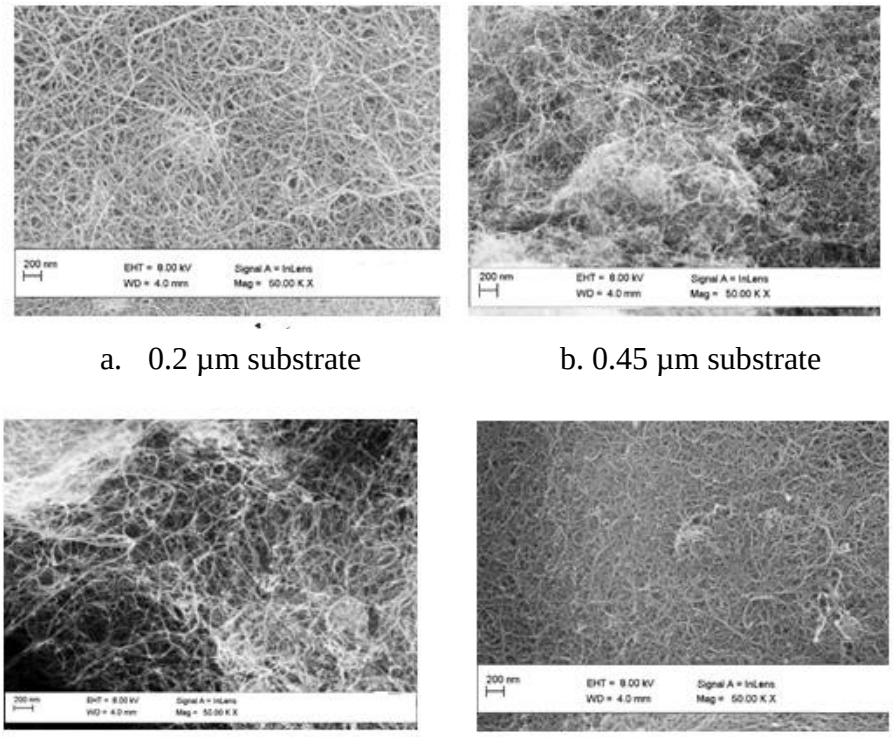

a. 0.2 µm substrate

b. 0.45 µm substrate

c. 1.0 µm substrate

d. 10 µm substrate

Figure 40 SEM images on the Effect of the pore size of the substrate on the porosity of BP

5.5 Investigating the effectiveness of the three different variables on Porosity

In the previous sections, the results of the investigating the change of acetone exposure time, change of boiling solvents, and change in pore size of membrane filter on porosity were presented. First, time of exposure of acetone as a boiling solvent was tested. Then, the effect of using different boiling solvents (acetone, THF, DMF, IPA) was chosen with an exposure to 40 minutes. Then, the effect of changing the substrate pore size on the porosity was tested in combination with exposing the BP to 40 minutes of DMF, since DMF was thought to be more effective in changing the porosity than the other solvents. In order to consider whether an interaction between these three variables would result in a change of porosity, a statistical analysis was carried out. A statistical model called ANOVA was chosen to test for the effect of these three different variables (type of solvent, pore size of the membrane filter and the time of exposure) combined on the porosity. The model gives an indication of whether the variables tested are of significance to the response or output one being testing for (in this case: average pore size and the BET surface area) or not. Secondly, it indicates what variables out of the three are the most influential to the output, but most importantly if the interaction between the variables themselves could be of significance to the output being tested for [84].

Different samples were then prepared to account for the combination of three variables. Each sample had a unique combination of the three variables values or properties. Each unique combination was prepared three times and this was called a trial. Trial one, for example, had the combination of the lowest time exposure (5 minutes) of

the boiling solvent with low vapor pressure (DMF) and the smallest pore size of the filter membrane (in this case 0.2 µm).

The statistical analysis was designed to investigate the effect of three variables: (1) pore size of substrate, (2) type of boiling solvent, (3) time of exposure to the boiling solvent. The model was programmed to test two responses that are needed to compare the porosity of the different samples individually. The first response is the BET surface area, and the second response is the average pore size of the sample.

As explained earlier in Chapter 4, the Design Expert software was used to generate the combinations of variables to be tested. These combinations are generated by a random order by the software to ensure the randomization factor of the results obtained (Table A2 in the appendix). The values for the different responses are then entered according to the combination of variables. Values of +1 and -1 are entered to show the high value and low value of the variable respectively. For example, Run number one (1) has low value (-1) of pore size of substrate (0.2 µm), low value (-1) type of boiling solvent (DMF) and high value (+1) of time of exposure of boiling solvent (40 minutes).

Fabrication of additional BPs was carried out by changing the three variables (see appendix), and the values of BET surface area and the average pore size were obtained from the BET adsorption method, as seen in Table 6.

Table 6 BET surface area and average pore size of the BPs produced by three combination of variables

BP	BET Surface area (m^2/g)	Average pore size (nm)
Trial 1(0.2 µm, DMF, 5 minutes)	179.5	20.1
Trial 2 (10 µm, DMF, 5 minutes)	192.7	20.3
Trial 3 (0.2 µm, acetone 5 minutes)	194.8	21.4
Trial 4(10 µm, acetone, 5 minutes)	197.5	18.0
Trial 5 (0.2µm, DMF, 40 minutes)	180.7	21.1
Trial 6 (10 µm, DMF, 40 minutes)	184.3	20.1
Trial 7 (0.2 µm, acetone, 40 minutes)	192.9	18.2
Trial 8 (10 µm, acetone, 40 minutes)	181.4	20.5

5.5.1 First Response: BET surface area

According to the statistical analysis done on the BET surface area as the first response, the model has proved to be successful. The program first shows the percentage contribution of each factor. From the table (Table 7), (C) time of exposure variable, the interaction AC between the pore size of fiter membrane (A) and time of exposure (C), the interaction (BC) between type of boiling solvent and time of exposure have the highest percentage contritbution. . ABC is not considered in this case because according to the sparsity of effects principle, that states in such an unreplicated system, the main effects

and the low order interactions such as AB, AC, and BC are the ones to be considered and most high interactions like ABC are to be negligible[84].

Table 7 Table poduced by the software showing the highest contribution variables on the BET surface area as a response

Term	Stdized Effect	Sum of Squares	% Contribution
Intercept			
A- Pore Size of filter membrane	2.02	8.12	2.22
B-Type of Boiling Solvent	0.30	0.18	0.048
C-Time of Exposure	-6.31	79.73	21.77
AB	-1.28	3.28	0.89
AC	-5.96	70.94	19.37
BC	-4.95	48.91	13.36
ABC	8.81	155.11	42.35
Lenth's ME	27.92		
Lenth's SME	66.83		

The variables with the highest contribution (C, AC, BC, and ABC) are then chosen to run the model (this is denoted by the letter M next to each of these variables). When ANOVA statistical analysis is run, the overall model was found to be significant at level of $\alpha = 0.05$. The p value is less than 0.05, which indicates that the model terms chosen are significant. In this particular case, C, AC, and BC are significant model terms, and thus are the most effective combination of variables to affect the BET surface area.

Results of the first response (The BET surface area):

Variable C: Time of exposure

The effect of time exposure on the BET surface area as seen in Figure 41 . A larger BET surface area is obtained when the time of exposure is shorter and a lower BET surface area is obtained when the time of exposure is longer.

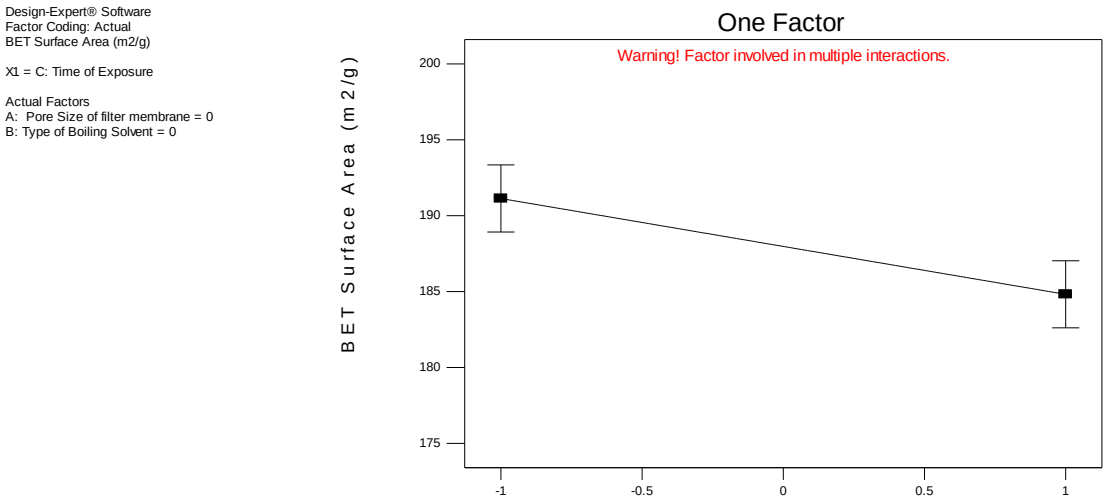

Figure 41 The effect of the time exposure of boiling solvent on the BET surface area

Interaction AC: Interaction between the pore size of filter membrane and the exposure time of boiling solvent

Figure 42 shows the interaction between the pore size of filter membrane and the exposure time of boiling solvent. A higher BET surface area is achieved, when the pore size of the filter membrane is high and the type of boiling solvent is of a lower vapor pressure. size of the filter membrane is high and the type of boiling solvent is of a lower vapor pressure.

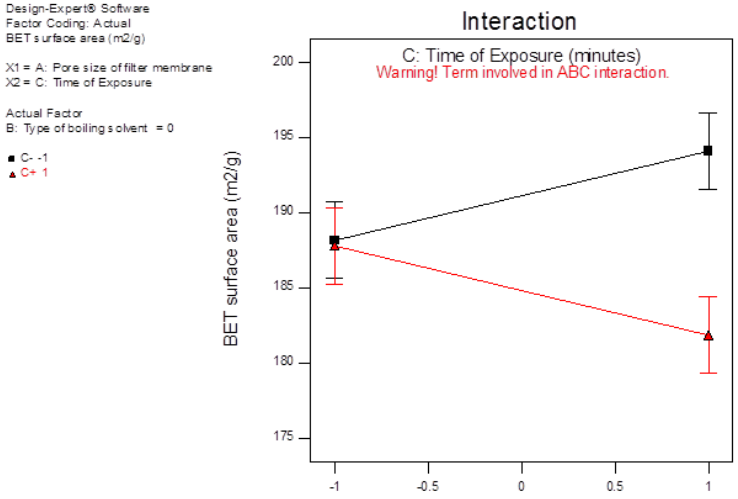

Figure 42 The effect of the interaction of pore size of filter membrane and the time exposure of boiling solvent on the BET surface area

Interaction BC: Interaction between the type of boiling solvent and the time of exposure

Figure 43 shows the effect of the interaction between the type of boiling solvent and the time of exposure on the BET surface area. A boiling solvent with a higher vapor pressure in combination of shorter exposure time results in higher BET surface area.

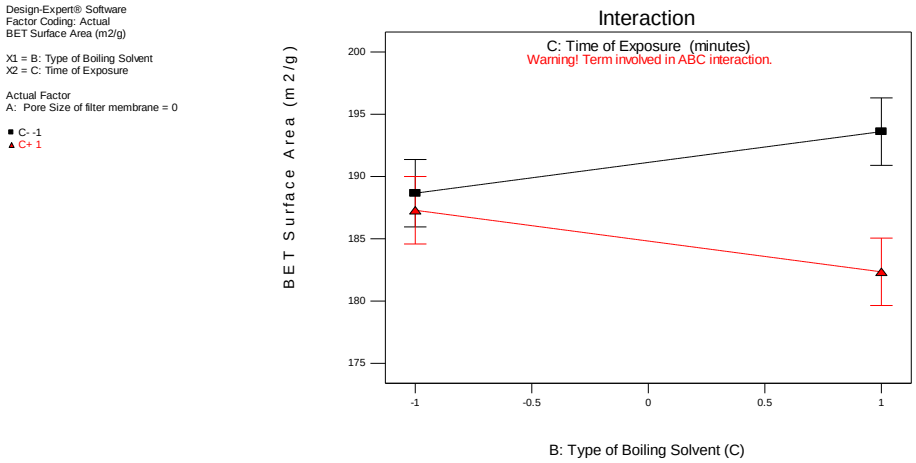

Figure 43 The effect of the interaction between type of boiling solvent and the time of exposure on the BET surface area

5.5.3 Second Response: Average pore size

According to the statistical analysis done on the average pore size as the second response, the model has proved to be successful. The program first shows the percentage contribution of each factor. From the table (Table 8), (B) type of boiling solvent, the interaction AC between the pore size of fiter membrane (A) and time of exposure (C) had the highest contribution. Again, ABC is not considered for reasons explained earlier. The variables with the highest contribution (B, AC and ABC) are then chosen to run the model (this is denoted by the letter M next to each of these variables). When ANOVA

statistical analysis is run, the overall model was found to be significant at level of α = 0.05. The p value is less than 0.05, which indicates that the model terms chosen are significant. In this particular case B and AC are significant model terms.

Table 8 Table produced by the software showing the highest contribution variables on the average pore size as a response

Term	Stdized Effect	Sum of Squares	% Contribution
Intercept			
A- Pore Size of filter membrane	-0.49	0.47	4.47
B-Type of Boiling Solvent	1.48	4.38	41.54
C-Time of Exposure	0.055	6.114E-003	0.058
AB	-0.55	0.60	5.71
AC	1.14	2.59	24.55
BC	-0.29	0.17	1.64
ABC	-1.08	2.32	22.04
Lenth's ME	3.10		
Lenth's SME	7.41		

Results of the second response (average pore size):

1. Type of boiling solvent

Figure 44 shows the effect of boiling solvent on the average pore size. A lower value of the average pore size of BP is achieved when the type of boiling solvent is of a lower vapor pressure.

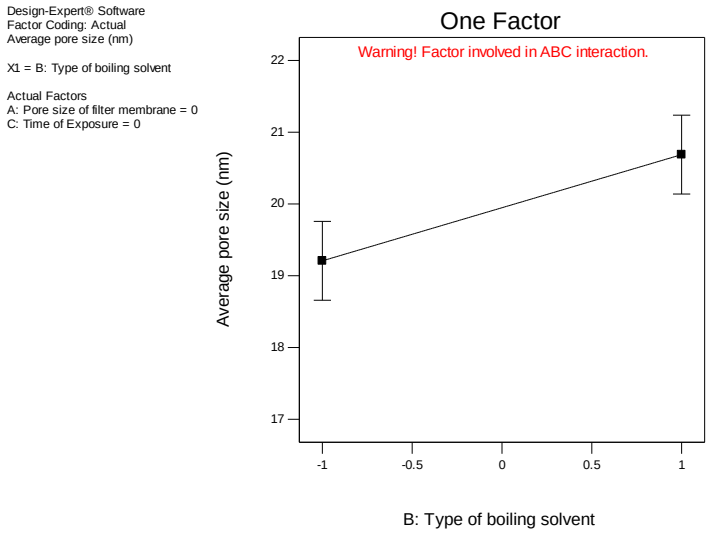

Figure 44 The effect of boiling solvent on the average pore size

2. *AC: Interaction between the pore size and the time of exposure*

Figure 45 shows the interaction between the pore size of the pore size of the substrate and time of exposure of boiling solvent on the average pore size. A smaller pore size of the substrate along with the long exposure by the solvent results in a smaller average pore size of the BP.

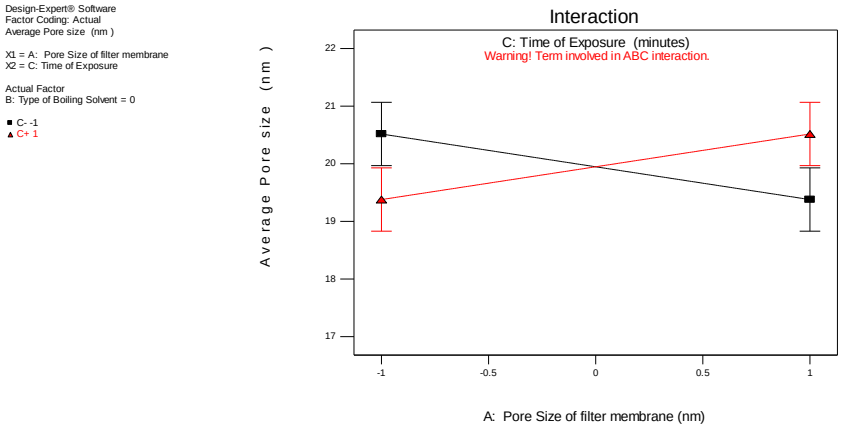

Figure 45 The effect of the interaction between the pore size of the substrate and time of exposure of the boiling solvent on the average pore size

To summarize the results of the statistical model, Table 9 shows the main variables or the interaction of variables that are responsible to produce a change in the BET surface area and the average pore size. The interaction between the pore size of the filter membrane and the time of exposure is influential combination for both the BET surface area and the average pore size. Time of exposure alone as a variable and the interaction between the type of boiling solvent and time it is being exposed are both influential on changing the BET surface area. On the other hand, the type of boiling solvent alone as a variable seems to be influential on the average pore width. The table

summarizes how the change of this variable might lead to the increase/decrease of the BET surface area/average pore width of the BPs, respectively.

Table 9 Summary of the results of the statistical model used

	C (Time of exposure)	AC (Interaction of Pore Size and time of exposure)	BC (Interaction between Type of boiling solvent and time of exposure)	B (Type of boiling solvent)
BET Surface area	A larger BET surface area is obtained when the time of exposure is shorter.	A higher BET surface area is achieved, when the pore size of the filter membrane is high and the type of boiling solvent is of a lower vapor pressure.	A boiling solvent with a higher vapor pressure in combination of a shorter exposure time results in higher BET surface area	
Average Pore width		A smaller pore size of the substrate along with the long exposure time results in a smaller average pore size of the BP.		A lower value of the average pore size of BP is achieved when the type of boiling solvent is of a lower vapor pressure.

5.6 Filtration of latex solution using the BP:

In accordance to the statistical results of the ANOVA model regarding the average pore size of the BP, it was found that a smaller pore size of membrane filter along with the longer time of exposure of solvent results in smaller average pore size. A comparison was then made between a blank BP (produced by 0.45 µm) and a modified BP (produced by the smallest pore size 0.2 µm of substrate exposed to 40 minutes of DMF). Two sizes of polystyrene beads were used for the filtration (0.3 µm and 0.6 µm that are comparable with the size of virus and colloids found in waste water [5].

Figure 46 presents the retention rate results obtained for filtering the two sizes of polystyrene beads using both the blank BP and the modified BP. By using the UV spectroscopy it was found that for the 0.3 µm polystyrene beads, the blank BP has a retention percentage of 71 in comparison to the modified one which has a retention percentage of 73. For the 0.6 µm polystyrene beads, the blank BP has a retention percentage of 67, while the modified one has a percentage of 76. This shows that there is an increase of around 3% by the modified BP in comparison to the blank one when filtering the small size of polystyrene beads, while there is an increase of around 9 % when filtering on the modified BP in comparison to the blank one. This in turn shows, that, the modified BP in both sizes of PS was more efficient than the blank BP, which

indicates that it possesses more of the small pores that helped in capturing more of the PS beads than when capturing using the blank BP.

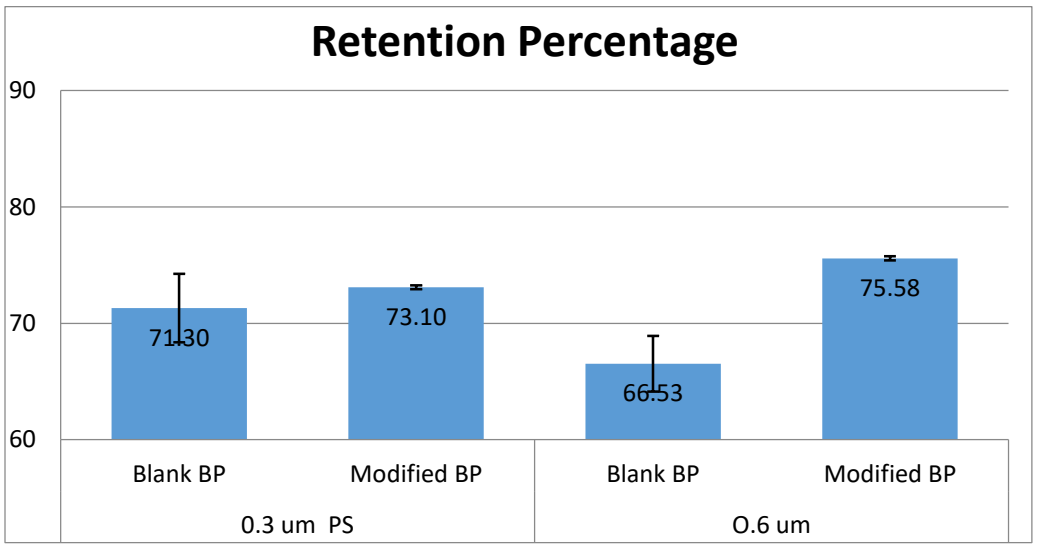

Figure 46 Retention Rate of polystyrene beads (0.3 µm and 0.6 µm) by the blank and modified BP

The SEM images below in Figure 47 show top-view images of the surfaces of the BP membranes after the filtration test at magnification of 20,000X . The PS beads that were retained by the BP membranes are clearly visible on the surface. It is evident that modified BPs have retained more PS beads in agreement with UV spectroscopy results.

0.6 um

PS

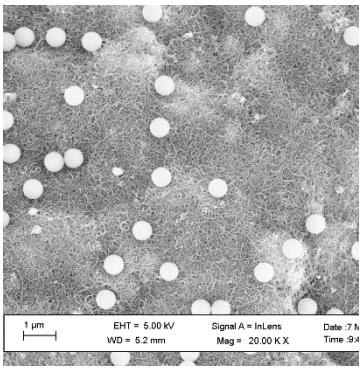

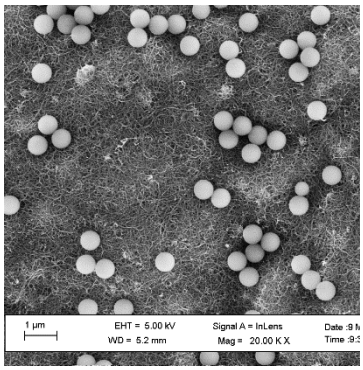

Blank **Modified BP**

0.3 um

PS

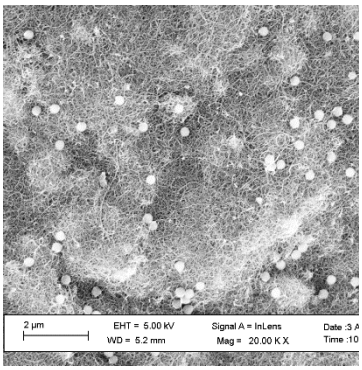

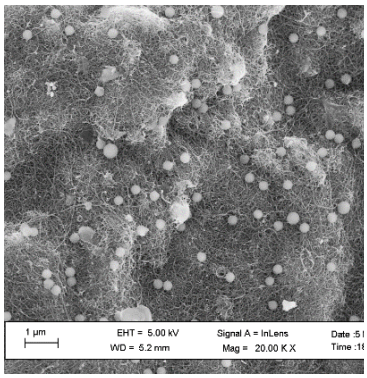

Blank **Modified BP**

Figure 47 SEM images of the blank BP and the modified BP after filtration at magnification of 20,000X for both the 0.3 µm and 0.6 µm of polystyrene beads

To explain why the retention rate of the BPs above was not 100%, a look at the range of pores sizes of the BP measured experimentally in the current study. The BPs were found to have pores sizes with sizes in the micron and the nano ranges. The BPs had the maximum micron pore size of 104 µm were explored, and the maximum nano pore size of 86 nm. This means that some of the bead particles passed through the BP because

of the micron range of the pore sizes, while some were retained because of the nano range that these BPs have. Thus, the efficiency of the retention was not fully achieved because some of the beads have already managed to escape through the micron pore sizes the BPs already have.

Another reason that may explain why the retention of BPs was not full efficiently working. BPs were used in the literature to filter Natural Organic matter (NOM) and Trace Organic Contaminants (TOC)[20], [22]. BPs have been proved to have good adsorbent capacity for these molecules, due to their mesoporous structure and the less number of negative surface charges of the CNTs. However, better results are obtained when the BPs are tailored to be more hydrophilic especially for filtering aqueous solutions. In the case of the BP used in this work, they are hydrophobic by nature [38] possessing an average angle of 121.9° measured by the contact angle analyzer presented earlier (Figure 48).

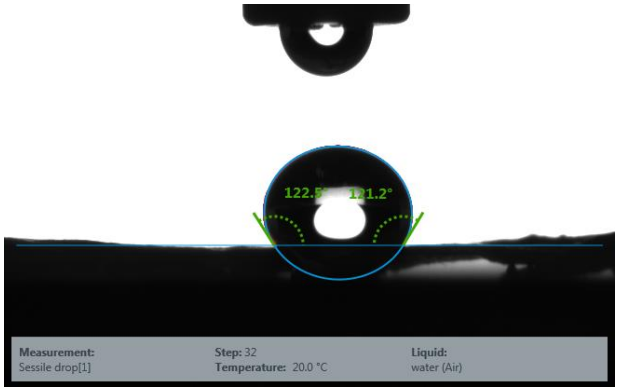

Figure 48 Contact angle of the BP

5.7 Relationship between the statistical model and the already tested variables

The main of objective of this work is to find the variables that would contribute change of porosity and specifically to produce the highest number of small pores possible. The statistical analysis aimed specifically to find the influential variables (or combination of variables) that would contribute to the highest surface area (which usually means more pores available) and to lowest average pore size of the BPs. The analysis done produced different variables that were responsible for optimizing these two products, however the verification of how influential the variables (or the combination of variables) to these products is not fully done.

According to the statistical analysis, an increase in the BET surface area is produced by shortening the time of exposure of a solvent. This was particularly not verified when testing the effect of the time of exposure of acetone on the change of the BET surface area. As the acetone time increased from 20 to 40 minutes of acetone exposure, the BET surface area increased as seen in Figure 29. However, this was particularly verified on the smaller pore ranges between 0-16 nm, as the shorter the time of exposure to acetone, the higher the differential surface area that was present. On the other hand, the two interactions AC (pore size of filter membrane with time of exposure) and BC (type of boiling solvent and time of exposure) that were produced by the statistical program to be influential on the BET surface area were not examined within the scope of this work in order to see if they verify or not.

The other output of this work is investigating is the lowering of the average pore size. According to the statistical model, the type of boiling solvent is influential in

changing the average pore size of BP. According to the model, a lower size of the average pore size is achieved when the type of boiling solvent is of a lower vapor pressure. This has been verified by testing of the effect of changing the boiling solvents (acetone, IPA, THF, DMF) on the average pore size. DMF had the lowest vapor pressure, and it resulted in the lowest average pore size produced (14 nm) in comparison to its counterparts which produced average pore size in the range of (16.5-17 nm). DMF was particularly successful in producing high number of pores at the size of 3.4 nm, where it contributed the most to the average pore size by lowering it. Acetone (solvent with the highest vapor pressure), on the other hand, was more responsible to produce the highest number of pores on the large pore ranges ≥~54 nm.

Also, according to the statistical model the interaction between the pore size of the filter membrane and the exposure time of solvent could be influential in decreasing the average pore size of the BP. This is still not verified within this work scope. However, the statistical model did not result in having the pore size of the filter membrane as a variable alone to influence the pore size of the BPs. This has been successfully verified by testing the effect of the change of filter membrane (0.2, 0.45, 1.0, 10 μm) where it showed that there is no much effect on the average pore size of the BPs was seen by changing the pore size (Table 5).

Thus, according to the influential variables already verified within the scope of this work, it would be safe to conclude that long time of exposure of the boiling solvent of the lowest vapor pressure (also the highest surface tension) are the optimum conditions that led to the production of the BP with the lowest average pore size relative to all the other BPs examined. Influential interactions between the variables need to be verified,

by changing both variables in the interaction, to see if this would result in having BPs with higher number of small pores, and eventually to the BP with the smallest average pore size possible. This would then lead to better retention percentages of the polystyrene beads, and thus better filtration results.

CHAPTER SIX

Conclusions and Future Work

CHAPTER SIX: CONCLUSIONS AND FUTURE WORK

6.1 Conclusions

The study aimed at tailoring the porosity of BPs by changing some preparation parameters; namely: varying the time for boiling solvent acetone exposure, varying the type of boiling solvent, varying the pore size of the membrane filter, and finally changing three parameters at the same time (type of solvent, time of exposure, and pore size of membrane filter). Statistical analysis on the three variables was carried out to see the most effective combination of parameters that result in a change in porosity and on the average pore size of the BPs. Different characterization techniques, such as SEM, Hg porosimetry and BET were used to investigate the change in porosity. The solvent exposure based on the densification method proved to be successful for tailoring the porosity of the BP.

BPs were successfully produced using vacuum filtration and Triton-X 100 as surfactant. They were then, successfully and completely peeled off from PTFE filter membranes.

First, the effect of changing the time of exposure to acetone vapor on BP was investigated. Porosity investigation was carried out using N_2 adsorption at 77K and Hg porosimetry. Samples were exposed to 20, 25, 30, 35, 40 minutes of acetone vapor. An increase in the number of pores in the range of (58 nm – 120 nm) resulted in all the BPs being exposed to acetone, as compared to their counterparts with no exposure to acetone vapor. Although, there is no clear linear relationship between the increase in time of acetone exposure and the BET surface area, there was an overall general successful

increase in the BET surface area and a general successful decrease of average pore size of the BPs, as the time of acetone exposure increased.

Second, the effect of changing the type of boiling solvent on the porosity of BPs was investigated. Different BPs were exposed to 40 minutes of four solvents (acetone, IPA, THF, and DMF) to test for a change in porosity. A significant decrease of the average pore size of BPs in case of the exposure to DMF. BET results showed that there is a variation in the values of differential volume and differential surface values for the same distinct pore widths exhibited by the different BPs. A new pore size range (3.4 nm) was observed for the cases of exposure to THF and DMF. The results confirmed that the porosity of BP can be modified and that DMF has the greatest effect in producing BPs with highest number of small pores and shifting the pores to smaller sizes because it has the highest surface tension and lowest vapor pressure of all solvents. The findings confirm the potential of the solvent evaporation technique in tailoring the porosity of BPs.

Third, the effect of changing the pore size of membrane filters on the BPs was also tested. PTFE membrane filters of different pore sizes (0.2µm, 0.45 µm, 1.0 µm, 10 µm) were used as membrane filter for BP along with exposing the BPs to 40 minutes of DMF vapor. The results showed that there is no linear relationship between the pore size of the filter membrane and the average pore size of the BP. However, the 0.45 µm membrane showed the highest number of small pores, while that of 10 µm showed the second highest. But in general, the 10 µm one possessed more pores in most of the

distinctive pores highlighted by both the differential volume and differential surface area graphs.

Fourth, statistical analysis was carried out to test for the effect of three different variables on (a) the BET surface area and (b) the average pore size of the BP. The three variables were (1) type of boiling solvent (2) time of exposure of the boiling solvent and (3) the pore size of the membrane filter. The analysis showed that the three variables have significant effect on these two responses. Specifically, time of exposure variable, the interaction between the pore size of filter membrane and time of exposure and the interaction between type of boiling solvent and time of exposure, all have significant effect on changing the BET surface area. While, time of boiling solvent and the interaction between the type of boiling solvent and time of exposure had the largest effect on the average pore size of the BPs. This last noteworthy finding had led to the use of the BPs produced using these two variables to be used to test for the efficiency of filtration of latex beads.

Last but not least, filtration procedures were carried out on the BP using PS beads as model pollutants. Blank and modified BP were compared according to their retention rate using two different sizes of the PS (0.3 μm and 0.6 μm). The results showed a small difference in the behavior between the blank and the modified BP when filtering the small size PS, while a better performance was observed when filtering the larger size of BPs.

The overall findings confirmed that the use of DMF as a solvent with a long exposure time was successful in producing BP with the most number of small pores, and the lowest average pore size. The statistical model confirmed that the type of boiling

solvent with low vapor pressure is effective in decreasing the average pore size of the BPs. Interaction between the pore size and time of exposure is an important factor to consider to tackle later in order to see if this produces lower average pore sized BP with relatively high number of small pores.

6.2 Future Recommendations

- Other types of boiling solvents should be considered to see the effect of changing them on the average pore size.
- Interaction between the pore size of the filter membrane and time of exposure of boiling solvent is to be varied to see the effect on changing the average pore size.
- Mechanical compacting techniques can be tested as an alternative technique for controlling the porosity the BPs.
- Use of bacteria and colloids as a media to be tested for filtration on BPs.
- Try filtration using different sizes of beads (maybe in the nano range) since there is a change in pores of nano- size which we are not capturing by the micron sized PS beads.

References: -

[1] S. Kar, R. C. Bindal, and P. K. Tewari, "Carbon nanotube membranes for desalination and water purification: Challenges and opportunities," *Nano Today*, vol. 7, no. 5, pp. 385–389, Oct. 2012.

[2] R. Das, S. B. Abd Hamid, M. E. Ali, A. F. Ismail, M. S. M. Annuar, and S. Ramakrishna, "Multifunctional carbon nanotubes in water treatment: The present, past and future," *Desalination*, vol. 354, pp. 160–179, Dec. 2014.

[3] C. H. Ahn *et al.*, "Carbon nanotube-based membranes: Fabrication and application to desalination," *J. Ind. Eng. Chem.*, vol. 18, no. 5, pp. 1551–1559, Sep. 2012.

[4] V. K. K. Upadhyayula, S. Deng, M. C. Mitchell, and G. B. Smith, "Application of carbon nanotube technology for removal of contaminants in drinking water: A review," *Sci. Total Environ.*, vol. 408, no. 1, pp. 1–13, 2009.

[5] R. Das, M. E. Ali, S. B. A. Hamid, S. Ramakrishna, and Z. Z. Chowdhury, "Carbon nanotube membranes for water purification: A bright future in water desalination," *Desalination*, vol. 336, pp. 97–109, Mar. 2014.

[6] V. K. Gupta, I. Ali, T. a. Saleh, A. Nayak, and S. Agarwal, "Chemical treatment technologies for waste-water recycling—an overview," *RSC Adv.*, vol. 2, no. 16, p. 6380, 2012.

[7] N. Academies, "Safe Drinking Water Is Essential," *Reports from Natl. Acad.*, 2007.

[8] K. Sutherland, "Developments in filtration: What is nanofiltration?," *Filtr. Sep.*, vol. 45, no. 8, pp. 32–35, 2008.

[9] K. Sears *et al.*, "Recent developments in carbon nanotube membranes for water purification and gas separation," *Materials (Basel).*, vol. 3, no. i, pp. 127–149, 2010.

[10] Y. Manawi, V. Kochkodan, M. A. Hussein, M. A. Khaleel, M. Khraisheh, and N. Hilal, "Can carbon-based nanomaterials revolutionize membrane fabrication for water treatment and desalination?," *Desalination*, vol. 391, pp. 69–88, 2016.

[11] L. Hu, D. S. Hecht, and G. Gru, "Carbon Nanotube Thin Films : Fabrication , Properties , and Applications," *Am. Chem. Soc.*, vol. 110, pp. 5790–5844, 2010.

[12] T. Kuilla, S. Bhadra, D. Yao, N. H. Kim, S. Bose, and J. H. Lee, "Recent advances in graphene based polymer composites," *Prog. Polym. Sci.*, vol. 35, no. 11, pp. 1350–1375, Nov. 2010.

[13] M. J. O'Connell, *Carbon nanotubes: properties and applications*, vol. 43, no. 19. 2006.

[14] A. Srivastava, O. N. Srivastava, S. Talapatra, R. Vajtai, and P. M. Ajayan,

"Carbon nanotube filters.," *Nat. Mater.*, vol. 3, pp. 610–614, 2004.

[15] O. Bakajin *et al.*, *Nanotechnology Applications for Clean Water*, Second Edi. Elsevier, 2014.

[16] J. Guo, J. Liu, L. Wang, and H. Liu, "Modification of ultrafiltration membranes with carbon nanotube buckypaper for fouling alleviation." *Membrane Water Treatment.*, vol.6, pp. 1-13, 2016"

[17] L. J. Sweetman *et al.*, "Bacterial filtration using carbon nanotube/antibiotic buckypaper membranes," *J. Nanomater.*, vol. 2013, 2013.

[18] R. J. Narayan, C. J. Berry, and R. L. Brigmon, "Structural and biological properties of carbon nanotube composite films," *Mater. Sci. Eng. B*, vol. 123, no. 2, pp. 123–129, 2005.

[19] Z. G. Z. & F. L. Jenny Hilding, Eric A. Grulke, "Dispersion of Carbon Nanotubes in Liquids," *J. Dispers. Sci. Technol.*, vol. 24, no. 1, pp. 1–41, 2003.

[20] X. Yang *et al.*, "Removal of natural organic matter in water using functionalised carbon nanotube buckypaper," *Carbon N. Y.*, vol. 59, pp. 160–166, 2013.

[21] A. Anso´n-Casaos, J. M. Gonza´ lez-Domı´nguez, and M. T. Martı´nez, "Surfactant-free assembling of functionalized single-walled carbon nanotube buckypapers," *Carbon N. Y.*, vol. 48, no. 5, pp. 1480–1488, 2010.

[22] H. Rashid *et al.*, "Synthesis , properties , water and solute permeability of MWNT buckypapers," *J. Memb. Sci.*, vol. 456, pp. 175–184, 2014.

[23] Z. Li *et al.*, "Freestanding bucky paper with high strength from multi-wall carbon nanotubes," *Mater. Chem. Phys.*, vol. 135, pp. 921–927, 2012.

[24] Y. A. Kim, H. Muramatsu, T. Hayashi, M. Endo, M. Terrones, and M. S. Dresselhaus, "Fabrication of high-purity, double-walled carbon nanotube buckypaper," *Chem. Vap. Depos.*, vol. 12, pp. 327–330, 2006.

[25] M. S. Jorio, Ado;Dresselhaus, Gene; Dresselhaus, Ed., *Topics in Applied Physics Volume 111- Carbon Nanotubes: Advanced Topic in the Synthesis, Structure, Properties and Applications*. New York: Springer, 2008.

[26] Z. Špitalský *et al.*, "The effect of oxidation treatment on the properties of multi-walled carbon nanotube thin films," *Materials Science and Engineering: B*, vol. 165. pp. 135–138, 2009.

[27] L. F. Dumée *et al.*, "Characterization and evaluation of carbon nanotube Bucky-Paper membranes for direct contact membrane distillation," *J. Memb. Sci.*, vol. 351, pp. 36–43, 2010.

[28] M. O. Memon, S. Haillot, and K. Lafdi, "Carbon nanofiber based buckypaper used as a thermal interface material," *Carbon N. Y.*, vol. 49, no. 12, pp. 3820–3828, 2011.

[29] H. C. Ismaik, Ahmad Fauzi; Rana, Dipak; Matsuura, Takeshi; Foley, *Carbon*

based Membranes for Seperation Processes. New York: Springer, 2011.

[30] W. Knapp and D. Schleussner, "Carbon Buckypaper field emission investigations," *User Model. User-adapt. Interact.*, vol. 69, pp. 333–338, 2002.

[31] N. a. Prokudina, E. R. Shishchenko, O.-S. Joo, K.-H. Hyung, and S.-H. Han, "A carbon nanotube film as a radio frequency filter," *Carbon N. Y.*, vol. 43, pp. 1815–1819, 2005.

[32] M. P. Mattson, R. C. Haddon, and A. M. Rao, "Molecular functionalization of carbon nanotubes and use as substrates for neuronal growth.," *J. Mol. Neurosci.*, vol. 14, pp. 175–182, 2000.

[33] R. H. Baughman, "Carbon Nanotube Actuators," *Science*, vol. 284. pp. 1340–1344, 1999.

[34] A. Schwengber, H. J. Prado, D. A. Zilli, P. R. Bonelli, and A. L. Cukierman, "Carbon nanotubes buckypapers for potential transdermal drug delivery," *Mater. Sci. Eng. C*, vol. 57, pp. 7–13, 2015.

[35] V. Perez-Fernandez, A. Gentili, A. Martinelli, F. Caretti, and R. Curini, "Evaluation of oxidized buckypaper as material for the solid phase extraction of cobalamins from milk: Its efficacy as individual and support sorbent of a hydrophilic-lipophilic balance copolymer," *J. Chromatogr. A*, vol. 1428, pp. 255–266, 2016.

[36] L. Dumée, K. Sears, J. R. Schü tz, N. Finn, M. Duke, and S. Gray, "Carbon nanotube based composite membranes for water desalination by membrane distillation," *Desalin. Water Treat.*, vol. 17, no. 1–3, pp. 72–79, Aug. 2012.

[37] S. M. Cooper, H. F. Chuang, M. Cinke, B. A. Cruden, and M. Meyyappan, "Gas permeability of a buckypaper membrane," *Nano Lett.*, vol. 3, pp. 189–192, 2003.

[38] L. Dumée *et al.*, "Enhanced durability and hydrophobicity of carbon nanotube bucky paper membranes in membrane distillation," *J. Memb. Sci.*, vol. 376, no. 1–2, pp. 241–246, Jul. 2011.

[39] A. Koohestanian, M. Hosseini, and Z. Abbasian, "The Separation Method for Removing of Colloidal Particles from Raw Water," *Euras. J. Agric. Environ. Sci*, vol. 4, no. 2, pp. 266–273, 2008.

[40] K. Sears *et al.*, "Recent developments in carbon nanotube membranes for water purification and gas separation," *Materials (Basel).*, vol. 3, pp. 127–149, 2010.

[41] F. M. Blighe, P. E. Lyons, S. De, W. J. Blau, and J. N. Coleman, "On the factors controlling the mechanical properties of nanotube films," *Carbon N. Y.*, vol. 46, pp. 41–47, 2008.

[42] H. Muramatsu *et al.*, "Pore structure and oxidation stability of double-walled carbon nanotube-derived bucky paper," *Chem. Phys. Lett.*, vol. 414, pp. 444–448,

2005.

[43] X. Zhang, T. V Sreekumar, T. Liu, and S. Kumar, “Properties and Structure of Nitric Acid Oxidized Single Wall Carbon Nanotube Films,” *J. Phys. Chem. B*, vol. 108, pp. 16435–16440, 2004.

[44] B. a. Kakade and V. K. Pillai, “Tuning the wetting properties of multiwalled carbon nanotubes by surface functionalization,” *J. Phys. Chem. C*, vol. 112, pp. 3183–3186, 2008.

[45] H. J. Park *et al.*, “Dispersion of Single-Walled Carbon Nanotubes in Water with Polyphosphazene Polyelectrolyte,” *J. Inorg. Organomet. Polym. Mater.*, vol. 16, no. 4, pp. 359–364, Nov. 2006.

[46] Q. Liu, M. Li, Z. Wang, Y. Gu, Y. Li, and Z. Zhang, “Improvement on the tensile performance of buckypaper using a novel dispersant and functionalized carbon nanotubes,” *Compos. Part A Appl. Sci. Manuf.*, vol. 55, pp. 102–109, Dec. 2013.

[47] R. L. D. Whitby, T. Fukuda, T. Maekawa, S. L. James, and S. V. Mikhalovsky, “Geometric control and tuneable pore size distribution of buckypaper and buckydiscs,” *Carbon N. Y.*, vol. 46, no. 6, pp. 949–956, May 2008.

[48] L. Dumée *et al.*, “The impact of hydrophobic coating on the performance of carbon nanotube bucky-paper membranes in membrane distillation,” *DES*, vol. 283, pp. 64–67, 2011.

[49] R. Smajda, Á. Kukovecz, Z. Kónya, and I. Kiricsi, “Structure and gas permeability of multi-wall carbon nanotube buckypapers,” *Carbon N. Y.*, vol. 45, pp. 1176–1184, 2007.

[50] A. Deneuve *et al.*, “Bucky paper with improved mechanical stability made from vertically aligned carbon nanotubes for desulfurization process,” *Appl. Catal. A Gen.*, vol. 400, pp. 230–237, 2011.

[51] J. Zhang and D. Jiang, “Influence of geometries of multi-walled carbon nanotubes on the pore structures of Buckypaper,” *Compos. Part A Appl. Sci. Manuf.*, vol. 43, no. 3, pp. 469–474, Mar. 2012.

[52] J. Zhang, D. Jiang, and H.-X. Peng, “A pressurized filtration technique for fabricating carbon nanotube buckypaper: Structure, mechanical and conductive properties,” *Microporous Mesoporous Mater.*, vol. 184, pp. 127–133, Jan. 2014.

[53] M. F. Arif, S. Kumar, and T. Shah, “Tunable morphology and its influence on electrical, thermal and mechanical properties of carbon nanostructure-buckypaper,” *Mater. Des.*, vol. 101, pp. 236–244, 2016.

[54] J. Liu, “High-Resolution Scanning Electron Microscopy,” in *Handbook of Microscopy for Nanotechnology*, 2005, pp. 325–359.

[55] L. Jacob, “An Introduction to Electron Optics,” *American Journal of Physics*. 1952.

[56] W. Zhou, R. P. Apkarian, and Z. L. Wang, “Fundamentals of Scanning Electron Microscopy,” in *Scanning Microscopy for Nanotechnology*, 2007, pp. 1–40.

[57] B. Hafner, “Scanning Electron Microscopy Primer,” *Cities*, pp. 1–29, 2007.

[58] “Derivation of the BET and Langmuir Isotherms,” *Ulm University*, 2011.[Online].Available:http://www.uniulm.de/fileadmin/website_uni_ulm/nawi.inst.251/Lehre/PC3-SS14/BET.pdf [Accessed: 15-Jun-2015].

[59] “OpenStax CNX - Physical Methods in Chemistry and Nano Science,” *BET surface area analysis of nano particles*, 2015. [Online]. Available: www.quizover.com/online/course/2-1-bet-surface-area-analysis-of-nanoparticles#m38278. [Accessed: 15-Jun-2015].

[60] M. Thommes *et al.*, “Physisorption of gases, with special reference to the evaluation of surface area and pore size distribution (IUPAC Technical Report),” *Pure Appl. Chem.*, vol. 87, no. 9–10, pp. 1051–1069, 2015.

[61] “Brunauer, Emmett and Teller (BET) Theory"*Particle Analytical*.” [Online].Available: http://particle.dk/methods-analytical-laboratory/surface-area-bet-2[Accessed: 20-Jun-2015].

[62] P.Klobles; K. Meyer; R. G. Munro. "Porosity and Specific Area Measurments for Solid materials" *Natl. Inst.* Stand.Technol..*Special Publ. 960-17*, 2006.

[63] H. Giesche, “Mercury Porosimetry: A General (Practical) Overview,” *Part. Part. Syst. Charact.*, vol. 23, no. 1, pp. 9–19, Jun. 2006.

[64] "Porosimetry By Mercury Intrusion". *The United States Pharmacopeial Convention*. 2011. [Online] *http://www.usp.org/sites/default/files/usp_pdf/EN/USPNF/m99026267porosimetrybymercury_intrusion.pdf.* [Accessed: 20-Jun-2015].

[65] Micromeritics Instrument Corporation,.[Online] *Http://Www.Micromeritics.Com/Repository/Files/Mercury_Porosemitry_Theory_Poster_.Pdf*. [Accessed: 20-Jun-2015].

[66] T. S. Meiron, A. Marmur, and I. S. Saguy, “Contact angle measurement on rough surfaces,” *J. Colloid Interface Sci.*, vol. 274, no. 2, pp. 637–644, 2004.

[67] Yuan, Yuehua and T. Randall Lee. "Contact angle and wetting properties". *Surface Science Techniques*. G Bracco and B Holst. 1st ed. Berlin: Springer, 2013. 1-23. Print.

[68] A. Lafuma and D. Quéré, “Superhydrophobic states.,” *Nat. Mater.*, vol. 2, no. 7, pp. 457–60, 2003.

[69] J. H. Snoeijer and B. Andreotti, “A microscopic view on contact angle selection,” *Phys. Fluids*, vol. 20, no. 5, 2008.

[70] A. Hofmann, “12 Spectroscopic techniques : I Spectrophotometric techniques,”

Princ. Tech. Biochem. Mol. Biol., pp. 477–521, 2010.

[71] G. R. Chatwal, S. K. Anand, M. (Meenakshi) Arora, and A. Anand, *Spectroscopy (atomic and molecular)*. Himalaya Pub. House, 2009.

[72] G. R. Chatwal, S. K. Anand, M. (Meenakshi) Arora, and A. Anand, *Spectroscopy (atomic and molecular)*. Himalaya Pub. House, 2009.

[73] D. L. Pavia, G. M. Lampman, G. S. Kriz, and J. R. Vyvyan, *Introduction to spectroscopy*. Brooks/Cole Publishers,USA, 4th edition, 2009

[74] M. De Volder *et al.*, "Diverse 3D microarchitectures made by capillary forming of carbon nanotubes," *Adv. Mater.*, vol. 22, no. 39, pp. 4384–4389, 2010.

[75] M. M. Zaeri, S. Ziaei-Rad, A. Vahedi, and F. Karimzadeh, "Mechanical modelling of carbon nanomaterials from nanotubes to buckypaper," *Carbon N. Y.*, vol. 48, pp. 3916–3930, 2010.

[76] T. Wang, D. Jiang, S. Chen, K. Jeppson, L. Ye, and J. Liu, "Formation of three-dimensional carbon nanotube structures by controllable vapor densification," *Mater. Lett.*, vol. 78, pp. 184–187, 2012.

[77] D. N. Futaba *et al.*, "Dual porosity single-walled carbon nanotube material," *Nano Lett.*, vol. 9, no. 9, pp. 3302–3307, 2009.

[78] P. Lu, and Y.Xia, "Manuevering the Internal Porosity and Surface Morphology of Electrospun Polysterene Yarns by Controlling the Solvent and Humidity" Langmiur " vol. 141, no. 4, pp. 7070-7078, 2013..

[79] L. F. Dumee *et al.*, "Small angle X-ray scattering study of carbon nanotube forests densified into long range patterns by controlled solvent evaporation," *J. Colloid Interface Sci.*, vol. 407, pp. 556–560, 2013.

[80] D. N. Futaba *et al.*, "Shape-engineerable and highly densely packed single-walled carbon nanotubes and their application as super-capacitor electrodes.," *Nat. Mater.*, vol. 5, no. 12, pp. 987–994, 2006.

[81] L. Hussein, G. Urban, and M. Krüger, "Fabrication and characterization of buckypaper-based nanostructured electrodes as a novel material for biofuel cell applications.," *Phys. Chem. Chem. Phys.*, vol. 13, no. 13, pp. 5831–9, 2011.

[82] R. L. Muhlbauer, S. M. Joshi, and R. A. Gerhardt, "The effect of substrate pore size on the network interconnectivity and electrical properties of dropcasted multiwalled carbon nanotube thin films," *J. Mater. Res.*, vol. 28, no. 12, pp. 1617–1624, 2013.

[83] L. Liu, Q. Yang, and J. Shen, "Correlation between porosity and electrical-mechanical properties of carbon nanotube buckypaper with various porosities," *J. Nanomater.*, vol. 2015, 2015.

[84] Montgomery, Douglas C. *Design And Analysis Of Experiments*. 1st ed. [S.l.]: Wiley, 2013. Print.

APPENDIX

Anova Data Analysis:

Select	Std	Run	Factor 1 A: Pore Size ... nm	Factor 2 B:Type of Bo... C	Factor 3 C:Time of Ex... minutes	Response 1 BET Surface... m2/g	Response 2 Average Por... nm
	5	1	-1	-1	1	192.879	18.2432
	2	2	1	-1	-1	197.542	17.9571
	7	3	-1	1	1	180.703	21.0558
	3	4	-1	1	-1	194.813	21.3542
	8	5	1	1	1	184.29	20.0817
	6	6	1	-1	1	181.412	20.5222
	1	7	-1	-1	-1	179.485	20.1099
	4	8	1	1	-1	192.698	20.2604

Model results according to BET Surface Area as a response

Use your mouse to right click on individual cells for definitions.

Response 1 **BET Surface Area**

ANOVA for selected factorial model

Analysis of variance table [Partial sum of squares - Type III]

Source	Sum of Squares	df	Mean Square	F Value	p-value Prob > F	
Model	354.69	4	88.67	22.98	0.0138	significant
C-Time of Exposure	*79.73*	*1*	*79.73*	*20.66*	*0.0199*	
AC	*70.94*	*1*	*70.94*	*18.38*	*0.0233*	
BC	*48.91*	*1*	*48.91*	*12.68*	*0.0378*	
ABC	*155.11*	*1*	*155.11*	*40.20*	*0.0079*	
Residual	11.58	3	3.86			
Cor Total	366.27	7				

The Model F-value of 22.98 implies the model is significant. There is only a 1.38% chance that an F-value this large could occur due to noise.

Values of "Prob > F" less than 0.0500 indicate model terms are significant. In this case C, AC, BC, ABC are significant model terms.

Normal Probability Assumption

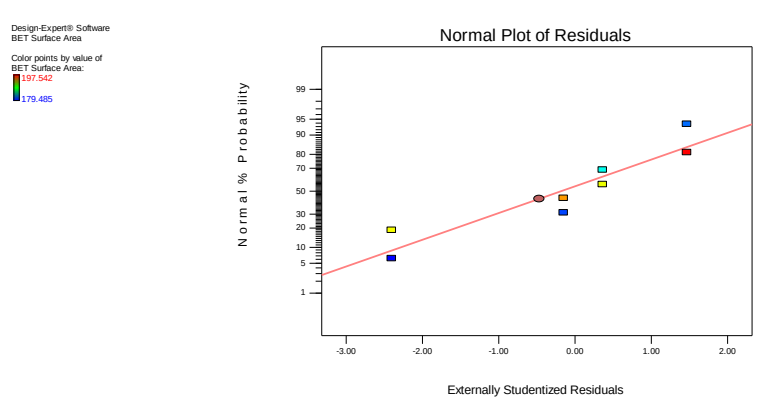

From examining the normal probability of residuals, error distribution is approximately normal. There is also no outlier in the plot.

Independence Assumption

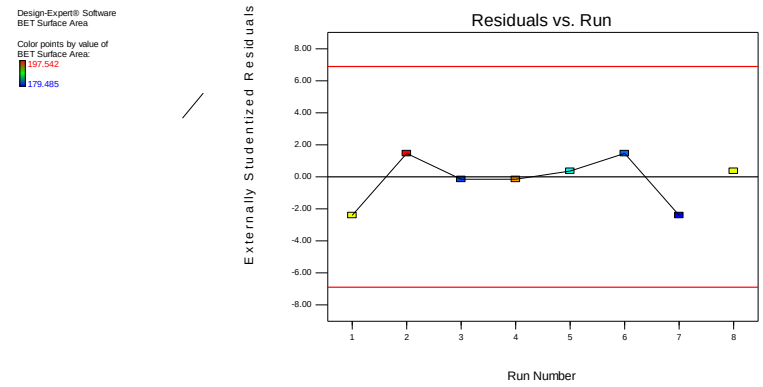

The residuals vs. run plot does not reveal obvious pattern, which means that there is no correlation and that the residuals satisfy the independence assumption.

Constant Variance Assumption

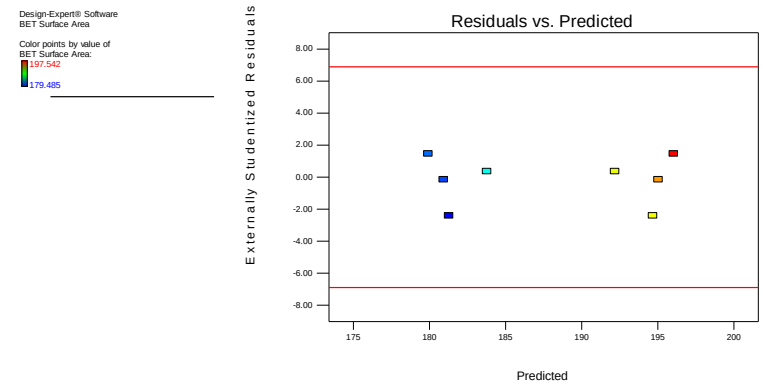

The Residual Vs Predicted plot does not reveal any obvious pattern i.e. there is no correlation. The residuals tend to cluster around the zero line of the y axis. They are well

distributed on both sides of the line, with no formation of any clear pattern.It will be safe to say that the residuals meet constant variance, because the residuals neither form an outward opening funnel nor skewed distribution.

Model results according to BET Average Pore size

Use your mouse to right click on individual cells for definitions.

Response 2 **Average Pore size**

ANOVA for selected factorial model

Analysis of variance table [Partial sum of squares - Type III]

Source	Sum of Squares	df	Mean Square	F Value	p-value Prob > F	
Model	9.29	3	3.10	9.90	0.0254	significant
B-Type of Boiling Solvent	*4.38*	*1*	*4.38*	*14.00*	*0.0201*	
AC	*2.59*	*1*	*2.59*	*8.27*	*0.0452*	
ABC	*2.32*	*1*	*2.32*	*7.43*	*0.0527*	
Residual	1.25	4	0.31			
Cor Total	10.55	7				

The Model F-value of 9.90 implies the model is significant. There is only a 2.54% chance that an F-value this large could occur due to noise.

Values of "Prob > F" less than 0.0500 indicate model terms are significant. In this case B, AC are significant model terms.

Normality assumption

The normal plot of residuals resembles a straight line. The analysis of variance satisfies Normality assumption. Since there is no outlier, it is safe that the experiment is ok.

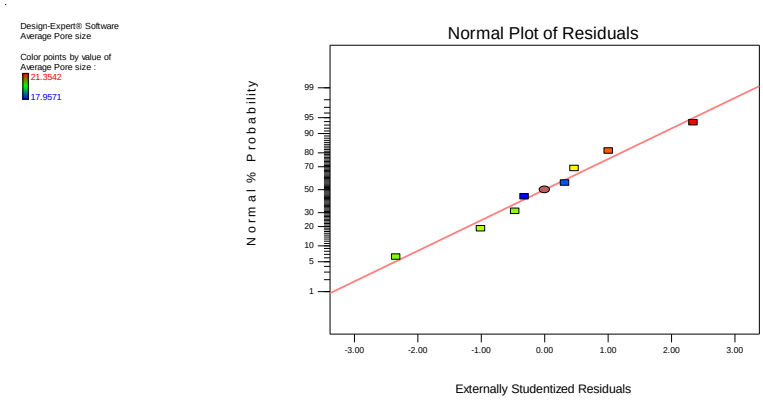

IIndependence Assumption

Finding: The Residual vs Run plot does not reveal any obvious pattern i.e there is no correlation.The independence of variance assumption holds good

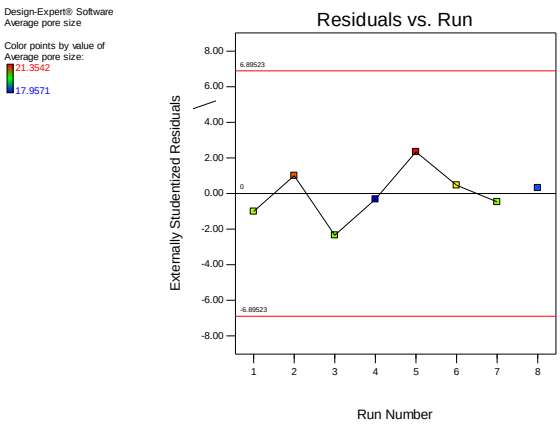

Constant Variance Assumption:

The predicted versus actual plot shows how the model predicts over the range of data. Plot exhibits random scatter about the 45 degree line. Clusters of points above or below the line indicate problems of over or under predicting. The line is going through the middle of the data over the whole range of the data, which is good.

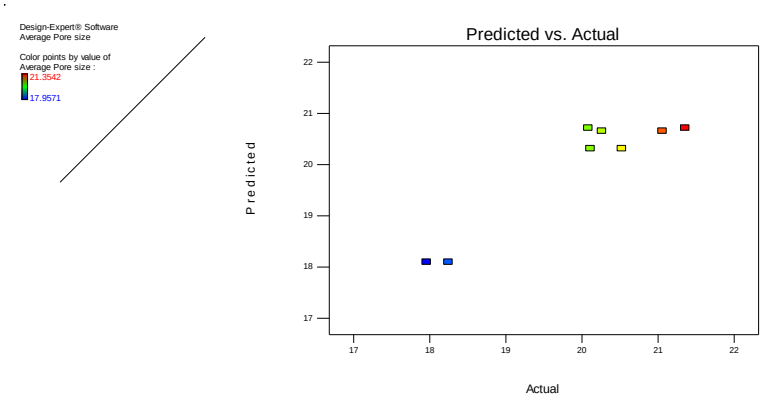

The Residual Vs Predicted plot does not reveal any obvious pattern i.e. there is no correlation. The residuals tend to cluster around the zero line of the y axis. They are well distributed on both sides of the line, with no formation of any clear pattern. It will be safe

to say that the residuals meet constant variance, because the residuals neither form an outward opening funnel nor skewed distribution.

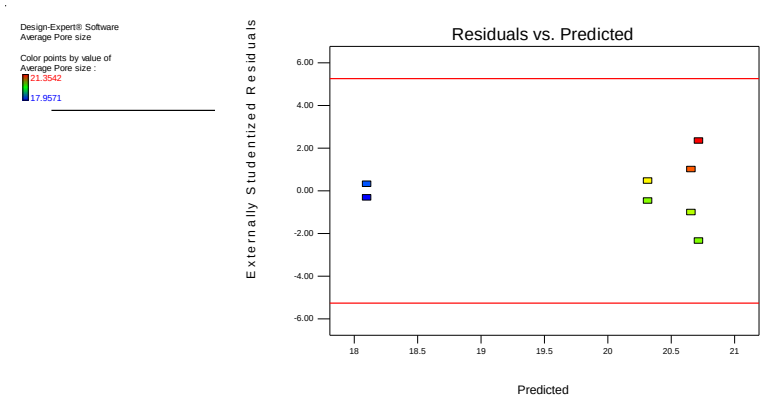

Calibration Curves:

0.3 µm PS beads

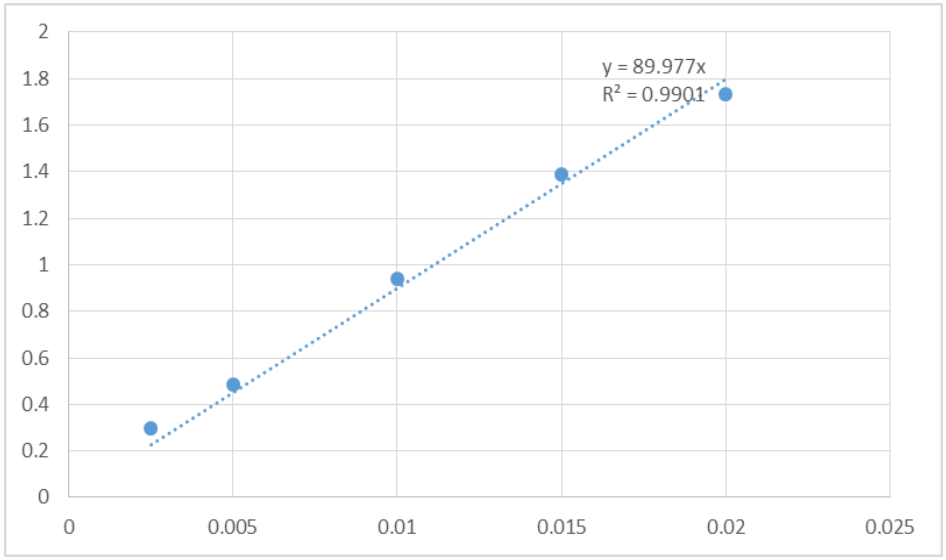

0.6 µm polystyrene beads